University of Windsor
Scholarship at UWindsor

Electronic Theses and Dissertations

1976

Evaluation of particle collection by thermophoresis and diffusiophoresis.

Ed. Alias
University of Windsor

Follow this and additional works at: http://scholar.uwindsor.ca/etd

Recommended Citation
Alias, Ed., "Evaluation of particle collection by thermophoresis and diffusiophoresis." (1976). *Electronic Theses and Dissertations.* Paper 1988.

This online database contains the full-text of PhD dissertations and Masters' theses of University of Windsor students from 1954 forward. These documents are made available for personal study and research purposes only, in accordance with the Canadian Copyright Act and the Creative Commons license—CC BY-NC-ND (Attribution, Non-Commercial, No Derivative Works). Under this license, works must always be attributed to the copyright holder (original author), cannot be used for any commercial purposes, and may not be altered. Any other use would require the permission of the copyright holder. Students may inquire about withdrawing their dissertation and/or thesis from this database. For additional inquiries, please contact the repository administrator via email (scholarship@uwindsor.ca) or by telephone at 519-253-3000ext. 3208.

INFORMATION TO USERS

THIS DISSERTATION HAS BEEN MICROFILMED EXACTLY AS RECEIVED

This copy was produced from a microfiche copy of the original document. The quality of the copy is heavily dependent upon the quality of the original thesis submitted for microfilming. Every effort has been made to ensure the highest quality of reproduction possible.

PLEASE NOTE: Some pages may have indistinct print. Filmed as received.

Canadian Theses Division
Cataloguing Branch
National Library of Canada
Ottawa, Canada K1A ON4

AVIS AUX USAGERS

LA THESE A ETE MICROFILMEE TELLE QUE NOUS L'AVONS RECUE

Cette copie a été faite à partir d'une microfiche du document original. La qualité de la copie dépend grandement de la qualité de la thèse soumise pour le microfilmage. Nous avons tout fait pour assurer une qualité supérieure de reproduction.

NOTA BENE: La qualité d'impression de certaines pages peut laisser à désirer. Microfilmée telle que nous l'avons reçue.

Division des thèses canadiennes
Direction du catalogage
Bibliothèque nationale du Canada
Ottawa, Canada K1A ON4

EVALUATION OF PARTICLE COLLECTION BY THERMOPHORESIS AND DIFFUSIOPHORESIS

A Thesis
Submitted to the Faculty of Graduate Studies
Through the
Department of Chemical Engineering
in Partial Fulfillment of the Requirements
for the Degree of
Master of Applied Science
at the
University of Windsor
by

Ed Alias

Windsor, Ontario
1975

© Ed Alias 1976

ACKNOWLEDGEMENTS

I wish to express my sincere gratitude to my advisors, Professor A. W. Gnyp and Professor C. C. St. Pierre for their unfailing help, guidance and encouragement throughout the preparation of this report. I also wish to express my thanks to Professor R. A. Stager and Professor G. P. Mathur for their help. I have benefited from discussions which I had with many, especially Mr. Doug Smith. To Mrs. Betty Sheehan, I wish to express my special thanks for her fine job of typing the manuscript and splendid co-operation.

ABSTRACT

A critical review of theoretical and experimental studies on thermophoretic and diffusiophoretic phenomena indicates that these flux force mechanisms represent potentially powerful techniques for the removal of fine particulate material in wet collectors. The magnitudes of the flux forces and flux velocities are presented as functions of temperature, pressure and particle size normally encountered in practice.

Overall flux force collection efficiency expressions indicate that significant fine particle collection can be achieved in counter-current spray scrubbers developing realistic temperature gradients, concentration gradients and drop collection surface areas. Initial attempts at modelling the performance of counter-current spray scrubbers show that practical design efficiency curves require the development of a computer program to simultaneously solve heat, mass and momentum transport rate equations.

CONTENTS

FIGURES

TABLES

I. INTRODUCTION

This report outlines the progress made during the 16 month period from 1 September, 1973 to 31 December 1974 on the research grant "Continuation and Extension of the Evaluation of Wet Collector Performance for Particulate Removal" awarded by the Ontario Ministry of the Environment to the air pollution research group in the Department of Chemical Engineering at the University of Windsor.

A. Aims

The objective of the 1973-74 research program, as determined by Ontario Ministry of the Environment priorities, was to continue the development of a design manual that would permit the evaluation of performance characteristics of industrial wet gas cleaning devices. Under the terms of the grant, the research personnel were

i. to continue the collection and critical evaluation of literature pertinent to the operation of wet collectors

ii. to develop a detailed theoretical analysis of the chemical and physical processes involved in the operation of wet collectors and

iii. to develop a preliminary outline of a design manual that can be used for the analysis of the performance characteristics of industrial wet gas cleaning equipment.

B. Program Development

In order to achieve the desired aims, the research group was organized to permit investigations on

i. Fundamentals of Gaseous-Particulate Flow Around Solid and Liquid Spherical Obstructions

ii. Atomization and Generation of Liquid Droplets with Respect to Solid Capture

iii. Solid Particle Collection in Wet Scrubbers by Thermophoretic and Diffusiophoretic Effects Including Condensation and Evaporation and

iv. Fundamentals of Venturi Scrubber Performance

II. INFORMATION SEARCH

A. Open Literature

To date, a total of 169 references pertaining to the evaluation of gas cleaning equipment performance have been collected and critically evaluated.

B. Conferences

The following conferences, where relevant papers were presented, were attended:

Twelfth Annual Purdue Air Quality Conference
Indianapolis, Indiana 6-8 Nov., 1973

Fourth Annual Environmental Engineering and Science Conference
Louisville, Kentucky 4-5 March, 1974

Pollution Control Association of Ontario Educational Seminar
Toronto, Ontario 14 March, 1974

Ministry of the Environment Research Seminar
Toronto, Ontario 21 March, 1974

Ontario Section APCA Spring Meeting
Waterloo, Ontario 6-8 May, 1974

Canadian Symposium on Fluid Dynamics
London, Ontario 21 June, 1974

University of Waterloo Special Lecture Series
Waterloo, Ontario 26 June, 1974

In addition, papers were obtained from the following conferences which were not attended:

The New York Academy of Sciences Conference on Odors: Evaluation, Utilization and Control
New York, New York 1-3 October, 1973

Sixty-Sixth Annual Meeting, AIChE Philadelphia, Pennsylvania	11-15 November, 1973
ASHRAE 1974 Semi-Annual Meeting Los Angeles, California	3-7 February, 1974
State-of-the-Art of Odor Control Technology Conference, APCA Pittsburgh, Pennsylvania	7-8 March, 1974
Seventy-Sixth National Meeting, AIChE Tulsa, Oklahoma	7-14 March, 1974
American Industrial Hygiene Conference Miami Beach, Florida	12-17 May, 1974
Seventy-Seventh National Meeting, AIChE Pittsburgh, Pennsylvania	2-5 June, 1974
Sixty-Seventh Annual Meeting, APCA Denver, Colorado	9-13 June, 1974

C. Advanced Seminars

In its effort to remain knowledgeable on the current state of technology associated with stack sampling for gaseous and particulate pollutants, the research group offered six stack sampling courses during the past year. Two of these were tailored specifically for members of the Ontario Ministry of the Environment. A third was designed to fulfill the needs of 18 officials selected from across the country by the Air Pollution Control Directorate of Environment Canada.

Interactions with engineers, chemists, technicians and administrators from industrial and regulatory organizations provide the group with added insight into the problems related to testing and performance of gas cleaning devices.

D. Equipment Manufacturers and Suppliers

A significant effort has been made to up-date the collection of trade literature available from manufacturers and suppliers of gas cleaning equipment and related components. This will be particularly important to future work involving the assessment of the performance of typical commercially available wet collectors.

E. Regulatory Agencies

Mutually profitable contacts were maintained during this period with personnel at:

Ontario Ministry of the Environment	Toronto, Ontario
U. S. Environmental Protection Agency Office of Air Programs	Research Triangle Park, North Carolina
Air Pollution Control Directorate, Environment Canada	Ottawa, Ontario
Montreal Urban Community	Montreal, Quebec

F. Universities and Research Institutes

Correspondence and personal visits were maintained with individuals at:

University of Waterloo Waterloo, Ontario	Chemical Engineering
University of Western Ontario London, Ontario	Dr. J. M. Beeckmans
University of British Columbia Vancouver, British Columbia	Chemical Engineering
The University of Texas Austin, Texas	Chemical Engineering

Oakland University Rochester, Michigan	School of Engineering
University of Bristol Bristol, England	Aeronautical Engineering
Illinois Institute of Technology Chicago, Illinois	Odor Sciences Centre
Lawrence Livermore Laboratory University of California Livermore, California	Technical Information Department
University of Bridgeport Bridgeport, Connecticut	Dr. E. S. Tillman, Jr.
The University of Leeds Leeds, England	Prof. N. Dombrowski
Indian Institute of Science Banglore, India	Prof. R. Kumar
Jet Propulsion Laboratory California Institute of Technology Pasadena, California	George A. Mitchell Document Review Group
Syracuse University Department of Chemical Engineering and Materials Science Syracuse, New York	Dr. R. Rajagopalan
Environmental Protection Agency Air Pollution Technical Information Centre Research Triangle Park North Carolina	Johon E. Knight
Research Centre The British Petroleum Co. Ltd. Sunburn on Thames Middlesex, United Kingdom	Dr. E. L. Howe
Department of Chemical Engineering Iowa State University Ames, Iowa	Dr. J. C. Hill

III. FUNDAMENTALS OF PARTICLE COLLECTION

A. Introduction

As Federal and Provincial environmental regulatory agencies continue to release new emission guidelines for chemical and metallurgical operations the need for the development of economical methods of removing particulate matter from stack emissions increases significantly. Future emphasis will be focussed on the improvement of techniques for the collection of sub-micron particles at the source because such material is

i. capable of penetrating to the furthest extremities of the human respiratory system when inhaled

ii. partly responsible for reduced visibility in urban centres

iii. accumulating in the atmosphere because of low agglomoration and settling rates.

In principle, particulate matter can be removed from dirty gas streams by subjecting the particles to forces which divert them from their original paths or change the relative motion between the particles and obstacles (collecting elements) in the moving gas streams. To be effective, these forces must be of sufficient magnitude to significantly influence the behavior of particles in the vicinity of the collecting elements.

B. Particle Collection Mechanisms

It is generally recognized that there are at least ten basic mechanisms responsible for particulate removal from dirty gas streams. Conventional gas cleaning devices have utilized

i. gravitational forces
ii. centrifugal forces
iii. electrostatic forces
iv. magnetic forces
v. inertial impaction
vi. direct interception
vii. Brownian diffusion
viii. thermophoretic forces
ix. diffusiophoretic forces
x. wake entrainment

to effect particle collection.

Since this report represents part of a broader study whose basic goal is to provide a comprehensive and systematic analysis of the parameters affecting the performance of wet scrubbers for particulate removal from gases, emphasis is focussed, in general, on mechanisms directly operative in wet collectors. As a result, the first four mechanisms have not been considered in the present investigation.

In particular this study is limited to the analysis of thermophoretic and diffusiophoretic phenomena with respect to their contributions to particulate capture in wet collectors. An earlier publication [1] discussed particle removal by cylindrical collectors in terms of the inertial impaction, direct interception and Brownian diffusion mechanisms. The application of inertial impaction, direct interception, Brownian diffusion and wake entrainment to particle-spherical collector interactions has been initiated by recent additions to the research team.

A brief review of the fundamentals of particulate collection by inertial impaction, direct interception and Brownian diffusion will show that thermophoresis and diffusiophoresis represent potentially powerful techniques for the removal of the sub-micron material that will come under increasingly critical scrutiny in future emission guidelines.

1. Inertial Impaction

Particle collection by inertial impaction is a function of the inertial impaction parameter [2],

$$N_I = \frac{C_1 \, v_p \rho_p \, D_p^2}{18 \, \mu \, D_c} \qquad \text{where} \qquad (3\text{-}1)$$

N_I = inertial impaction parameter, dimensionless

C_1 = Cunningham correction factor, dimensionless

v_p = particle velocity, cm/sec

ρ_p = density of particle, gm/cm^3

μ = gas viscosity, gm/(cm sec)

D_c = diameter of collecting element, cm

D_p = diameter of particle, cm

Figure 3-1 depicts the particle velocity required to achieve 90% target efficiency as a function of the diameter of the collecting body and the diameter of the particle to be captured. According to this plot, the collection of submicron particles by inertial impaction requires velocities beyond the capabilities of commercially available control equipment.

2. Interception

The efficiency of particle collection by the interception mechanism is dependent on the interception parameter [2].

$$N_R = \frac{D_p}{D_c} \qquad \text{where} \qquad (3\text{-}2)$$

N_R = interception parameter, dimensionless

D_p = diameter of particle, cm

D_c = diameter of collecting element, cm

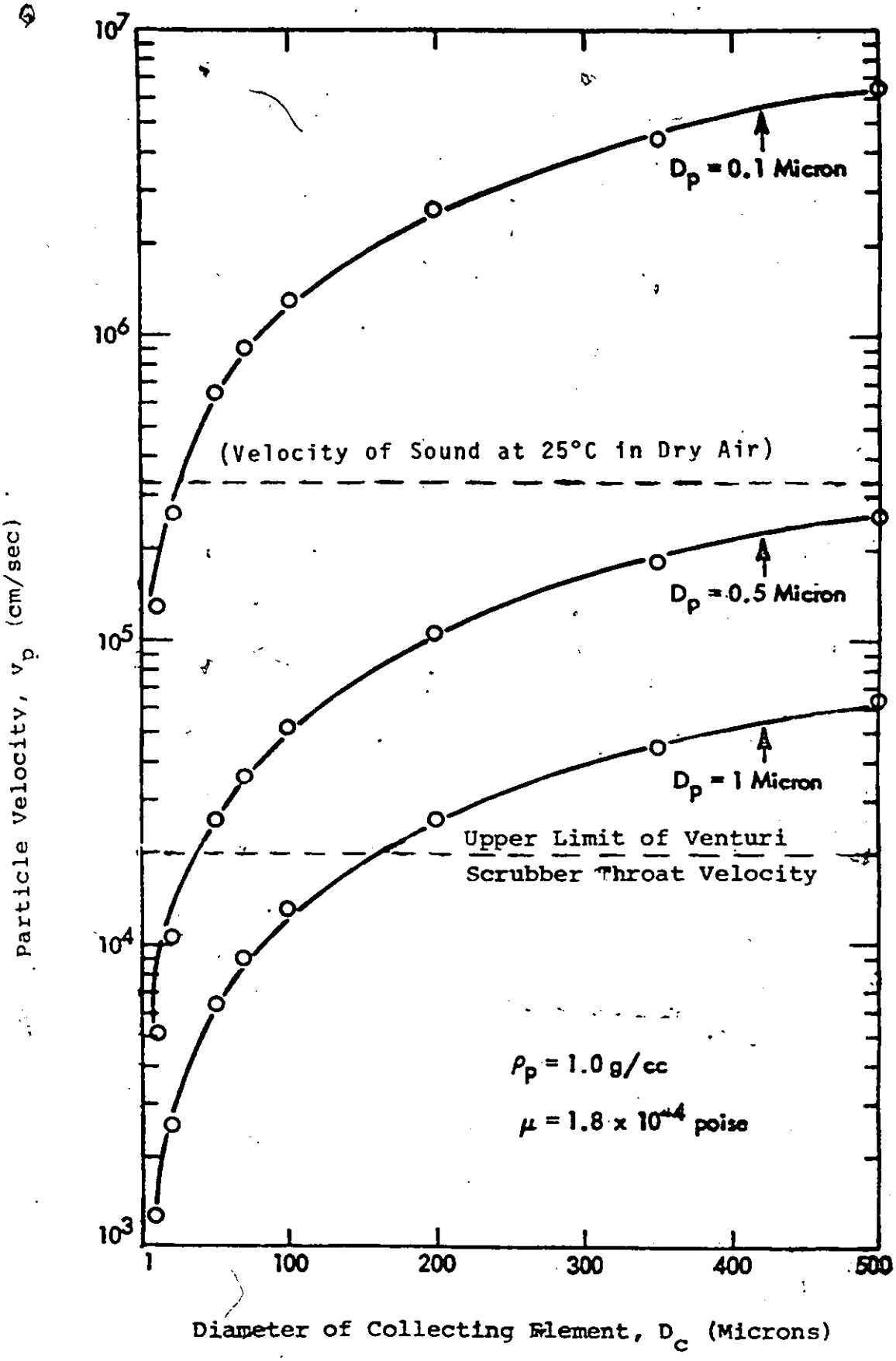

FIGURE 3-1: Particle Velocities Required to Achieve 90% Target Efficiency for Inertial Impaction [2]

The relationship between the interception parameter, N_R and Reynolds number, N_{Re_c}, for target efficiencies, η_{Int}, of 0.5 and 0.9 is provided by Figure 3-2 which indicates that interception is significant as a collection mechanism only when the diameter of the collecting element is of the same order of magnitude as the particles to be collected. In practice the diameters of liquid drops generated in wet scrubbers would never approach sub-micron particle dimensions because gas velocities even as high as 20,000 cm/sec would normally never produce drops smaller than 25 microns.

3. Brownian Diffusion

The target efficiency for particulate collection by Brownian diffusion is an inverse function of the diffusion parameter which is the Peclet number [2]

$$N_{Pe} = \frac{D_c \, v_{rel}}{\mathscr{D}_p} \qquad \text{where} \qquad (3\text{-}3)$$

N_{Pe} = Peclet number, dimensionless

v_{rel} = particle velocity relative to collecting element, cm/sec

D_c = diameter of collecting element, cm

$\mathscr{D}_p$ = diffusivity of particle, cm^2/sec

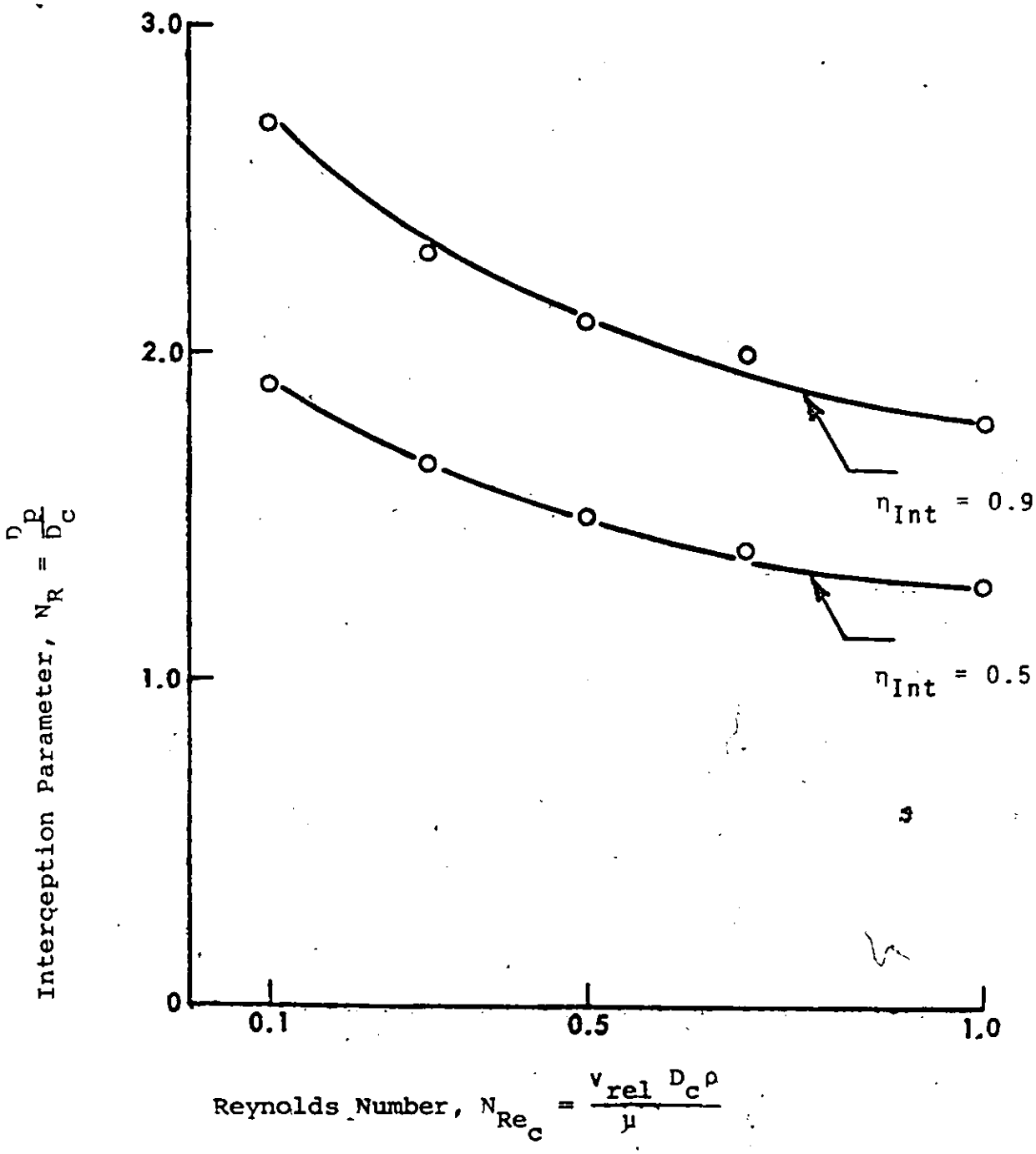

FIGURE 3-2: Interception Parameter as a Function of Reynolds Number for Selected Target Efficiencies [2]

Figure 3-3 represents graphical solutions of the equations for target efficiencies developed by Ranz [3], Freidlander [4] and Langmuir [5]. It is apparent from Figure 3-3 that the collection efficiency for Brownian diffusion is not significant if the value of the Peclet number, N_{Pe}, is much above 10. For sub-micron particles whose diffusion coefficients are of the order of 10^{-6} cm^2/sec, normal wet scrubber operating conditions lead to Peclet numbers exceeding 1000.

4. Flux Forces

Thermophoretic and diffusiophoretic forces are classified as flux forces because they are dependent on temperature and concentration gradients respectively. According to Shannon [2] the magnitudes of flux forces do not approach zero as the size of the particles to be collected approaches the sub-micron range. This characteristic of flux forces indicates that thermophoretic and diffusiophoretic phenomena should be seriously considered as potentially useful techniques for the removal of sub-micron particulate material in wet collectors.

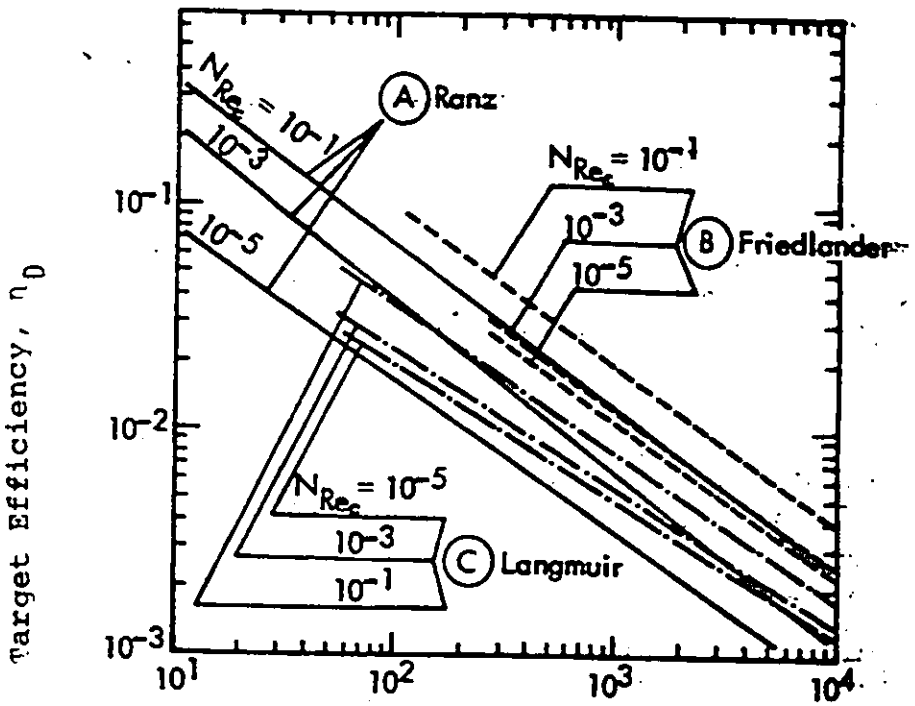

FIGURE 3-3: Target Efficiency by Diffusion on an Isolated Cylinder [2]

REFERENCES

1. Gnyp, A. W., Price, S. J. W., St. Pierre, C. C., Mozzon, D., and Smith, D., An Evaluation of Wet Collector Performance for Particulate Removal, Part I: Fundamentals, The Industrial Research Institute of the University of Windsor (1973).

2. Shannon, L. J., Control Technology for Fine Particulate Emissions, Midwest Research Institute, Kansas City, Missouri, U.S. Environmental Protection Agency Report, EPA-650/2-74-027 (May 1974).

3. Ranz, W. E., The Impaction of Aerosol Particles on Cylindrical and Spherical Collectors, Contract Report AT (30-3)-28; University of Illinois Technical Report No. 3 (1951).

4. Friedlander, S. K., Mass and Heat Transfer to Single Spheres and Cylinders at Low Reynolds Numbers, AIChE Journal, 3, 43 (1957).

5. Langmuir, I., U.S. Office of Scientific Research and Development No. 865, Part 4 (1942).

IV. THERMAL FORCE

The thermal force is presently defined as "a force, other than that caused by convection, which acts on a body suspended in a gas not in thermal equilibrium" [1]. This thermal or radiometric force on a particle originates from the interaction of gas molecules with the particle surface. The mechanism of the gas-solid interaction is dependent upon the ratio of the mean free path length of the gas to the particle radius, which is called the Knudsen number, N_{Kn}.

A simple model illustrating the thermal force would consider only the relative velocities of the gas molecules hitting a single solid spherical particle. Molecules striking the particle from the hotter side have a mean velocity which is greater than that of molecules impinging from the colder side and thus a net momentum is imparted to the particle which tends to move it towards the cold surface (i.e. in the direction of decreasing temperature).

A complex model would take into account the shape of the solid as well as the interaction of two or more solid particles with the gas molecules.

A. Background

It is of interest to consider the chronological development of the explanation for the existence of thermal force and

thermal creep which dates back to 1870 when Tyndall [2] discovered that small dust particles, suspended in a gas, will tend to move from a hot surface to a cold surface under the influence of a temperature gradient. He observed the existence of a dust-free space around a heated wire suspended in a dusty atmosphere. Tyndall assumed that the dust-free region was caused by incineration of dust particles in the vicinity of the heated wire. In 1876, Osborne Reynolds [3] suggested that "the existence of heat reactions", consistent with the kinetic theory of gases, was the cause of the phenomenon and attempted to measure the magnitude of the force by using so called "light mills". Lord Rayleigh [4] pointed out that small temperature differences between the wire and the surrounding air were sufficient to establish the dust-free space.

Maxwell [5] in 1879 expanded his theory on stresses in rarefied[a] gases arising from inequalities of temperature to express the conditions which must be satisfied by a gas in contact with a solid body. The equations developed by Maxwell indicated that the gas may slide over the solid surface in the direction of increasing temperature. The magnitude of these thermal stresses is negligible in a normal gas[b], but in a rarefied gas the magnitude becomes appreciable. In the presence of a temperature gradient along the surface, Maxwell deduced, using the kinetic theory of gases, that there would be "a velocity of sliding of the gas over the surface due to a given tangential stress". A

---

a density of a rarefied gas is approximately one-millionth of a normal gas

b 1 gm-mole of a normal gas occupies 22.4 litres at standard temperature and pressure

statistical analysis which accounted for reflection and adsorption of the molecules indicated that there will be a flow of gas from the colder to the hotter end of the surface if the pressure is uniform. This movement of gas due to a temperature gradient along a solid boundary has been named 'thermal creep'. Maxwell's formula for the thermal creep velocity was of the form:

$$v_{tc} = \frac{3}{4} \frac{\mu}{\rho T} \frac{\partial T}{\partial S} \quad \text{where} \tag{4-1}$$

v_{tc} = thermal creep velocity, cm/sec

μ = gas viscosity, gm/(cm sec)

ρ = gas density, gm/(cm)^3

T = absolute gas temperature, °K

$\frac{\partial T}{\partial S}$ = temperature gradient along surface in the S-direction, °K/cm

In a series of experiments Aitken [6] eliminated gravitational, evaporative, combustive, centrifugal and electrical forces and radiation heat transfer as possible explanations for the removal of particles from the vicinity of a hot surface. Experimental evidence suggested the existence of a force unique to regions of unequal temperature. He called this force 'thermal repulsions' and postulated that higher temperature gradients produced greater force.

A more realistic expression for the thermal stress was developed by Jones [7] whose relationship differed from that of Maxwell since second and higher order terms were considered. To a first approximation, both thermal stress expressions were in agreement.

In 1910, Knudsen [8] developed an acceptable theory for thermal repulsion which was applicable to systems at very low pressures.

Einstein [9] was the first to provide an equation of quantitative validity. He considered the force to be exerted on a peripheral zone of a vane radiometer having a width of the order of the mean free path of the gas. His formula was derived by developing Maxwell's point of view [5] that the thermal force on a single plate was an edge rather than a surface effect. The equation

$$F_t = -\frac{S}{2} p \frac{\lambda^2}{T} \frac{dT}{dx} \qquad \text{where} \qquad (4\text{-}2)$$

F_t = thermal force, dynes

S = length of periphery, cm.

p = absolute pressure, dynes/cm^2

λ = mean free path of gas, cm

T = absolute temperature, °K

$\frac{dT}{dx}$ = temperature gradient in the x-direction, °K/cm

predicts the experimentally observed dependence of thermal force as well as its relation to the temperature gradient.

Epstein [10] pointed out that Einstein's equation was correct only for particles which have a very low thermal conductivity in comparison to the gas because Einstein had assumed the particles did not affect the temperature distribution of the gas. Epstein was the first to consider the temperature of the sphere as an important parameter. In addition, he assumed that the tangential gas velocity at the particle surface was Maxwell's creep velocity.

Cawood [11] suggested that the thermal force on a body is caused by a stronger molecular bombardment from the direction of the heat source. He rejected the earlier postulation that the repulsion stems from radiation pressure because a strong effect could be observed at temperatures too low to produce any appreciable radiation, and also because the force did not seem to depend on the nature of the repulsing surface. By calculating the excess of momentum of molecular impacts in the direction of decreasing temperature, Cawood [11] derived the following equation for the thermal force, F_t, as:

$$F_t = - \frac{D_p^2}{8} \frac{p\lambda}{T} \left(\frac{dT}{dx}\right) \quad \text{where} \qquad (4\text{-}3)$$

F_t = thermal force in the x-direction, dynes

D_p = diameter of spherical particle, cm

T = absolute gas temperature, °K

λ = mean free path of gas, cm

p = pressure, dynes/cm^2

$\frac{dT}{dx}$ = temperature gradient in the x-direction, °K/cm

Because of the dual nature of the force mechanisms, and of the variety of initial assumptions that may be made regarding the temperature gradients of the particle and the gas, a large number of thermal force equations (9-21) have appeared. The available thermal force equations are summarized in Table 4.1.

B. Theoretical Analysis

In order to appreciate the thermal force phenomenon, consider a small spherical particle to be suspended between two parallel plates maintained at different temperatures as shown in Figure 4.1. In order to eliminate convection currents, the plates are positioned horizontally with the upper plate kept at the higher temperature. There are three important length parameters:

i. the radius of the particle, R_p

ii. the plate spacing, L and

iii. the mean free path of the gas, λ

from which two relevant Knudsen numbers can be obtained:

NO.	NAME	YEAR	REGIME	THERMOPHORETIC FORCE EQUATIONS
1	Einstein, A. (9)	1926	—	$F_t = -\frac{2}{3} p \frac{d}{dT} \delta$
2	Epstein, P. (10)	1929	Slip-Flow $\alpha_{Kn_L} = 0$	$F_t = -9\pi\eta_g \left[\frac{\eta_g}{\rho_g T_g + \rho_p T_p}\right] \frac{d}{dT} \delta$
3	Cawood, W. (11)	1936	Transition $\alpha_{Kn_L} = 0$	$F_t = -\frac{\eta_g^2}{\rho_g} \frac{d}{dT} \frac{dT}{dr}$
4	Waldmann, L. (12)	1959	Free Molecular $\alpha_{Kn_L} = 0$	$F_t = -\frac{8}{3\pi} \eta_g^2 \sqrt{\frac{2\pi}{RT}} (\delta_t)_{tr}$
5	Brock, J.R. (13)	1962	Slip-Flow $\alpha_{Kn_L} = 0$	$F_t = -9 \cdot \eta_g \left(\frac{\eta}{\rho}\right)^2 \left[\frac{1}{1 + 3 C_m \frac{\lambda}{r_p}}\right] \left[\frac{\frac{\lambda}{r_p} + c_1 \frac{\lambda}{r_p}}{1 + 2\frac{\lambda}{r_p} + 2 c_1 \frac{\lambda}{r_p}}\right] \delta$
6	Derjaguin, B. V. and Bakanov, S. P. (14)	1962	Slip-Flow $\alpha_{Kn_L} = 0$	$F_t = -6\pi \left(\frac{\eta_g \rho_g + \rho_p}{2\rho_g + \rho_p}\right) \frac{d}{dT} \delta T$
7	Derjaguin, B. V. and Yalanay, Yu. L. (15 and 16)	1964	Slip-Flow $\alpha_{Kn_L} = 0$	$F_t = -6\pi \left[\frac{\eta_g \rho_g + \frac{\lambda}{r_p} + c_1 \frac{\lambda}{r_p} \rho_g}{2\rho_g + \rho_p + 2 c_1 \frac{\lambda}{r_p} \rho_g}\right] \frac{d}{dT} \delta T$
8	Brock, J. R. (17)	1967	Transition	$F_t = -\frac{8}{3\pi} \eta_g^2 \sqrt{\frac{2\pi}{RT}} \rho_g \left\{1 + [0.66 + 0.09\alpha + 0.28\alpha (1 - \frac{\alpha}{2+\alpha})] \frac{\lambda}{r_p}\right\} \delta T$
9	Dwyer, H. A. (18)	1967	$0 < \alpha_{Kn_g} < \infty$ $\alpha_{Kn_L} = 0$	$F_t = \frac{-6\pi\eta_g^2 \left(\frac{r_p}{\lambda}\right)^{1/2} \rho_g \left(\frac{\lambda}{r_p}\right) \left\{\alpha_1 \cdot \frac{\lambda}{r_p} + \frac{1}{2}\alpha_3 \left(\frac{\lambda}{r_p}\right)^2 \frac{1}{\alpha + \frac{1}{2}\alpha_2 \left(\frac{\lambda}{r_p}\right)} \left(1 + 2\frac{\lambda}{r_p}\right) + \left(\frac{\lambda}{r_p}\right)\left(\frac{\lambda}{r_p}\right) + \frac{\alpha_1 \alpha_2 \left(\frac{\lambda}{r_p}\right)}{\alpha + \frac{1}{2}\alpha_2 \left(\frac{\lambda}{r_p}\right)}\right\} \delta T}{\frac{1}{2\pi}\left(\frac{\lambda}{r_p}\right)\left[\alpha + 2\alpha \left(\frac{\lambda}{r_p}\right)^2 \left\{\frac{1 + \alpha_2 \left(\frac{\lambda}{r_p}\right)}{\alpha + \frac{1}{2}\alpha_2 \left(\frac{\lambda}{r_p}\right)}\right\}\right](1 + 2\frac{\lambda}{r_p}) + \frac{1}{2\pi}\left[\alpha + 2\alpha \left(\frac{\lambda}{r_p}\right)^2 \left\{\frac{1 + \alpha_2 \left(\frac{\lambda}{r_p}\right)}{\alpha + \frac{1}{2}\alpha_2 \left(\frac{\lambda}{r_p}\right)}\right\}\right] \alpha_1 + \frac{\alpha}{2} \frac{\partial \alpha}{\partial \left(\frac{\lambda}{r_p}\right)}}$
10	Sprenger, H. S. (19)	1971	$0 < \alpha_{Kn_g} < \infty$ $\alpha_{Kn_L} = 0$	$F_t = -\frac{8}{3\pi} \eta_g^2 \sqrt{\frac{2\pi}{RT}} \rho_g \left[1 + \left(\frac{\alpha}{2} \frac{\lambda}{r_p}\right) \frac{1 + \frac{2\lambda}{r_p} + \frac{1}{r_p}[2 c_1 + 2 c_m (1 + \frac{2\lambda}{r_p} + 2 c_1 \frac{\lambda}{r_p})]}{\frac{\lambda}{r_p} + \frac{1}{r_p} c_1 + 3.2 c_m \frac{1}{r_p}\left[\left(\frac{\lambda}{r_p}\right) + c_1 \frac{\lambda}{r_p} \cdot \right]}\right]^{-1} \delta T$
11	Phillips, W. F. (20, 21)	1972	$\alpha_{Kn_g} = \infty$ $0 < \alpha_{Kn_L} < \infty$	$F_t = -\frac{\eta_g^2}{\rho_g} \sqrt{\frac{2\pi}{RT}} \rho_g \left[\frac{\frac{2}{3}\alpha_{Kn_L} + \frac{111}{1115}}{\alpha_{Kn_L}^2 + (\alpha_{Kn_L} + \frac{2}{3}\alpha_{Kn_L}) \left(\frac{\alpha_1 + \alpha_2 - \alpha_1 \alpha_2}{\alpha_1 \alpha_2}\right) + \frac{16}{115}\alpha_{Kn_L} + \frac{16}{115}}\right] \frac{(T_2 - T_1)}{T_1} \delta$

TABLE A.1: THERMAL FORCE EQUATIONS

$$N_{Kn_{R_p}} = \frac{\lambda}{R_p} \quad \text{and}$$

$$N_{Kn_L} = \frac{\lambda}{L}$$

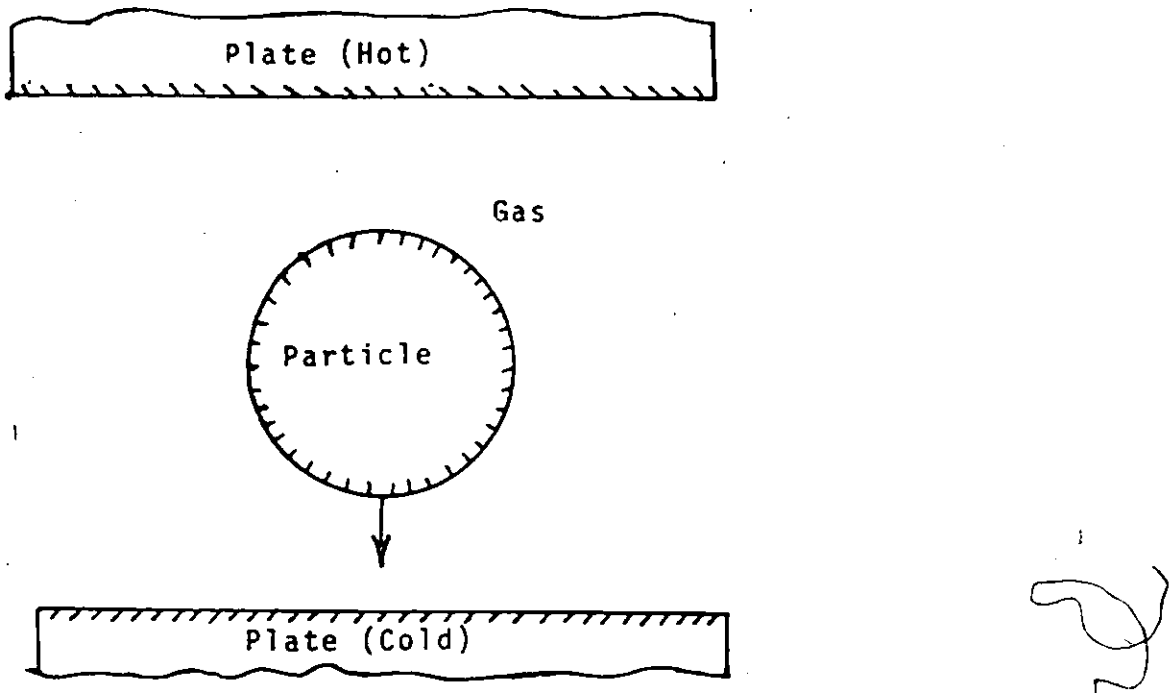

FIGURE 4-1: Spherical Particle in a Gas with a Temperature Gradient

Most of the experimental investigations (1, 22, 23 and 24) of the thermal force acting on aerosol particles have been carried out for so-called "infinite gases", in which the plate spacing is much larger than the mean free path length of the gas and so $N_{Kn_L} \rightarrow 0$. Thus for an infinite gas, the thermal

force can only depend on the Knudsen number, $N_{Kn_{R_p}}$. To date there is no analysis for an infinite gas which will predict the thermal force over the entire range of Knudsen number $0 < N_{Kn_{R_p}} < \infty$. Three arbitrary classifications are defined to facilitate analysis of the thermal force for an infinite gas [34]

i. the slip-flow regime $0 < N_{Kn_{R_p}} < .25$

ii. the free-molecular regime, $10 < N_{Kn_{R_p}} < \infty$

iii. the transition regime $.25 < N_{Kn_{R_p}} < 10$

In the slip-flow regime, the mean free path of the gas, λ, is small compared to the size of the aerosol particle [$\lambda << R_p$ and $N_{Kn_{R_p}} \to 0$]. The "slip" term can be related to the boundary condition employed in the theoretical analysis in which a slippage of gas is assumed to occur over the particle surface. An acceptable theory, developed by Epstein [10], was later modified by Brock [13].

In the free-molecular regime, the mean free path of the gas, λ, is much greater than the size of the aerosol particle ($\lambda >> R_p$ and $N_{Kn_{R_p}} \to \infty$). In this limiting case, the gas molecule velocity distribution function is not affected by the presence of the particle and the particle is considered to be a large molecule. For this case, designated as the free-molecular regime, the most acceptable theory is that of Waldmann [12].

For the third regime, where the mean free path of the gas, λ, is of the same order of magnitude as the size of the particle, Brock's [16] 'transition' regime theory is considered most acceptable.

No quantitative analysis has been reported in the literature for the thermal force over the entire range of $0 < N_{Kn_{R_p}} < \infty$ and $0 < N_{Kn_L} < \infty$.

1. Slip-Flow Regime

In the slip-flow regime, a molecule sees a particle as a solid surface. If the temperature is higher to the top as shown in Figure 4.2, any gas molecules impinging on an element of surface from the top have, on the average, a greater momentum than those hitting from the bottom. As a result, the surface receives an impulse directed to the bottom, (i.e. in the direction of decreasing temperature). An equal but opposite impulse is imparted to the gas, making it slip along the surface to the top (i.e. in the direction of increasing temperature).

Epstein [10] developed a comprehensive theory for the thermophoretic force in the slip-flow regime. He considered the following factors in his derivation:

i. the thermal conductivity of the gas, k_g

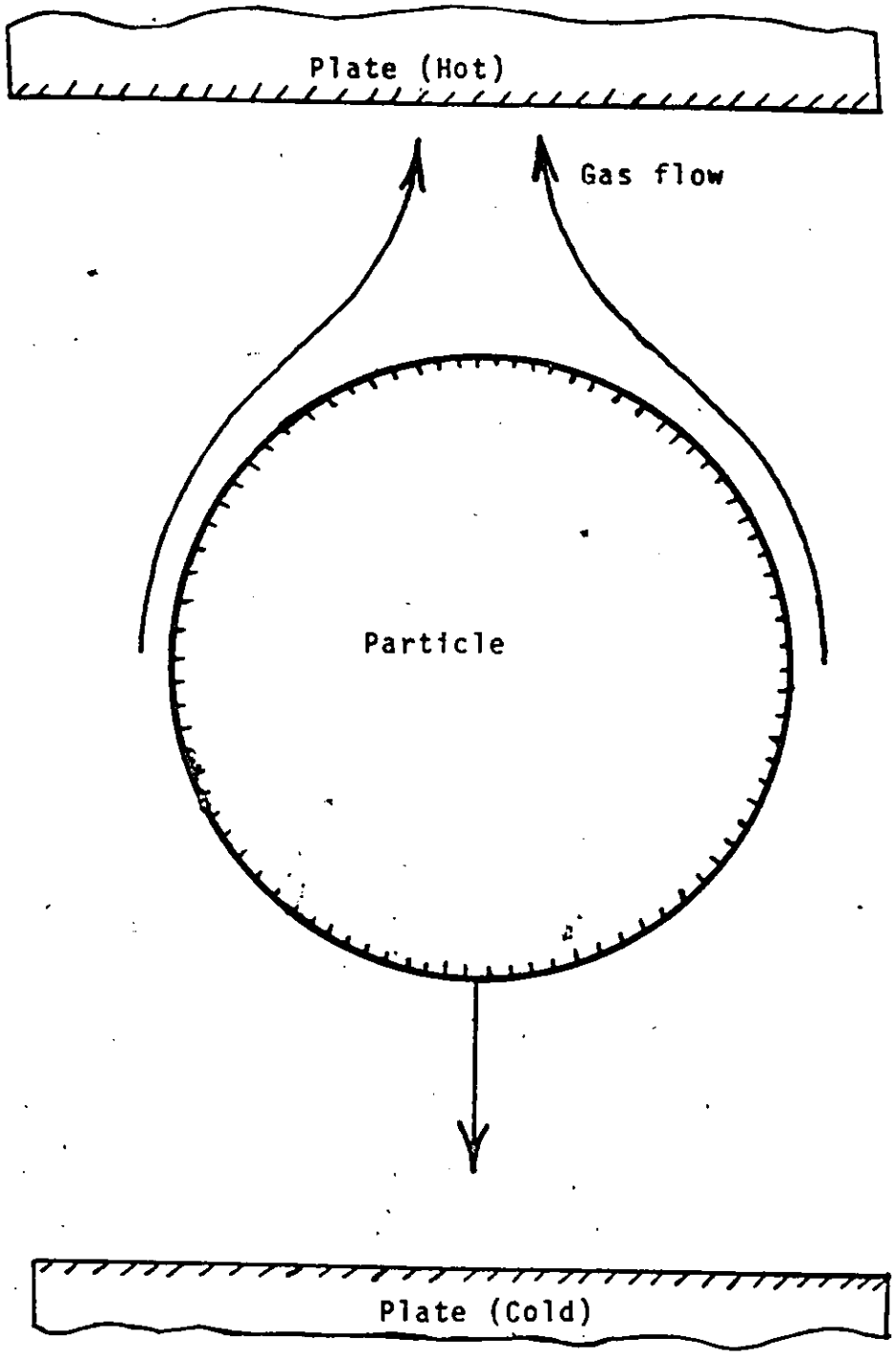

FIGURE 4.2: Flow of Gas and Spherical Particle Under a Temperature Gradient

ii. the thermal conductivity of the aerosol particle, k_p

iii. the ratio of heat transported through the particle (internal conduction) to the heat input rate from molecular impacts (external conduction), and

iv. the kinetic and hydrodynamic aspects of the problem

a. Temperature Distribution

Since a detailed derivation of Epstein's thermal force model is given in Appendix I, only the essential steps are outlined here. Beginning with the steady-state form of the heat conduction equation

$$\nabla^2 T = 0$$

Epstein expanded Laplace's equation for the spherical co-ordinate system (Figure 4-3) in order to study the heat transfer through both the spherical particle and the surrounding gas:

$$\frac{\partial}{\partial r}\left(r^2 \frac{\partial T}{\partial r}\right) + \frac{1}{\sin\theta} \frac{\partial}{\partial \theta}\left(\sin\theta \frac{\partial T}{\partial \theta}\right) + \frac{1}{\sin^2\theta} \frac{\partial^2 T}{\partial \phi^2} = 0 \qquad (4.5)$$

By making use of axial symmetry and a separation of variables type solution, the temperature distribution was obtained as:

$$T = \begin{cases} r^n & P_n(\cos\theta) \\ r^{-(n+1)} & Q_n(\cos\theta) \end{cases} \quad \text{where} \qquad (4\text{-}6)$$

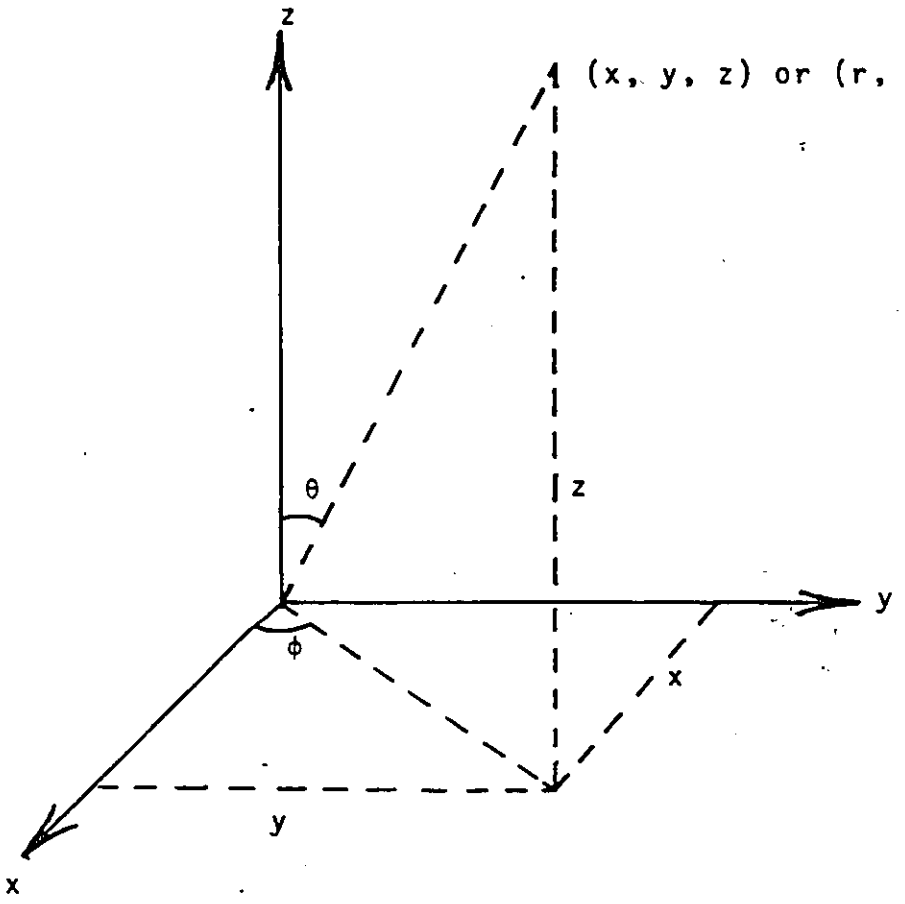

FIGURE 4.3: Spherical Co-ordinates. The ranges of variables are $0 \leq r \leq \infty$, $0 \leq \theta \leq \pi$ and $0 \leq \phi \leq 2\pi$

$P_n(\cos\theta)$ is the n'th Legendre polynominal in $\cos\theta$ and $Q_n(\cos\theta)$ is the reciprocal of the (n + 1)'th Lengendre polynomial in $\cos\theta$.

Further application of the boundary condition that the temperature must be finite at all points inside the sphere, including $r \to 0$ and $\cos\theta = \pm 1$, allowed simplification to:

$$T_i(r,\theta) = \sum_{n=0}^{\infty} (A_n r^n)\, P_n\,(\cos\theta) \qquad (4\text{-}7)$$

On the basis of Epstein's assumption that on the surface of the sphere where $r = R_p$, the inside, T_i, and outside T_o, temperatures as well as the heat fluxes must be the same at thermal equilibrium it follows that

$$-k_p\left(\frac{\partial T_i}{\partial r}\right)_{r = R_p} = -k_g\left(\frac{\partial T_o}{\partial r}\right)_{r = R_p} \qquad \text{where} \qquad (4\text{-}8)$$

k_p = thermal conductivity of particle, cal/(sec cm °K)

k_g = thermal conductivity of gas, cal/(sec cm °K)

The final form of the temperature distribution inside the spherical particle becomes:

$$T_i(r,\theta) = G\left(\frac{3\,k_g}{k_p + 2k_g}\right) r\cos\theta \qquad (4\text{-}9)$$

where

$r \leq R_p$

$0 \leq \theta \leq \pi$

G = uniform temperature gradient away from the particle, °K/cm

The temperature distribution in the gas surrounding the solid spherical particle was obtained in a similar manner as

$$T_o\ (r,\theta) = G\ [r + \frac{(k_g - k_p)}{(k_p + 2\ k_g)}\ \frac{R_p^3}{r^2}]\ \cos\theta \qquad (4\text{-}10)$$

where

$$r \geq R_p$$

$$0 \leq \theta \leq \pi$$

Using this temperature distribution over the surface, which is a function of θ only, the temperature gradient is obtained by differentiating partially with respect to, S, the distance along the surface in the direction of increasing temperature:

$$\frac{\partial T}{\partial S} = (\frac{1}{r}\ \frac{\partial T}{\partial \theta})_{r\ =\ R_p}$$

$$= \frac{1}{R_p}\ (\frac{\partial T_o}{\partial \theta})_{r\ =\ R_p} = \frac{1}{R_p}\ (\frac{\partial T_i}{\partial \theta})_{r\ =\ R_p} \qquad (4\text{-}11)$$

which reduces to

$$\frac{\partial T}{\partial S} = -\ (\frac{3\ k_g}{2\ k_g + k_p})G\ \sin\theta \qquad (4\text{-}12)$$

b. Velocity Distribution

The velocity components in rectangular co-ordinates for the steady state creeping flow of a constant density gas past a fixed spherical particle, as shown in Figure 4.3, are given by Lamb [25] as

$$v_x = (B - \frac{Ar^2}{6\mu}) \frac{\partial}{\partial x} (\frac{z}{r^3}) \qquad (4\text{-}13)$$

$$v_y = (B - \frac{Ar^2}{6\mu}) \frac{\partial}{\partial y} (\frac{z}{r^3}) \qquad (4\text{-}14)$$

$$v_z = v + (B - \frac{Ar^2}{6\mu}) \frac{\partial}{\partial z} (\frac{z}{r^3}) + \frac{2A}{3\mu r} \qquad (4\text{-}15)$$

where A and B are constants to be evaluated using the appropriate boundary conditions. The appropriate boundary conditions in rectangular co-ordinates are

i. $v_x = 0$, $v_y = 0$, $v_z = 0$ for $r = R_p$, and

ii. $v_x = 0$, $v_y = 0$, $v_z = v$ for $r = \infty$

However, a solution is desired in terms of the spherical co-ordinate variables r, θ and ϕ.

The transformation into the variables r, θ and ϕ from x, y and z makes use of:

$$x = r \sin\theta \cos\phi \tag{4-16}$$

$$y = r \sin\theta \sin\phi \tag{4-17}$$

$$z = r \cos\theta \tag{4-18}$$

$$r = + \sqrt{x^2 + y^2 + z^2} \tag{4-19}$$

$$\theta = \arctan\left[\frac{\sqrt{x^2 + y^2}}{z}\right] \tag{4-20}$$

$$\phi = \arctan y/x \tag{4-21}$$

In Appendix I a detailed transformation of the velocity distribution equations is given. First $\frac{\partial}{\partial x}\left(\frac{z}{r^3}\right)$, $\frac{\partial}{\partial y}\left(\frac{z}{r^3}\right)$ and $\frac{\partial}{\partial z}\left(\frac{z}{r^3}\right)$ are evaluated and substituted into equations (4-13), (4-14) and (4-15).

Simplification of the standard transformations

$$v_r = (\sin\theta \cos\phi)\, v_x + (\sin\theta \sin\phi)\, v_y + (\cos\theta)\, v_z \tag{4-22}$$

$$v_\theta = (\cos\theta \cos\phi)\, v_x + (\cos\theta \sin\phi)\, v_y + (-\sin\theta)\, v_z \tag{4-23}$$

$$v_\phi = (-\sin\phi)\, v_x + (\cos\phi)\, v_y + (0)\, v_z \tag{4-24}$$

yields

$$v_r = \left(v - \frac{2B}{r^3} + \frac{A}{\mu r}\right) \cos\theta \tag{4-25}$$

$$v_\theta = -\left(v + \frac{B}{r^3} + \frac{A}{2\mu r}\right) \sin\theta \tag{4-26}$$

$$v_\phi = 0 \tag{4-27}$$

The boundary conditions which are applicable to the slip-flow regime are:

i. there is no gas flow except near the surface of the sphere. Hence, $v = 0$

ii. the normal velocity, v_r, must be zero at the surface of the particle where $r = R_p$, and

iii. the tangential velocity, v_θ, at the surface of the particle where $r = R_p$, is assumed to be Maxwell's slip velocity given by equation (4-1).

These boundary conditions allow A and B to be determined as

$$A = \frac{9\ R_p}{4} \left(\frac{\mu}{\rho T}\right)^2 \left(\frac{k_g}{2\ k_g + k_p}\right) G \tag{4-28}$$

$$B = \frac{AR_p^{\ 2}}{2\mu} \tag{4-29}$$

Finally, the velocity over the surface of the sphere, v_θ, is obtained in the form

$$v_\theta = -\ \frac{9}{4} \left(\frac{\mu}{\rho T}\right) \left(\frac{k_g}{2\ k_g + k_p}\right) G \sin\theta \tag{4-30}$$

by substitution of equations(4-28) and (4-29) into equation (4-26).

c. The Thermal Force

The force acting on the sphere in the direction of flow as shown in Figure 4.4 is given by the integral over the surface in the z-direction.

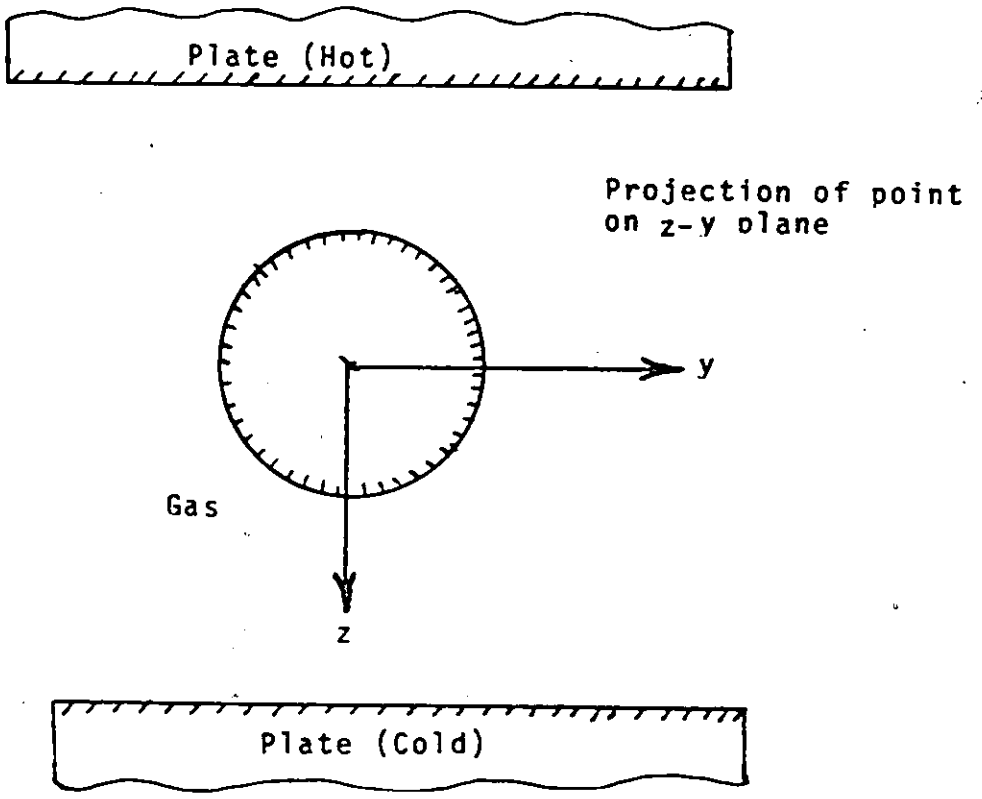

FIGURE 4.4: Flow of a Spherical Particle in a Gas Under a Temperature Gradient

At each point on the particle surface, there is a fluid stress acting perpendicularly to the surface. The surface area, on which the fluid stress acts, is $R^2 \sin\theta \, d\theta \, d\phi$ [26].

Therefore:

$$F_t = \int_0^{2\pi} \int_0^{\pi} p_{r,z=R_p} (r, \theta) R^2 \sin\theta \, d\theta \, d\phi \qquad (4\text{-}31)$$

and

$$F_t = 2\pi R_p^2 \int_0^{\pi} p_{r,z=R_p} (r,\theta) \sin\theta \, d\theta \qquad (4\text{-}32)$$

The total fluid stress acting on the surface of the sphere in the z-direction is given by Lamb [25] as

$$p_{r,z} = \frac{-x}{r} p_o + (Ar - \frac{6\mu B}{r}) \frac{\partial}{\partial z} (\frac{z}{r^3}) - \frac{A}{r^2} \qquad (4\text{-}33)$$

Substitution of equation (4-33) into equation (4-32) and simplification leads to Epstein's thermal force equation:

$$F_t = - 9\pi R_p (\frac{k_g}{2k_g + k_p})(\frac{\mu^2}{\rho T}) G \text{ where} \qquad (4\text{-}34)$$

F_t = the thermal force, dynes

R_p = radius of the particle, cm

k_g = thermal conductivity of gas, cal/(sec cm°K)

k_p = thermal conductivity of spherical particle, cal/(sec cm°K)

μ = gas viscosity, gm/(cm sec)

T = gas temperature, °K

G = uniform temperature gradient at large distances from particle, °K/cm

Brock [13] extended Epstein's analysis of the slip-flow regime by taking into consideration temperature jump and velocity slip [27 and 28].

Brock made use of the Poisson concept that at a wall bounding an unequally heated gas there might be a temperature discontinuity as shown in Figure 4-5:

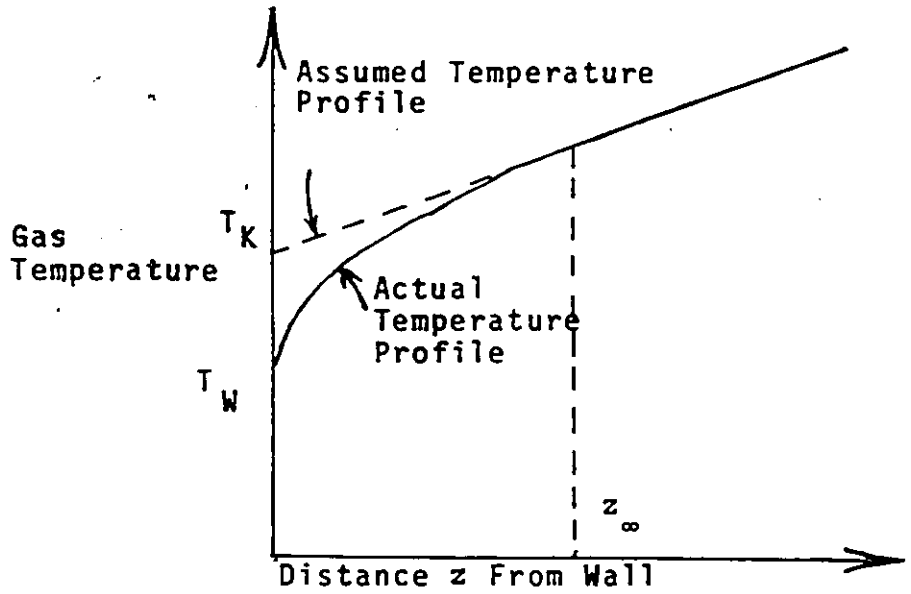

FIGURE 4-5: The Variation of Gas Temperature T With Distance, z, From the Wall [28]

Poisson's equation for the temperature discontinuity at a wall or particle surface is

$$T_K - T_W = g\left(\frac{\partial T}{\partial n}\right) \qquad \text{where} \qquad (4\text{-}35)$$

T_W = wall or particle surface temperature , °K

T_K = gas temperature at wall or particle surface obtained by extrapolating uniform gas temperature profile back to wall or particle surface , °K

$\frac{\partial T}{\partial n}$ = G = uniform gas temperature gradient away from wall or particle surface, °K/cm

z_∞ = distance from wall or particle surface beyond which gas temperature gradient is uniform, cm

g = temperature jump distance, cm

Experimental evidence obtained by Smoluchowski [29] confirmed the kinetic theory prediction that the temperature jump distance, g, was inversely proportional to the pressure and thus directly proportional to the mean free path length of the gas. Knudsen introduced a slightly different constant of proportionality called the "thermal accommodation coefficient". The thermal accommodation coefficient can be defined as the fractional extent to which those molecules that fall on the surface and are reflected or re-emitted from it have their mean energy adjusted or "accommodated" toward what it would be if the returning molecules were issuing as a stream out of a mass of gas at the temperature of the wall or particle surface [27].

The gas slip velocity can be defined in an analogous manner as illustrated by Figure 4.6 where the gas slip velocity parallel to the surface is depicted by v_K (the wall or particle surface velocity being zero).

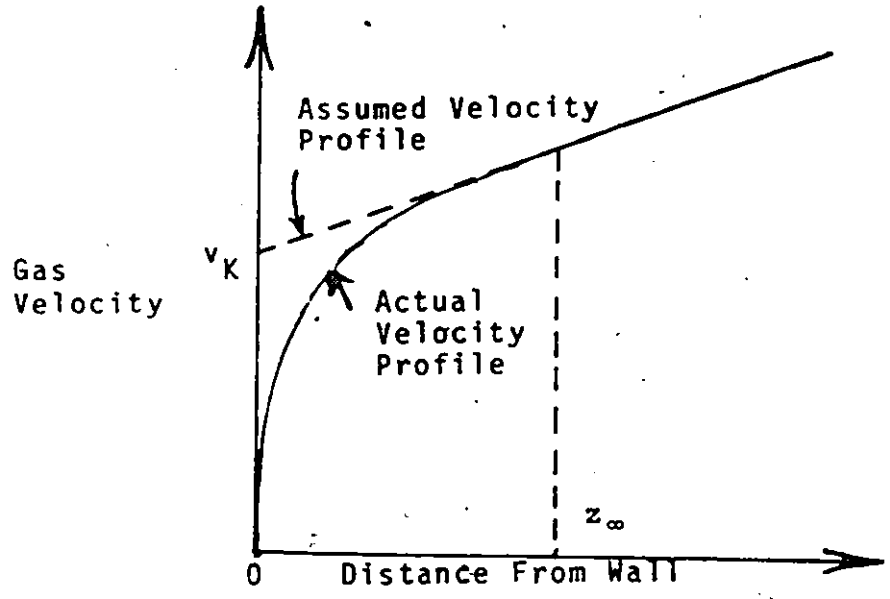

FIGURE 4.6: The Variation of Gas Velocity, v, with Distance, z, from the Wall [28]

The velocity of slip, v_K, relative to the wall or particle surface is written as:

$$v_K = \zeta\left(\frac{dv}{dz}\right) \qquad \text{where} \qquad (4\text{-}36)$$

ζ = is a constant commonly called the coefficient of slip,

$\left(\frac{dv}{dz}\right)$= gas velocity gradient, taken positive in the direction away from the wall or particle surface, sec^{-1}

z_∞ = distance from wall or particle surface beyond which the gas velocity gradient is uniform, cm

The constant ζ represents a length which Kundt and Warburg [30] found to be inversely proportional to the pressure. The constant of proportionality which is called the 'momentum accommodation coefficient', is dependent upon the nature of the gas-surface interaction.

The thermal accommodation coefficient, a_t, and momentum accommodation coefficient, a_m, are defined by [13]:

$$a_t = \frac{E_i - E_r}{E_i - E_w} \tag{4-37}$$

$$a_m = \frac{G_i - G_r}{G_i} \tag{4-38}$$

where

E_i = average energy flux for incoming molecules at a point on the wall or particle surface, $\frac{cal}{cm^2 hr}$

E_r = average energy flux for departing molecules at the point on the wall or particle surface, $\frac{cal}{cm^2 hr}$

E_w = energy flux which would prevail if the molecules leaving were in equilibrium with the wall or particle surface at that point, $\frac{cal}{cm^2 hr}$

G_i = average tangential components of the momentum of molecules striking the wall or particle surface, $\frac{gm\ cm}{sec}$

G_r = average tangential components of the momentum of molecules leaving the wall or particle surface, $\frac{gm\ cm}{sec}$

Brock [13] introduced two semi-empirical constants c_t, and c_m which were associated with the temperature jump and the velocity slip respectively. Values of the constants based upon simple semi-macroscopic derivations were:

$$c_t = \frac{15}{8}\left(\frac{2 - a_t}{a_t}\right) \tag{4-39}$$

$$c_m = \frac{\left(2 - a_m\right)}{a_m} \tag{4-40}$$

The following boundary conditions were applied at the gas-particle interface by Brock [13].

$$\text{i.}\quad v_r = 0 \text{ at } r = R_p \tag{4-41}$$

$$\text{ii.}\quad v_\theta = c_m \lambda \left(r \frac{\partial}{\partial r}\left(\frac{v_\theta}{r}\right) + \frac{1}{r}\frac{\partial v_r}{\partial \theta}\right)_{r=R_p} + \frac{3}{4}\frac{\mu}{\rho T}\frac{1}{R_p}\left(\frac{\partial T_o}{\partial \theta}\right)_{r=R_p} \tag{4-42}$$

$$\text{iii.}\quad T_o - T_i = c_t \lambda \left(\frac{\partial T_o}{\partial r}\right), \qquad r = R_p \tag{4-43}$$

$$\text{iv.}\quad k_p \left(\frac{\partial T_i}{\partial r}\right) = k_g \left(\frac{\partial T_o}{\partial r}\right), \qquad r = R_p \tag{4-44}$$

where

c_m = constant associated with the velocity slip

c_t = constant associated with the temperature jump

μ = gas viscosity, gm(cm sec)

ρ = gas density, gm/cm^3

λ = mean free path of gas, cm

R_p = radius of spherical particle, cm

T = gas temperature, °K

T_i = temperature inside the spherical particle, °K

T_o = gas temperature on the surface of spherical particle, °K

k_g = thermal conductivity of gas, cal/(cm sec °K)

k_p = thermal conductivity of particle, cal/(cm sec°K)

v_r = radial velocity of gas, cm/sec

v_θ = tangential velocity of gas, cm/sec

Epstein [10], in his analysis, did not consider the first term of equation (4-42) containing c_m the constant associated with the velocity slip and equation (4-43) containing c_t the constant associated with the temperature jump. Brock [13] obtained, with these boundary conditions, the thermal force equation:

$$F_t = -9\pi R_p \left(\frac{\mu^2}{\rho T}\right) \left[\frac{1}{1 + 3\, c_m \frac{\lambda}{R_p}}\right] \left[\frac{\frac{k_g}{k_p} + c_t \frac{\lambda}{R_p}}{1 + 2\frac{k_g}{k_p} + 2c_t \frac{\lambda}{R_p}}\right] G \quad \text{where} \quad (4\text{-}45)$$

F_t = the thermal force, dynes

c_m = constant associated with velocity slip whose value depends on the nature of gas-particle interaction

c_t = constant associated with temperature jump whose value depends on the nature of gas-particle interaction

μ = gas viscosity gm/(cm sec)

T = gas temperature, °K

k_g = thermal conductivity of gas, cal/(sec cm°K)

k_p = thermal conductivity of particle, cal/(sec cm °K)

R_p = radius of spherical particles, cm

G = uniform temperature gradient, at large distance from the particle, °K/cm

λ = mean free path of gas, cm

The effect of changes in the constants c_t and c_m can be appreciated from equation (4-45). It should be noted that when $c_t = c_m = 0$, the expression reduces to Epstein's equation for the thermal force. Values of $a_t = a_m = 1$ correspond to the situation where incident molecules achieve thermodynamic equilibrium with the surface before leaving. On the other hand $a_t = a_m = 0$ corresponds to complete specular reflection of incident molecules. More rigorous derivations [31] produce, usually, relatively small changes in the form of the expressions for c_t and c_m developed by the simpler semi-macroscopic arguments. According to the

rigorous treatments, for $a_t = a_m = 1.0$, values of c_t range from 1.875 to 2.48 while values of c_m range from 1.00 to 1.27 in contrast to the constant values predicted by equations (4-39) and (4-40).

2. Free-Molecular Regime

In the free-molecular regime, where the mean free path of gas, λ, is much greater than the size of the aerosol particle ($\lambda >> R_p$ and $N_{Kn_{R_p}} \to \infty$), the thermal force can be considered to be due to the net momentum imparted to the particle. If there is a temperature gradient within the surrounding gas, the gas molecules striking the particle from the hot side will have a greater velocity than the gas molecules hitting from the cold side. The resulting inequality in momentum balance over the two hemispheres of the particle defines the force.

Waldmann [12] based his analysis of the thermal force in the free-molecular regime on the kinetic theory of gases assuming that:

i. the distribution function of molecules striking the particle is not influenced by the presence of the particle

ii. a fraction of the departing molecules undergoes specular reflection (i.e. the particle acts as an optical surface and thermodynamic equilibrium with the

surface is not achieved while the remaining fraction undergoes diffuse reflection (i.e. incident molecules achieve complete thermodynamic equilibrium with the surface before leaving)

iii. the particle surface temperature is equal to the local gas temperature

The thermal force, F_t, on a single particle due to momentum transfer in an effectively infinite gas can be represented by [7].

$$F_t = -\int d\vec{s} \cdot \sum_{\pm} \int_{\pm} d\left(\vec{v}\, m\, \vec{v}\, \vec{v}\, f^{\pm}\right) \quad \text{where} \qquad (4\text{-}46)$$

+ and - indicate regions of molecular velocity space appropriate for molecules leaving and hitting the particle surface respectively

f^+ = velocity distribution of leaving gas molecules

f^- = velocity distribution of gas molecules striking the surface of the particle assuming absence of the particle

$d\vec{s}$ = unit normal of a surface element

m = molecular mass of the gas, gm

$\vec{v}$ = molecular velocity of the gas, cm/sec

To calculate the thermal force on a surface element, it is necessary to know the undisturbed distribution function of the gas and the law of reflection at the surface. Waldmann

assumed the velocity distribution of approaching molecules to be that of the undisturbed gas. The distribution function of the molecules reflected from the surface of the particle, f^+, is

$$f^+ = (1 - \alpha)\, f' + \alpha F^{(+)} \qquad \text{where} \qquad (4\text{-}47)$$

f' = the distribution function resulting from specular reflection on the surface element of the distribution function, f^-

$F^{(+)}$ = the Maxwellian distribution arising from completely diffuse reflection

α = accommodation coefficient of particle

In the free-molecular regime, Waldmann [13] assumed the coefficient of diffuse reflection to be equal to unity. The thermal force could be evaluated by integrating the net momentum transfer over the surface of the particle based on the distribution function. Using this approach, Waldmann obtained for polyatomic molecules, a thermal force

$$F_t = \frac{-8}{15} R_p^{\,2} \sqrt{\frac{2\pi m}{kT}}\; (k_g)_{tr}\; \nabla T \quad \text{where} \qquad (4\text{-}48)$$

F_t = the thermal force, dynes

k = Boltzmann constant, dynes cm/°K

R_p = radius of spherical particle, cm

m = molecular mass of gas, gm

T = gas temperature, °K

$(k_g)_{tr}$ = translational component of the thermal conductivity of gas, cal/(sec cm °K)

∇T = temperature gradient, °K/cm.

Introducing a mean molecular velocity [21] as:

$$\bar{v} = 4 \sqrt{\frac{kT}{2\pi m}} \tag{4-49}$$

yields

$$F_t = \frac{-32}{15} \frac{R_p^2}{\bar{v}} (k_g)_{tr} \nabla T \tag{4-50}$$

Equation (4-48) defines a force independent of the gas pressure and the nature of the particle.

In order to make use of equation (4-48), the translational component of the thermal conductivity of the gas must be known exactly. It is difficult to determine the translational constituent except for a pure monatomic gas.

The energy of molecules composed of more than one atom is made up of several forms, including rotational, vibrational and electronic contributions in addition to the translational component. Nevertheless, k_g is primarily dependent on the translational energy contribution.

3. Transition Regime

Brock [17] developed a theory for the thermal force in the region by considering the net momentum transferred by gas

molecules striking and reflecting from a particle surface.

In his development, Brock assumed that

i. the gas is in mechanical equilibrium so that at large distances from the particle there is no pressure gradient

ii. the thermal conductivity of the particle, k_p, is greater than or of the same order of magnitude as the thermal conductivity of the gas, k_g, and

iii. a fraction of gas molecules, α, equal to the accommodation coefficient, undergoes diffuse reflection and the remaining fraction, $(1 - \alpha)$ is specularly reflected.

For the transition regime, it is no longer valid to assume that the particle does not affect the velocity distribution of approaching molecules.

Brock obtained the velocity distribution function of approaching molecules, f_o^-, by solution of the BGK (Bhatnagar, Gross and Krook) model [32].

Using assumption (iii) given previously, the velocity distribution function of molecules leaving the surface of the particle is given by equation (4-47).

$$f^+ = \alpha F^{(+)} + (1 - \alpha)\, f' \quad \text{where} \tag{4-47}$$

f^+ = velocity distribution function of molecules leaving the surface of the particle

$F^{(+)}$ = the Maxwellian distribution of molecules due to completely diffuse reflection

f' = the distribution function arising from specular reflection on the surface element of the distribution function f_0^- obtained from the solution of the BGK model

α = the accommodation coefficient of particle

Table 4.2 gives typical experimentally determined values of α.

Data Source	α
1. Jacobsen and Brock [33] spherical sodium chloride aerosols in argon	0.98
2. Schmitt [24] M 300 silicon oil aerosols in argon	0.80
3. Schmitt [24] PH 300 silicon oil aerosols in argon	0.82

TABLE 4.2: Experimental Values of Accommodation Coefficient [17]

Using the BGK model for the velocity distribution of approaching molecules and equation (4-47) for departing molecules, Brock determined the thermal force due to momentum transfer obtaining the following result which is first order in $1/N_{Kn_{R_p}}$:

$$F_t = F_t^* \left\{ 1 - [0.06 + 0.09\alpha + 0.28\alpha(1-\alpha \frac{k_g}{2k_p})] \frac{R_p}{\lambda} \right\} \qquad (4\text{-}51)$$

where

F_t = thermal force in the transition regime, dynes

F_t^* = thermal force in the free-molecular regime, dynes

α = accommodation coefficient

k_p = thermal conductivity of particle, cal/(cm sec °K)

k_g = thermal conductivity of gas cal/(cm sec °K)

R_p = radius of particle, cm

λ = mean free path of gas, cm

The thermal force in the free-molecular regime for monatomic molecules was given earlier by equation (4-48)

$$F_t^* = \frac{-8}{15} R_p^2 \sqrt{\frac{2\pi m}{kT}} (k_g)_{tr} \nabla T \qquad (4\text{-}48)$$

The thermal force equation (4-51) for monatomic molecules is an approximation since the Boltzmann equation has not been solved to obtain the velocity distribution function of incoming molecules, f^-. The BGK model was used instead for convenience.

REFERENCES

1. Rosenblatt, P., and Lamer, V. K., Motion of a Particle in a Temperature Gradient; Thermal Repulsion as a Radiometer Phenomenon , Phy. Rev. 70, 385 (1946).

2. Tyndall, J., On Dust and Disease , Proc. Roy. Inst. 6, 3 (1970).

3. Reynolds, Osborne, On Forces caused by Communication of Heat Between a Surface and a Gas , Phil. Trans., 166, 725 (1876).

4. Rayleigh, Lord, On the Dark Plane which is Formed over a Heated Wire in Dusty Air , Proc. Roy. Soc., 34, 414 (1882).

5. Maxwell, J.C., On Stresses in Rarefied Gases Arising from Inequalities of Temperature , Phil. Trans., 170, 231 (1979).

6. Aitken, J., On the Formation of Small Clear Spaces in Dusty Air , Trans. Roy. Soc. Ed., 32, 239 (1884).

7. Jones, J.E., On the Velocity Distribution Function and on the Stresses in a Non-Uniform Rarefied Monatomic Gas , Phil. Trans. 223, Series A, (1923).

8. Knudsen, M., Ein Absolute Manometer , Ann. der Phys, 32, 809 (1910).

9. Einstein, A., Zur Theorie der Radiometerkratte , Zeits. f. Phys., 27, 1 (1924).

10. Epstein, P., Zur Theorie des Radiometers , Zeits f. Phy., 54, 537 (1929).

11. Cawood, W., The Movement of Dust or Smoke Particles in a Temperature Gradient., Trans. Farad. Soc. 32, 1068 (1936).

12. Waldmann, L., Wher die Kraft eines Inhomogenen Gases auf Kleine Suspendierte Kugeln , Zeits. f. Naturf. 14a, 589 (1959).

13. Brock, J.R., On the Theory of Thermal Forces Acting on Aerosol Particles , J. Colloid, Sci., 17, 768 (1962).

14. Deryaguin, B. V., and Bakanov. S. P., Theory of the Thermophoresis of Large Solid Particles , Dokl. Akad. Nauk SSSR, 147 (1), 139 (1962).

15. Deryaguin, B. V., and Yalamov, Yu., Theory of the Thermophoresis of Moderately Large Aerosol Particles, Dokl. Akad. SSSR, 155(4), 886 (1964).

16. Deryaguin, B. V., and Yalamov, Yu., Theory of Thermophoresis of Large Aerosol Particles, J. Colloid Sci., 20, 555 (1965).

17. Brock, J. R., The Thermal Force in the Transition Region , J. Colloid and Interface Sci., 23, 448 (1967).

18. Dwyer, H. A., Thirteen-Moment Theory of the Thermal Force on a Spherical Particle , Phys. of Fluids, 10(5), 976 (1967).

19. Springer, G. S., Thermal Force on Particles in the Transition Regime , J. Colloid and Interface Sci., 34(2), 215 (1970).

20. Philips, W. F., Thermal Force on Spherical Particles in a Rarefied Gas , Phys of Fluids, 15(6), 999 (1972).

21. Philips, W. F., The Thermal Force on Spherical Aerosol Particles, Environmental Engineering and Science Conference, Second Annual, Louisville, Kentucky, p. 728, April 20-21, (1972).

22. Saxton, R. L., and Ranz, W. E., Thermal Force on an Aerosol Particle in a Temperature Gradient, J. of Applied Physics, 23, 917 (1952).

23. Schadt, C. F., and Cadle, R.D., Thermal Force on Aerosol Particles , J. Phys. Chem., 65, 1689 (1961).

24. Schmitt, K. H., Untersuchungen and Schwebstaffteilchen in Temperaturefied , Zeits. f. Naturfors., 14a, 870, (1959).

25. Lamb, H., Hydrodynamics , p. 597, Sixth edition Cambridge University Press, New York (1957).

26. Bird, R. B., Stewart, W. E., and Lightfoot, E. N., Transport Phenomena", p. 58, John Wiley and Sons, Inc. New York (1966).

27. Kennard, E. H., Kinetic Theory of Gases , p. 295-300, p. 327-330, McGraw Hill, New York (1938).

28. Payne, H., Temperature Jump and Velocity of Slip at the Boundary of a Gas , J. of Chem. Physics, 21(12), 2127 (1953).

29. Kennard, E. H., Kinetic Theory of Gases , p. 295, McGraw Hill, New York (1938).

30. Kennard, E. H., Kinetic Theory of Gases, p. 320, McGraw Hill, New York (1938).

31. Street, R. E., Rarefied Gas Dynamics, p. 276-292, Pergamon Press, New York (1960).

32. Bhatnagar, P. L., Gross, E. P., and Krook, M., A Model for Collision Processes in Gases.I.Small Amplitude Processes in Charged and Neutral One-Component Systems, Phys. Rev. 94, 511 (1954).

33. Jacobsen, S., Investigation of a Second Order Slip Flow Theory: Thermal Force on Solid Aerosols, Master's Thesis, The University of Texas, (1964).

34. Hidy, G. M., Theory of Diffusive and Impactive Scavenging, p. 355, Proceedings of Precipitation Scavenging 1970 Symposium, Richland, Washington, June 1970, NTIS No. Conf. 700601.

V. THERMOPHORETIC VELOCITY

Particles suspended in a gas exposed to a temperature gradient will be influenced by a thermal force. Such particles tend to move in the direction of decreasing temperature with a velocity known as the 'thermophoretic velocity'.

Under the influence of a temperature gradient and friction, the force exerted by the gas on a free particle, F_g, is given by [1]:

$$F_g = F_t - F_D \tag{5-1}$$

F_g = force exerted by the gas on the particle, dynes
F_t = thermal force, dynes
F_D = drag force, dynes

At steady state, the force exerted by the gas on the particle must vanish. Hence, if the drag force (i.e. the fluid resistance to the movement of a particle suspended in a fluid), F_D, is known, the thermophoretic velocity can be obtained from the thermal force, F_t. In other words, in order to predict the thermophoretic velocity, a knowledge of the drag force, F_D, applicable to the flow, is required.

A. Slip-Flow Regime

In the slip-flow regime, where the mean free path of gas, λ, is much smaller than the size of the aerosol particle ($\lambda << R_p$ and $N_{Kn_{R_p}} \to 0$)

The drag force is given by Stokes' law [2]:

$$F_D = 6\pi \mu R_p v_t \quad \text{where} \tag{5-2}$$

F_D = drag force, dynes

μ = gas viscosity, gm/(cm sec)

R_p = radius of the particle, cm

v_t = thermophoretic velocity of the particle relative to the stagnant fluid, cm/sec

Under steady state conditions the thermal force, F_t, must equal the drag force, F_D, and under the influence of a thermal force and friction, an otherwise free particle moves towards the region of lower temperature with a velocity:

$$v_t = \frac{F_t}{6\pi \mu R_p} \tag{5-3}$$

Epstein's equation (4-34) for the thermal force, gives a thermophoretic velocity:

$$v_t = -\frac{3}{2} \left(\frac{k_g}{2 k_g + k_p}\right) \frac{\mu}{\rho T} G \quad \text{where} \tag{5-4}$$

v_t = thermophoretic velocity, cm/sec

k_g = thermal conductivity of gas, cal/(sec cm°K)

k_p = thermal conductivity of particle, cal/(sec cm°K)

μ = gas viscosity, gm/(cm sec)

ρ = gas density, gm /cm ^{3}

T = absolute gas temperature, °K

G = uniform gas temperature gradient away from the particle, °K/cm.

By substituting Brock's equation (4-45) for the the thermal force in the slip-flow regime into equation (5-3) the following expression for the thermophoretic velocity results:

$$v_t = -\frac{3}{2}\left[\frac{1}{1 + 3\, c_m \frac{\lambda}{R_p}}\right]\left[\frac{\frac{k_g}{k_p} + c_t \frac{\lambda}{R_p}}{1 + 2\frac{k_g}{k_p} + 2\, c_t \frac{\lambda}{R_p}}\right]\frac{\mu}{\rho T} G \qquad (5\text{-}5)$$

where

v_t = thermophoretic velocity, cm/sec

c_m = momentum accommodation coefficient

c_t = temperature accommodation coefficient

λ = mean free path of gas, cm.

μ = gas viscosity, gm /(cm sec)

T = absolute gas temperature, °K

k_g = thermal conductivity of the gas, cal/(sec cm °K)

k_p = thermal conductivity of the particle, cal /(sec cm °K)

G = uniform gas temperature gradient away from the particle, °K/cm.

B. Free-Molecular Regime

In the free-molecular regime, where the mean free path of the gas, λ, is much greater than the size of the aerosol particle

($\lambda >> R_p$ and $N_{Kn_{R_p}} \to \infty$), Waldmann [3] derived the following expression combining frictional and thermophoretic forces acting on the particle:

$$F_g = -\frac{8}{3} R_p^2 \sqrt{\frac{2\pi m}{kT}} \left[\left(1 + \frac{\pi}{8}\alpha\right) p v_t + \frac{1}{5} (k_g)_{tr} \nabla T\right] \qquad (5\text{-}6)$$

where

F_g = force exerted by the gas on a moving particle, dynes

R_p = radius of the particle, cm

k = Boltzmann constant, (dynes cm)/°K

T = absolute gas temperature, °K

m = molecular mass of gas, gm

α = accommodation coefficient of particle

p = gas pressure, dynes/cm^2

$(k_g)_{tr}$ = translational component of the thermal conductivity of gas, cal/(cm sec °K)

v_t = thermophoretic velocity of the particle relative to the stagnant fluid, cm/sec

It should be noted that the first term of equation (5-6) is the drag force, F_D and the second term is the thermal force, F_t, acting on the particle. In the steady state case the force, F_g, exerted by the gas on the particle must vanish. An otherwise free particle thus moves towards the region of lower temperature with the velocity, v_t, relative to the stagnant fluid where

$$v_t = - \frac{1}{5(1 + \frac{\pi\alpha}{8})} \frac{(k_g)_{tr}}{p} \nabla T \qquad (5\text{-}7)$$

For polyatomic gases having molecular mass m and viscosity μ the translational component of the gas thermal conductivity [4]

$$(k_g)_{tr} = \frac{15k\mu}{4m} \qquad (5\text{-}8)$$

should be used in Equation (5-7) rather than the total thermal conductivity.

C. Transition Regime

In the transition regime, where the mean free path of the gas, λ, is of the same order of magnitude as the size of aerosol particle, the drag force, F_D, is given by Millikan [5] as

$$F_D = \frac{6\pi\mu R_p v_t}{1 + \frac{\lambda}{R_p}[A + B \exp(-CR_p/\lambda)]} \qquad (5\text{-}9)$$

where

A, B and C = empirical constants appearing in the slip-correction equation

It should be noted that the transition regime equation reduces to Stokes law for the slip-flow regime, where $\lambda/R_p \rightarrow 0$.

In order to apply equation (5-9), it is necessary to evaluate the mean free path length of the gas, λ, and the empirical constants A, B and C. The mean free path length, λ, from the pressure-independent viscosity concept of kinetic theory, is defined such that the pressure-mean free path product, $p\lambda$, for a given gas is a function of temperature, T, only. The appropriate relationship is given by [6]:

$$\lambda = \frac{\mu RT}{0.499\ M\ p\ \bar{v}} \qquad (5\text{-}10)$$

where

λ = mean free path of gas, cm

μ = gas viscosity, gm/(cm sec)

p = gas pressure, dynes/cm^2

R = gas constant, cm^3 atm/gm mole °K

$\bar{v}$ = mean molecular velocity, cm /sec

M = molecular weight of gas, gm/gm mole

The values of the empirical constants, A, B and C are given in Table 5.1.

	A	B	C
Davies [7]	1.270	0.400	1.100
Millikan [5]	1.230	0.410	0.880

TABLE 5.1: Values of Empirical Constants A, B and C.

Under steady state conditions, the thermal force, F_t must equal the drag force, F_D. A combination of Brock's equation (4-50) for the thermal force and equation (5-9) for the drag force, yields

$$v_t = \frac{F_t^{**} \left[1 + \frac{\lambda}{R_p} \left(A + B \exp\left(\frac{-CR_p}{\lambda}\right)\right)\right]}{6 \pi \mu R_p} \qquad (5\text{-}11)$$

where

F_t^{**} is the thermal force in the transition regime given by Brock [equation (4-50)].

REFERENCES

1. McNab, G. S., Thermophoresis in Sols , Ph.D. Thesis, University of British Columbia, p. 67 (1972).

2. Kennard, E. H., Kinetic Theory of Gases , McGraw-HillBook Company, Inc. New York, p. 309 (1938).

3. Waldmann, L., Uber die Kraft eines Inhomogenen Gases and Kleine Surpendierte Kugelen , Zeits. f, Naturf. 14a, 589 (1958).

4. Philips, W. F., Thermal Force on Spherical Particles , Environmental Engineering and Science Conference, Second Annual, Louisville, Kentucky, p. 728, April 20-21 (1972).

5. Millikan, R. A., The General Law of Fall of a Spherical Body Through a Gas and its Bearing Upon the Nature of Molecular Reflection From Surfaces , Phy. Rev. 22, 1 (1923).

6. Wilson, T. W., McAlister, J. A., and Orr, C., An Investigation of Thermal Force with Particular Reference to Materials of High Conductivity , Engineering Experiment Station of the Georgia Institute of Technology, Atlanta, Georgia, Final Report p. 39, (1961).

7. Davies, C. N., Definitive Equations for the Fluid Resistance of Spheres , Proceedings of the Physical Society, 57, 259 (1945).

VI. EXPERIMENTAL INVESTIGATIONS

The thermal force has been defined as "a force, other than that caused by convection which acts on a particle suspended in a gas exposed to a temperature gradient". Although various experimental techniques involving

i. vane radiometers [1]

ii. dust-free space [2]

iii. photophoresis [3]

iv. thermal precipitators [4 and 5] and

v. a modified Millikan oil drop apparatus

have been reported, almost all experiments testing the thermal force theory have been carried out with a modified Millikan oil drop apparatus using the technique of 'single particles in a temperature gradient' [6, 7, 8 and 9]. In the first four experimental categories, a quantitative calculation of the force presents a difficult problem and for this reason agreement between theory and experiment has been mainly qualitative.

The general experimental approach can be easily visualised. An aerosol is generated and subjected to a thermal field. The resulting thermal force causes migration of the suspended material. In the modified Millikan experiment the velocity of particulate migration is measured and the magnitude of the force deduced.

The Modified Millikan experiment employs an electrostatic field for the manipulation of a charged particle. The technique of dark field illumination is used to observe the particle. This adaptation provides for the establishment of a temperature gradient in the gas surrounding the particle through controlled heating and cooling of the electrodes.

A. The Modified Millikan Apparatus

1. Description of Equipment

The essential elements of a typical modified Millikan device, which provide for optical viewing and electrostatic field control, are schematically illustrated in Figure 6.1 [5]. The central cell containing electrodes and temperature control elements is shown in Figure 6.2 [5]. Two cylindrical brass electrodes, one inch in diameter, were positioned concentrically, one above the other with a separation of 0.075 cm. A resistance coil was used to heat the upper electrode while the lower electrode was equipped for cooling with an internal water jet. Copper-constantan thermocouples were inserted near the surfaces of both electrodes for temperature measurement. With the electrodes encased in Bakelite shells, the complete unit was rigidly mounted in a brass case. The entire assembly was suspended in the main chamber of the Millikan apparatus. A water bath was provided as a means of shielding the main chamber from ambient room temperature changes.

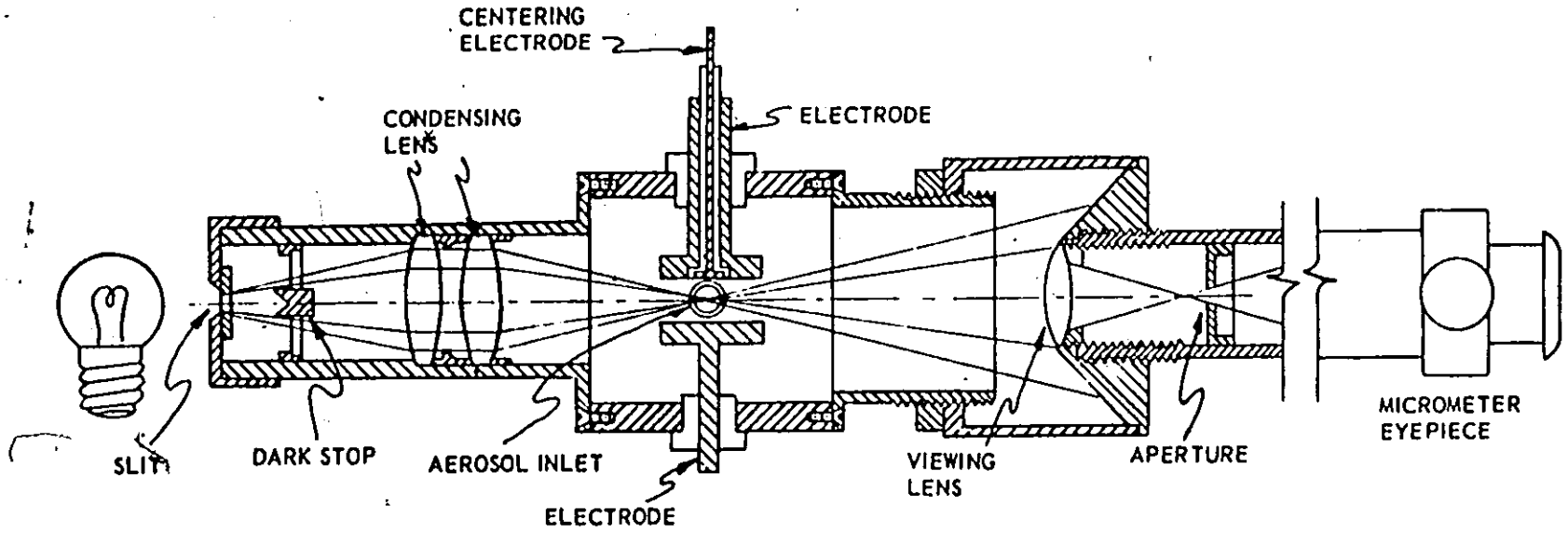

FIGURE 6.1: Essential Elements of Modified Millikan Device. Shown Above is a Schematic Diagram of the Optical System Providing Dark Field Illumination of Suspended Particulates [5]

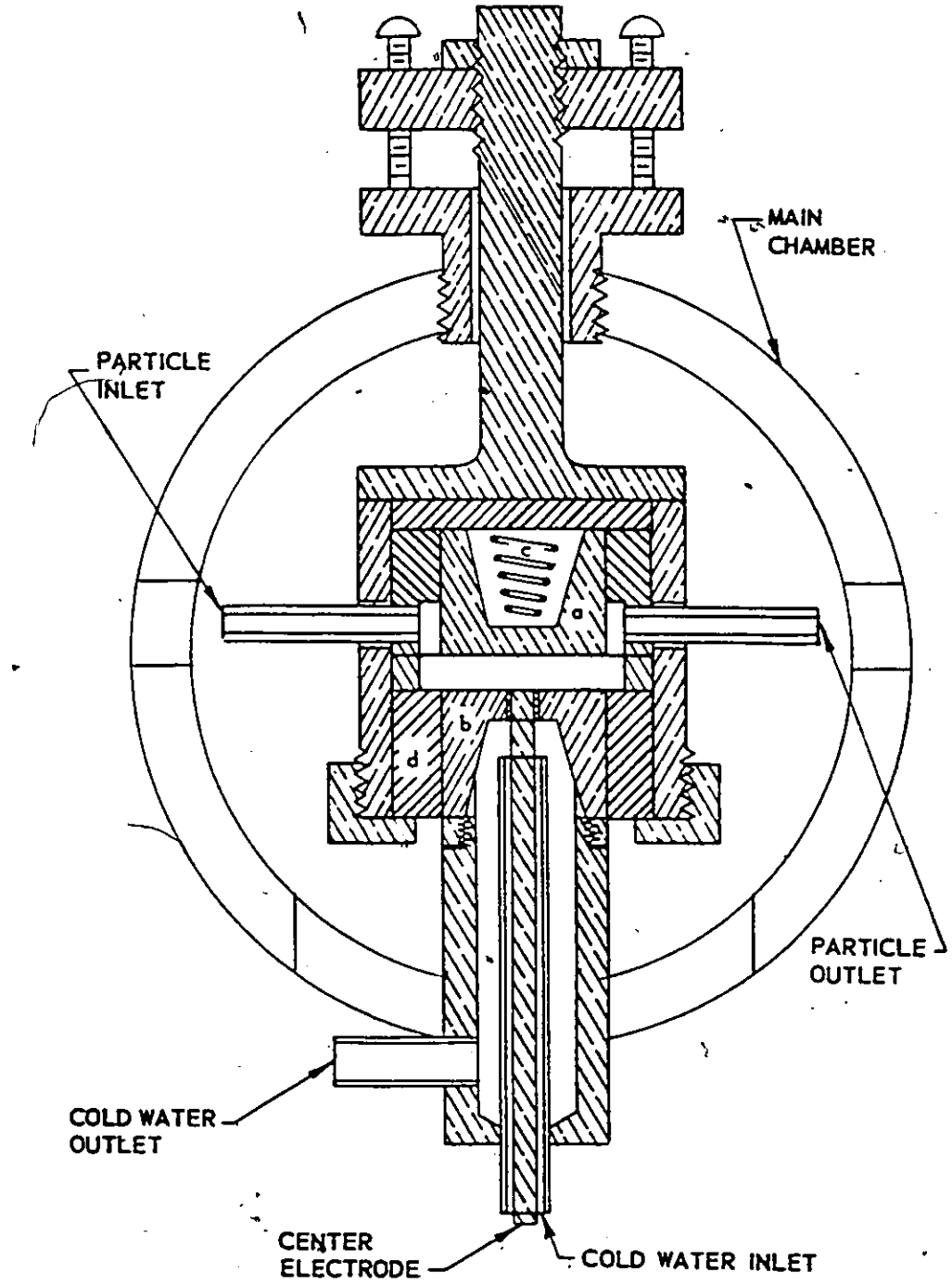

FIGURE 6.2: Detail of Central Cell of Modified Millikan Apparatus. (This Thermal Cell, Containing Electrodes and Temperature Control Elements, was Installed in the Objective Section of a Conventional Millikan Apparatus) [5]

2. Experimental Procedure

Charged aerosol particles to be studied in this apparatus were introduced into the central cell at very dilute concentrations. A single particle was suspended between the principal electrodes. This particle, observed through the optical system, could be raised or lowered by altering the electrical field strength. The effective diameter of the suspended particle was determined from repeated measurements of its terminal velocity under the influence of gravity in the absence of a temperature gradient. This was accomplished by switching off the current to the electrodes and timing the vertical descent of the particle between the calibrated cross-hairs of the micrometer eye-piece. In this manner particulate behavior could be observed through the optical system as many times as desired by reapplying the voltage to the electrodes.

In the absence of a temperature gradient, since the gravitational force, F_{gr}, must equal the drag force, F_D, it follows that: $F_{gr} = F_D$

$$\frac{4}{3}\pi R_p^3 (\rho_p - \rho) g = \frac{6\pi \mu R_p v_f}{1 + \frac{\lambda}{R_p}\left[A + B \exp(-CR_p/\lambda)\right]} \qquad (6\text{-}1)$$

where

R_p = radius of the particle, cm

ρ_p = particle density, gm/cm^3

ρ = gas density, gm/cm^3

g = gravitational acceleration, 980.6 cm/sec^2

μ = gas viscosity, gm/(cm sec)

v_f = velocity of fall of the particle, cm/sec

λ = mean free path of gas, cm

A, B and C = empirical constants, dimensionless

The charge on the particle could be computed from a determination of the velocity of rise of the particle, v_r, according to

$$\frac{qE}{300} = \frac{4}{3}\pi R_p^3 (\rho_p - \rho)g + \frac{6\pi\mu R_p v_r}{1 + \frac{\lambda}{R_p}[A + B\exp(-CR_p/\lambda)]} \qquad (6\text{-}2)$$

where

q = charge on a particle, statcoulombs

E = electric field intensity, practical volts per cm

300 = conversion factor, practical volts to stat volts

1 statvolt = a potential of one erg per statcoulomb

After the diameter and charge on the particle had been determined, a thermal field was established. From another series of velocity measurements, the thermal force, F_t, was obtained as the difference between this electrical force, F_E, and the sum of gravitational, F_{gr}, and drag, F_D, forces.

From

$$F_t = F_E - F_{gr} - F_D \qquad (6\text{-}3)$$

$$F_t = \frac{qE}{300} - \frac{4}{3}\pi R_p^3 (\rho_p - \rho)g - \frac{6\pi\mu R_p v_r}{1 + \frac{\lambda}{R_p}[A + B\exp(-CR_p/\lambda)]} \qquad (6\text{-}4)$$

B. Experimental Investigations

Typical experimental investigations are reviewed briefly to establish

i. the validity of theoretical analyses and

ii. the quantitative inconsistencies which have been reported.

1. Rosenblatt and LaMer

In 1945, Rosenblatt and LaMer [6] used an adaptation of the Millikan oil drop experiment to directly observe the behavior of a particle in a thermal field. From a measurement of the difference in velocities for a particle in free-fall and under an imposed temperature gradient, the thermal force was deduced.

In these experiments, the radius of tricresyl phosphate droplets ranged from 0.4 to 1.6 microns. The experimental observations covering a Knudsen number, $N_{Kn_{R_p}}$ range from 0.04 to 1.5 showed that

i. the thermophoretic velocity and hence the thermal force were directly proportional to the temperature gradient. Figure 6.3 shows the dependence of thermal velocity on temperature gradient and particle size at a fixed pressure. The dependence of thermal velocity on pressure and temperature gradient is illustrated by Figure 6.4. Figures 6.3 and 6.4 are plots of v_t against $\frac{dT}{dx}$ corrected to a standard temperature of 300°K.

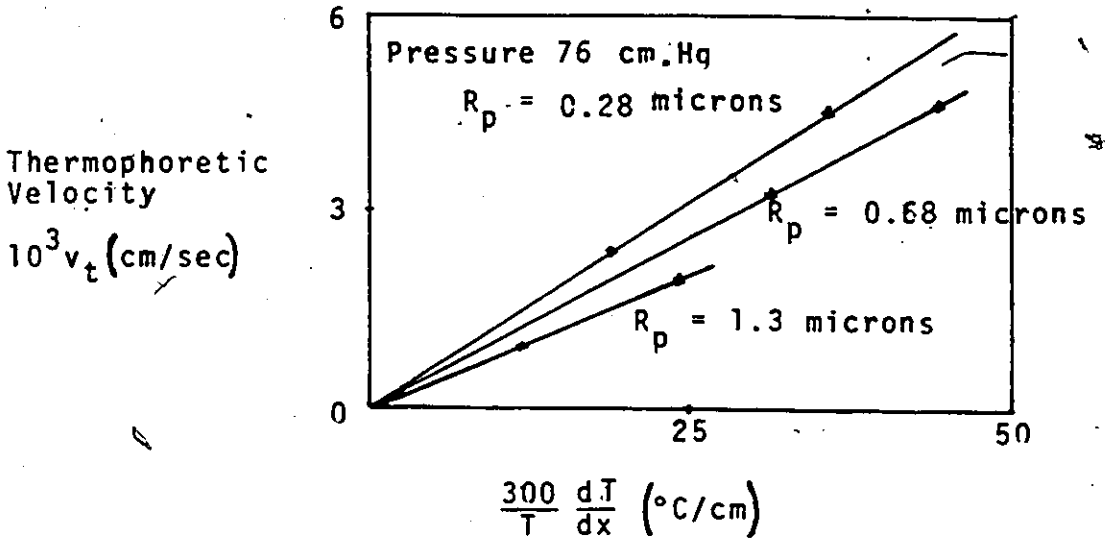

FIGURE 6.3: Dependence of Thermophoretic Velocity on Temperature Gradient and Particle Size at Constant Pressure [6]

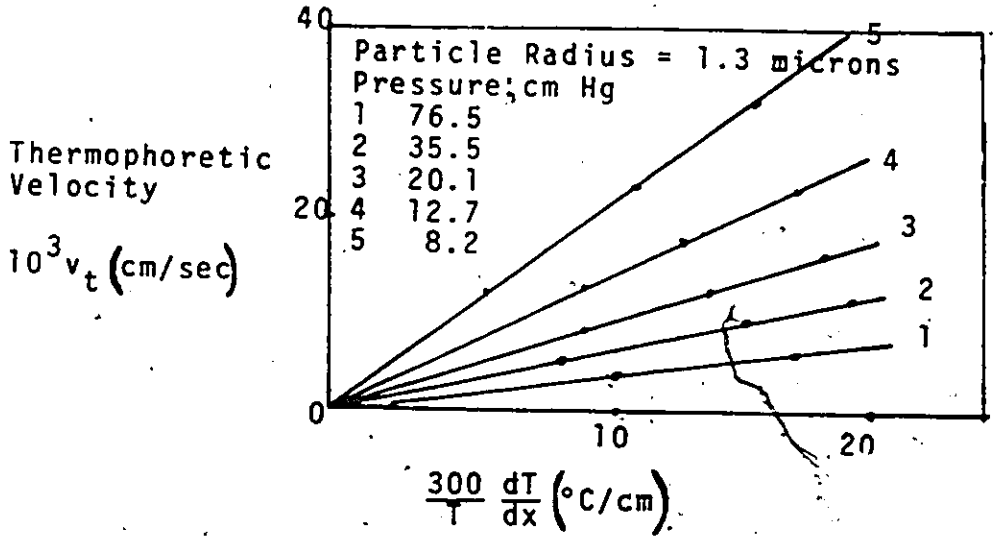

FIGURE 6.4: Dependence of Thermophoretic Velocity on Pressure and Temperature Gradient for Fixed Particle Size [6]

ii. the thermophoretic velocity was approximately inversely proportional to pressure for Knudsen numbers less than 0.5 as shown in Figure 6.5 [6].

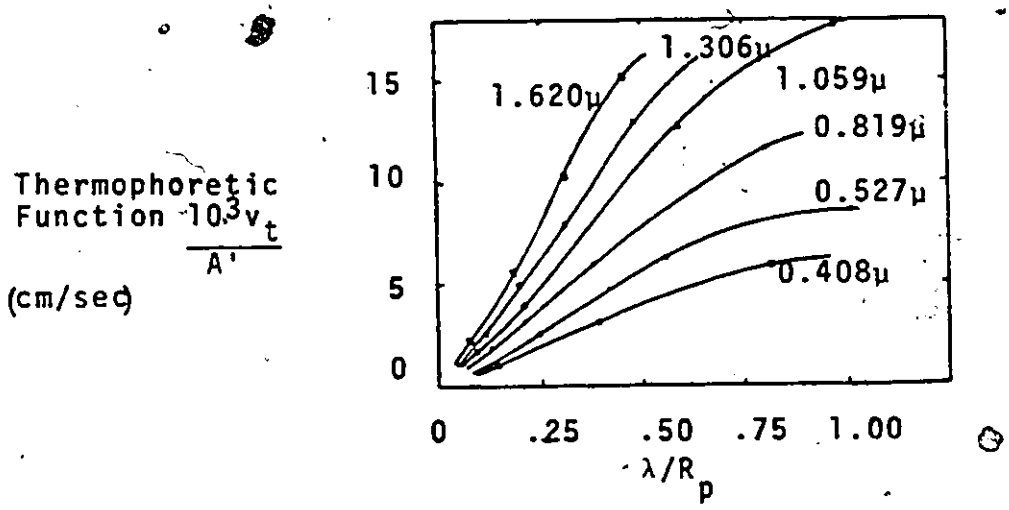

FIGURE 6.5 Dependence of Thermophoretic Function $\frac{v_t}{A'}$ on $\frac{\lambda}{R_p}$, the Ratio of the Mean Free Path of Gas to Radius of Aerosol Particle

[6] $[A' = 1 + \frac{\lambda}{R_p}[A + B \exp(-CR_p/\lambda)]$

$[\lambda = \mu\sqrt{\pi}/\sqrt{2p\rho}]$[12]

2. Saxton and Ranz

In 1952, Saxton and Ranz [7] utilized a modified Millikan apparatus to investigate the effect of particle size, temperature gradient and aerosol material on the magnitude of the thermal force. Castor oil and paraffin oil droplets with thermal conductivities of 4.3×10^{-4} and 2.95×10^{-4} cal/(cm sec °K) respectively were used. Knudsen numbers, $N_{Kn_{R_p}}$, ranged from 0.0615 to 0.277. Saxton and Ranz found that

i. the thermal force was directly proportional to both temperature gradient and particle radius in agreement with Epstein's equation as shown in Figure 6.6.

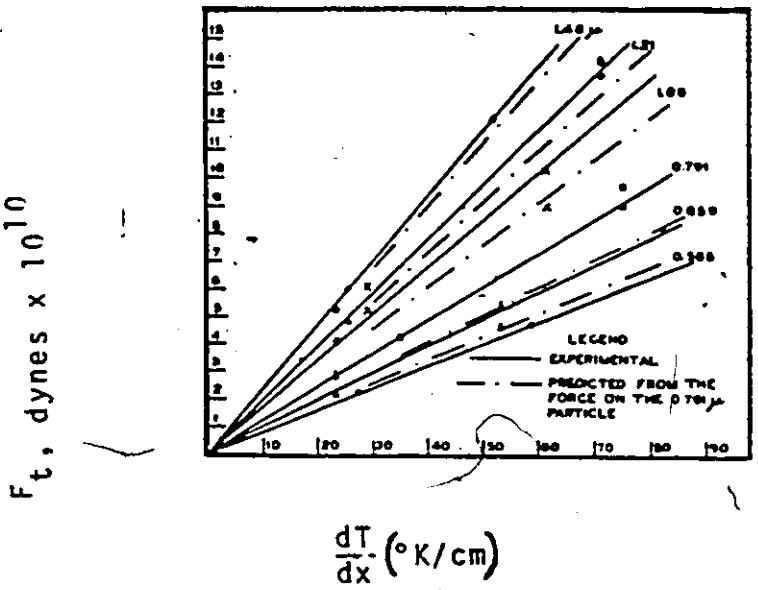

FIGURE 6.6: Effect of Particle Diameter and Temperature Gradient on the Thermal Force [7]

ii. the thermal force predicted by the equations of Cawood, Einstein and Epstein differed from the experimental value by 249, 68.5 and 5.4 percent, respectively. This study established the superiority of Epstein's equation over the Cawood and

Einstein expressions as shown in Figure 6.7

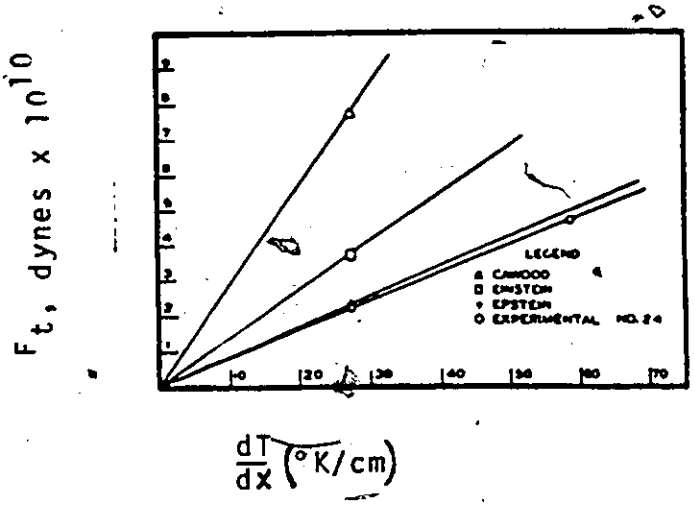

FIGURE 6.7: Comparison of Theoretical Equations of Cawood, Einstein and Epstein with Saxton and Ranz Experimental Data [7]

3. Schadt and Cadle

In 1961, Schadt and Cadle [8] employed a modified Millikan oil drop apparatus to investigate thermal forces on tricresyl phosphate droplets, sodium chloride particles, and mercury droplets with thermal conductivities of 4.8×10^{-4}, 1.55×10^{-2} and 2.8×10^{-2} cal/(cm sec °C) respectively. The radii of the tricresyl phosphate droplets, sodium chloride particles and mercury droplets ranged from 0.46 to 0.49, 0.22 to 1.15, and 0.096 to 0.145 microns respectively. The Schadt and Cadle study showed that:

i. thermal force measurements on tricresyl phosphate droplets and sodium chloride particles were in agreement with the predicted dependence on temperature gradient, particle radius and mean free path of gas as illustrated by Figures 6.8 and 6.9.

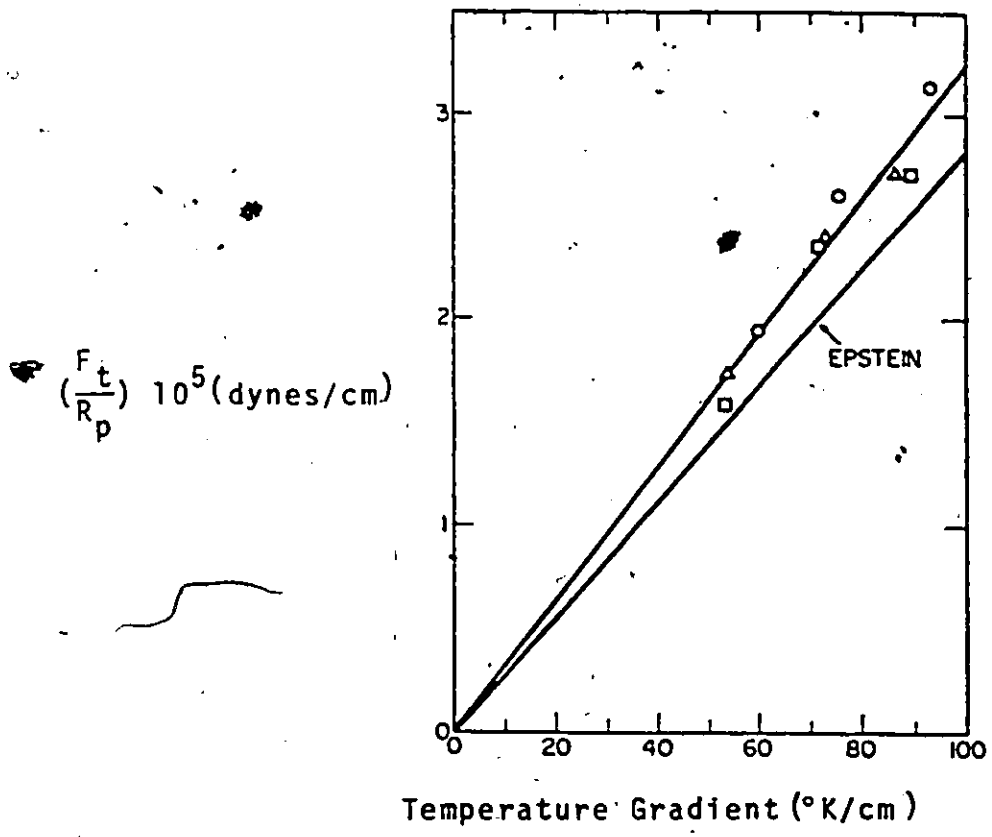

FIGURE 6.8: Dependence of Thermal Force on Temperature Gradient. Tricresyl Phosphate Droplets. Radius of Droplets in Microns: O, 0.46; □, 0.49; Δ, 0.49 [8]

It should be noted that there is a close agreement between Epstein's theory and experiment for low thermal conductivity particles. In contrast, agreement is poor for high

thermal conductivity sodium chloride particles.

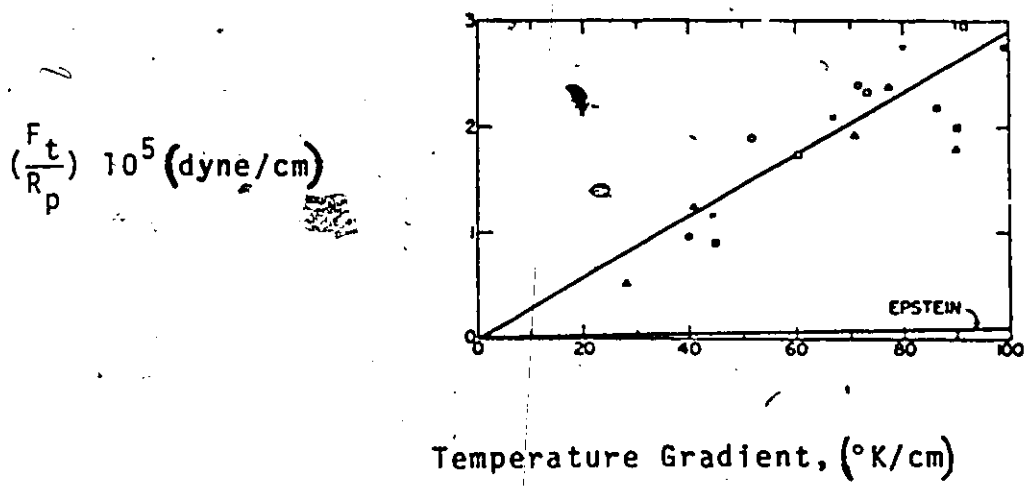

FIGURE 6.9: Dependence of Thermal Force on Temperature Gradient and Particle Radius at Atmospheric Pressure. Sodium Chloride Particles, Radius of Each in Microns:

No. 1	○	0.22	No. 5	●	0.41
No. 2	□	0.30	No. 6	■	1.02
No. 3	△	0.35	No. 7	▲	1.15
No. 4	X	0.40			

[8]

ii. measurements of thermal force on tricresyl phosphate droplets of low thermal conductivity indicated fairly close agreement with the Epstein equation as shown by Figure 6.10. Agreement between Epstein's theory and experiment is very good as the Knudsen number $N_{Kn_R} \to 0$.

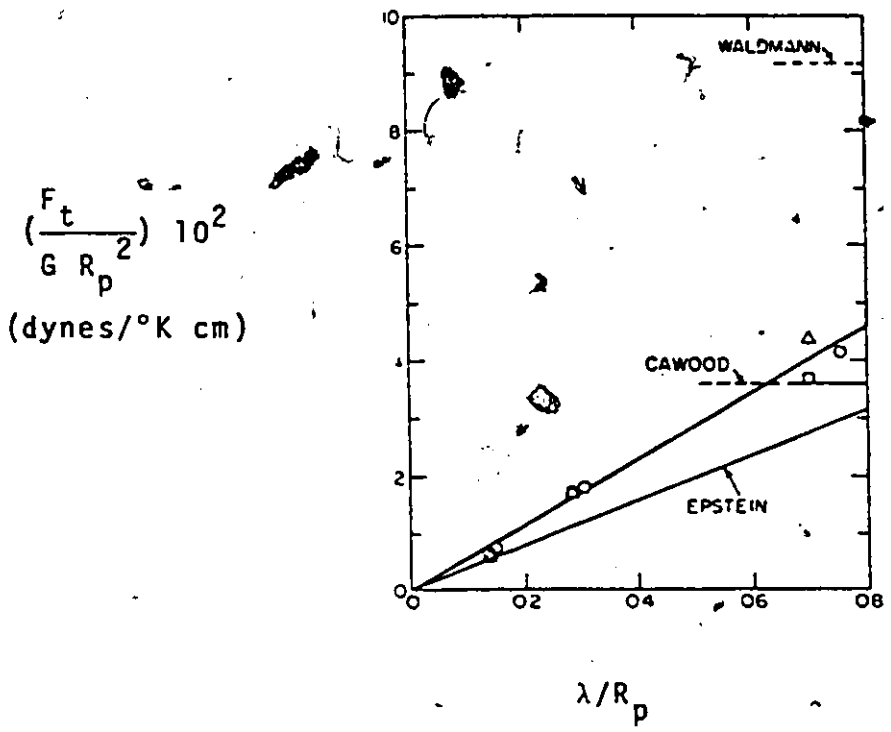

FIGURE 6.10: The Effect of the Ratio of Mean Free Path to Particle Radius on Thermal Force (Average Temperature was 307°K) for Tricresyl Phosphate Droplets. Radius of Each Droplet in Microns: ○, 0.46; △, 0.49; □, 0.49 [8])

iii. thermal forces on sodium chloride particles and mercury droplets, (involving much higher thermal conductivities) differed by 30 and 50 respectively. These differences are illustrated in Figures 6.11 and 6.12.

4. Schmitt

The 1959 experimental investigation by Schmitt [9, 10] was specifically oriented toward the confirmation of Waldmann's

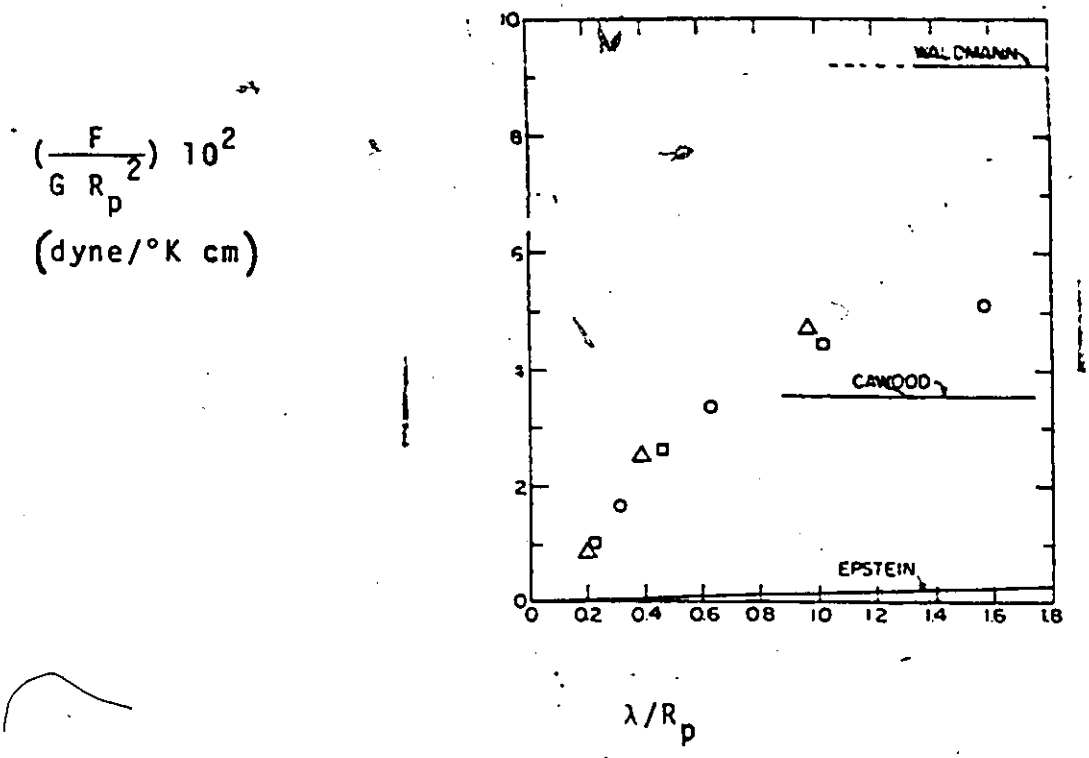

FIGURE 6.11: The Effect of the Ratio of Mean Free Path to Particle Radius on Thermal Force (Average Temperature was 307°K) for Sodium Chloride Particles Radius of Each Particle in Microns [8]

○	0.22	●	0.41
□	0.30	■	1.02
△	0.35	▲	1.15
×	0.40		

theory [11]. Schmitt was concerned with the dependence of thermal force and thermophoretic velocity upon the gas pressure, the particle radius and the nature of both the particle and the gas. His findings showed that:

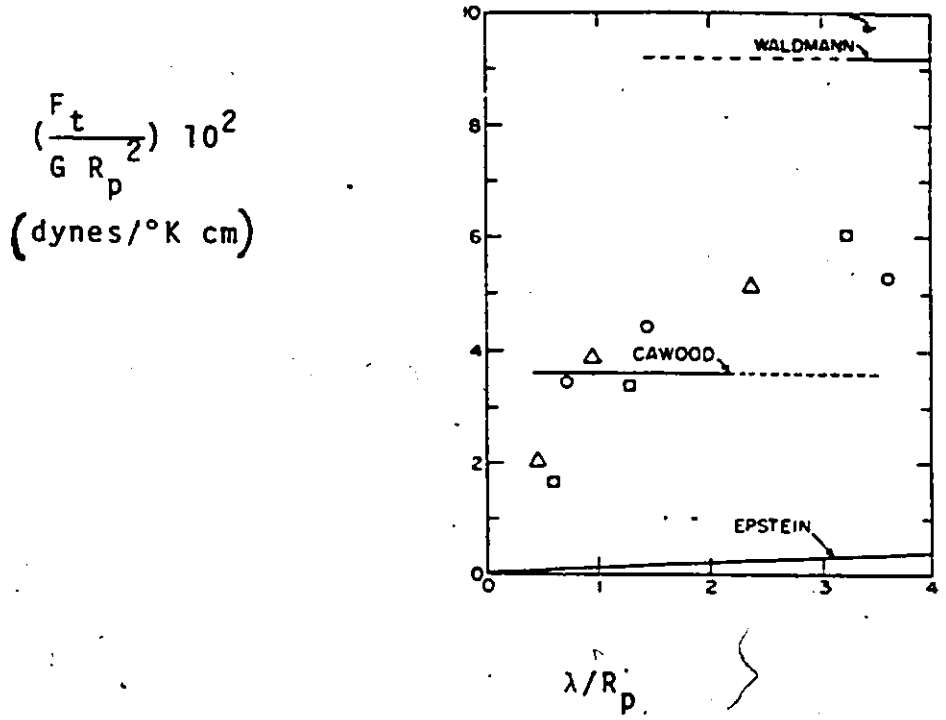

FIGURE 6.12: The Effect of the Ratio of the Mean Free Path to Particle Radius on Thermal Force for Mercury Droplets (Temperature of 307°K) Radius of Each Droplet in Microns: ○, 0.096; □, .0.115; △, 01.45) [8]

i. experimental results were in excellent agreement (5 percent deviation) with Waldmann's theory if $\alpha = 1$ was taken for the coefficient of diffuse reflection. Figure 6.13 provides a comparison of experimental data with several theoretical predictions.

When considering Figures 6.10 to 6.12 it should be recalled that Epstein's thermal force expression was derived for $\frac{\lambda}{R_p} \to 0$ while Waldmann's was for $\frac{\lambda}{R_p} \to \infty$.

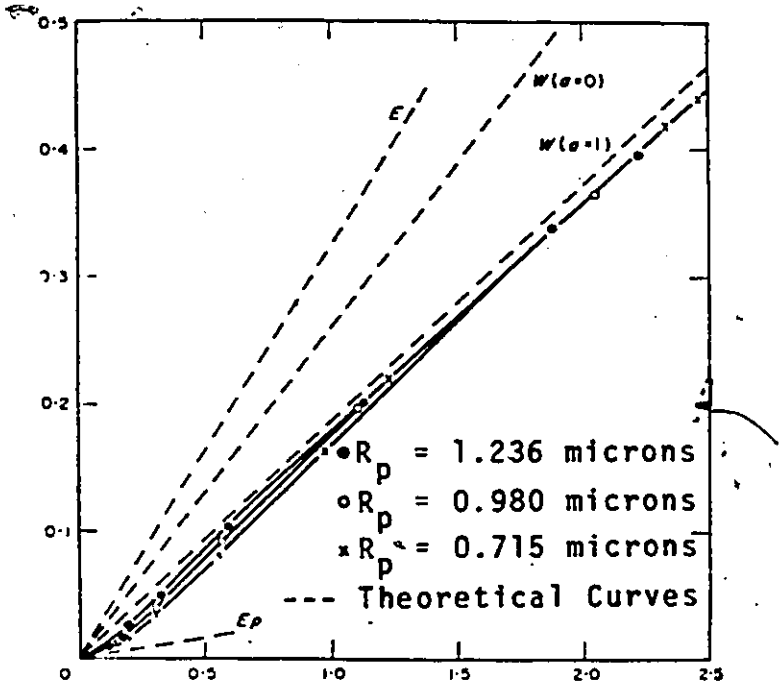

FIGURE 6.13: Comparison of the Expressions for the Thermophoretic Velocities of Waldmann, W, Epstein, Ep and Einstein, E, with Experiment. (For Theoretical Curves: $k_g = 0.40 \times 10^{-4}$ (Air) and $k_p = 2.95 \times 10^{-4}$ cal/(cm sec °K). Silicone Oil Drops have been used) [10].

ii. the thermal force approached a constant value with decreasing pressure when $\frac{\lambda}{R_p} > 2.0$ as shown in Figure 6.14.

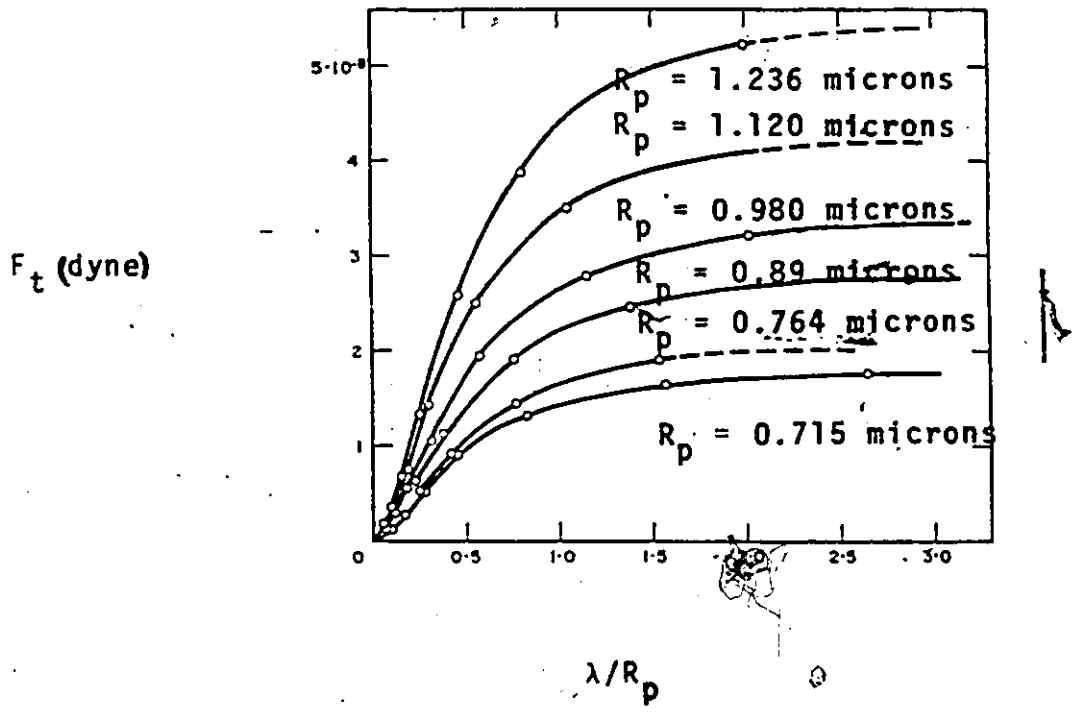

FIGURE 6.14: Dependence of Thermophoretic Force on the Mean Free Path (Silicone Oil Droplets in Argon $\nabla T = 49.4\,^{\circ}K/cm$) [11].
$[\lambda = \mu \sqrt{\pi}/\sqrt{2p\rho}]$ [12]

For large mean free paths ($\frac{\lambda}{R_p} >> 1$) Waldmann's thermal force expression Equation (4-48) applies; and in accordance with the theoretical prediction the force becomes independent of the pressure (i.e. force is constant for large λ) and

proportional to R_p^2. For small mean free path ($\frac{\lambda}{R} << 1$) and droplets of low thermal conductivity Epstein's expression (4-34) is applicable. Figure 6.14 shows that the force in the slip-flow regime is approximately proportional to λ (i.e. inversely proportional to pressure) and radius R_p.

iii. in the slip-flow regime, experimental results of thermophoretic velocity supported the theory of Epstein as shown in Table 6.1.

Gas	V_t, exp.(1 micron) 10^3cm/sec	$k_g \cdot 10^4$ cal/(cm sec °C)	$\frac{2k_g + k_p}{k_g}$	Gas Viscosity $\mu\ 10^4$ gm/(cm sec)	V_t, Ep. 10^3 cm/sec	V_t, $E_p./V_t$, exp.
Ä	3.40	0.401	13.32	2.270	2.82	0.830
N_2	4.00	0.594	9.65	1.788	4.35	1.090
CO_2	2.08	0.351	14.90	1.506	1.47	0.707
H_2	97.00	4.91	3.08	0.909	104.00	1.070

TABLE 6.1: Comparison of the Experimental Thermophoretic Velocities, V_t, exp. with the Calculated Velocities, V_t, Ep. According to Equation (5-4) [9]

REFERENCES

1. Crookes, W., On Repulsion from Radiation , Phil., Trans. Roy. Society London, 170, 87 (1878).

2. Watson, H. H., The Dust-Free Space Surrounding Hot Bodies , Trans. Farad. Soc., 32, 1073 (1973).

3. Reynolds, O., On the Forces by the Communication of Heat Between a Surface and a Gas; and on a New Photometer, Phil. Trans. Roy. Soc. London, 166, 725 (1876).

4. Schadt, C. F., and Cadle, R. D., Thermal Forces on Aerosol Particles in a Thermal Precipitator , J. Colloid Sci., 12, 356 (1957).

5. Wilson, T.W.M. McAlister, J. A., and Orr, C., An Investigation of Thermal Force with Particular Reference to Materials of High Conductivity , Engineering Experiment Station of the Georgia Institute of Technology, Atlanta, Georgia, Final Report p. 39, (1961).

6. Rosenblatt, P., and Lamer, V. K., Motion of a Particle in a Temperature Gradient, Thermal Repulsion as a Radiometer Phenomenon , Phy. Rev. 70, 385 (1946).

7. Saxton, R. L., and Ranz, W. E., Thermal Force on an Aerosol in a Temperature Gradient, J. of Applied Physics, 23, 917 (1952).

8. Schadt, C. F., and Cadle, R. D., Thermal Force on Aerosol Particles , J. Phys. Chem., 65, 1689 (1961).

9. Schmitt, K. H., Untersuchungen an Schwebstoffteilchen in Temperaturefied , Zeits. f. Naturfors, 14a, 870 (1959).

10. Waldmann, L., and Schmidt, K. H., Thermophoresis and Diffusiophoresis of Aerosols, Aerosol Science, Edited by Davies, C. N., Academic Press, New York, p. 137 (1966).

11. Waldmann, L., Wher die Kraft eines Inhomogenen Gases auf Kleine Suspendierte Kugeln, Zeits, f. Naturf, 14a, 589 (1959).

12. Golovin, M. N., and Putnam, A. A., Inertial Impaction on Single Elements, I and EC Fundamentals, 1, 264 (1962).

VII. DIFFUSIOPHORETIC FORCE

Aerosol particles suspended in a non-uniform but isothermal gas mixture move due to existing concentration gradients. In a binary mixture with vanishing average molecular velocity, the aerosol particles, in general, move in the same direction as the heavier component [1]. The force causing motion is called the 'diffusiophoretic force' and the velocity with which the aerosol particles move is known as the diffusiophoretic velocity. As in the case of the thermal force, the diffusiophoretic force originates from the interaction of gas molecules with the particle surface. The mechanism of the gas-solid interaction is dependent upon the ratio of the mean free path of the gas to the particle radius.

A simple model illustrating diffusiophoresis would consider a single spherical particle immersed in a binary gas mixture in which relative motion of gas molecules is due to a concentration gradient. Gas molecules of the heavier component have a greater momentum than the molecules of the lighter gas component. As a result a net momentum is imparted to the particle which tends to move the particle in the direction of the heavier gas component.

A complex model would take into account the shape of the solid as well as the interaction of two or more solid particles with the two or more gas components.

A. Background

Aitken [2] in 1883 first reported on diffusiophoresis in his paper "On the Formation of Small Clear Spaces". He observed a small dust-free space next to a moist surface when that surface was suspended in dry dusty air. Aitken thought this phenomenon was due to the evaporation of water from the surface, but he made no attempt to develop a quantitative explanation.

No further work on diffusiophoresis was reported in the open literature until 1956-57 when Deryaguin and Dukhin [3, 4, and 5] published three papers in Russian. They recognized that the mechanism of gas-solid particle interaction is dependent upon the ratio of the mean free path length of the gas to the particle radius, which is the Knudsen number, $N_{Kn_{R_p}}$. The Russian researchers attempted to use the kinetic theory of gases to develop a mathematical expression for the force which diffusing gas mixtures exert on large aerosol particles. In order to obtain the net momentum imparted to a particle by colliding gas molecules, it is necessary to have a knowledge of the velocity distribution function of the gas molecules. Since a rigorous approach involves solution of the Boltzmann equation, Deryaguin and Dukhin [3, 4, and 5] did not pursue this line of attack. Instead they postulated that a large aerosol particle moves with the Stefan flow velocity (i.e. the mass average velocity).

Facy and Freise [6, 7 and 8], who were completely unaware of Aitken's [2] earlier work, provided the first experimental evidence for diffusiophoresis in modern times. Facy [6] suspended a liquid drop in air containing tobacco or magnesium oxide smoke. His first set of experiments was conducted with a drop of water suspended in smoky air. As the drop evaporated he observed that the smoke particles moved away from the drop to form a clear space in its vicinity. In the second set of experiments involving a sulphuric acid drop in moist air, water vapour diffused towards the drop. Under these conditions smoke particles deposited on the drop surface. The Facy attempt [6] to develop a quantitative appreciation of the behavior of smoke particles in diffusing gases recognized the importance of the Knudsen number. The following force and velocity expressions were developed for small aerosol particles in diffusing binary mixtures where only component A, diffuses:

$$F_d = K_F A_p \nabla \gamma_A \qquad (7\text{-}1)$$

where

F_d = diffusiophoretic force, dynes

K_F = a constant to be determined experimentally, dynes/cm

A_p = projected area of an aerosol particle, cm^2

∇ = differential operator, cm^{-1}

γ_A = mole fraction of component A

and

$$v_d = K_F' D_{AB} \nabla \gamma_A \qquad (7\text{-}2)$$

where

v_d = diffusiophoretic velocity, cm/sec

D_{AB} = binary diffusivity of component A through B, cm^2/sec

K_F' = a constant to be determined experimentally

In his derivation, Facy assumed that the particle did not affect the velocity distribution of the gas molecules. Also the constants K_F and K_F' were not determined experimentally.

Facy [7] also developed an equation for large aerosol particles for which the Knudsen number is very small. The force exerted on such a particle in a diffusing binary gas mixture in which one component is stationary is given by:

$$F_d = K_F^* D_p \nabla \gamma_A \qquad (7\text{-}3)$$

K_F^* = a constant to be determined experimentally, dynes

D_p = particle diameter, cm

Facy evaluated the steady state velocity by equating the diffusiophoretic force to the Stokes drag force to obtain

$$v_d = K_F^{**} D_{AB} \nabla \gamma_A \qquad (7\text{-}4)$$

The constants K_F^* and K_F^{**} were not determined experimentally.

Freise [8] studied the diffusiophoresis of small natural particles in liquids. In his experiments a butyl iodide drop was suspended in water. Butyl alcohol diffused from the butyl iodide drop into the water when the drop was saturated with butyl alcohol. On the other hand when the water was saturated with butyl alcohol, the butyl alcohol diffused from the water to the butyl iodide drop. Rubber particles suspended in the water were found to move in the direction of the diffusing alcohol. Freise suggested the particle velocity was identical to the Stefan flow velocity.

Because of the complex nature of the force mechanisms and the variety of initial assumptions that may be made regarding the velocity distribution, a large number of diffusiophoretic force equations [9, 10, 11, 12, 13, 14 and 15] have appeared. The available diffusiophoretic equations are summarized in Table 7.1.

B. Theoretical Analysis

In order to appreciate the phenomenon of diffusiophoresis consider a spherical particle suspended in an isothermal binary fluid mixture in which a concentration gradient exists as shown in Figure 7.1. From the two important length parameters involved:

i. the radius of the particle, R_p and

ii. the mean free path of the gas, λ

No.	Name	Year	Region	Diffusiophoretic Force Equation
1	Deryaguin, B. V. and Bakanov, S. P. [9]	1957	Free-Molecular	$F_d = -\frac{32}{3} R_p^2 \Gamma P_1 \frac{(v_p - v_1)}{v_1}$
2	Pacy, H. L. [6]	1958	Free-Molecular	$F_d = k_F A_p \nabla Y_A$
3	Pacy, H. L. [7]	1958	Slip-Flow	$F_d = k_F D_p \nabla Y_A$
4	Waldmann, L [10]	1958	Free-Molecular	$F_d = -\frac{32}{3} R_p^2 \Gamma (1 + \frac{\pi}{8} a_1) P_1 \frac{(v_p - v_1)}{v_1}$
5	Schmitt, K. H., and Waldmann, L [11, 12]	1960	Slip-Flow	Case 1: Average molecular velocity = 0 $F_d = -6\pi \mu R_p \left(\frac{M_A - M_B}{Y_A M_A + Y_B M_B + \sqrt{M_A M_B}}\right) D_{AB} \nabla Y_A$ Case 2: $F_d = -6\pi \mu R_p \left[1 + \left(\frac{M_A - M_B}{Y_A M_A + Y_B M_B + \sqrt{M_A M_B}}\right) Y_B\right] \frac{D_{AB}}{Y_B} \nabla Y_A$
6	Mason, E. A. and Chapman, S [13]	1962	Free-Molecular	$F_d = -\frac{32}{3} R_p^2 \Gamma (1 + \frac{4}{9} a_1) P_1 \frac{(v_p - v_1)}{v_1}$
7	Waldmann, L. and Schmitt, K. H. [17]	1966	Slip-Flow	$F_d = -6\pi \mu R_p \left[1 + \left(A_w \frac{M_A - M_B}{M_A + M_B} + B_w \frac{d_A - d_B}{d_A + d_B} Y_B\right)\right] \frac{D_{AB}}{Y_B} \nabla Y_A$
8	Brock, J. R. [14, 15]	1968	Transition	$F_d = -\frac{8}{3} R_p^2 C(2\pi m_A kT)^{1/2} (1 + \frac{\pi}{8}) \frac{D_{AB}}{Y_B} (\nabla Y_A) \left[1 - 0.071 \frac{2m_B}{(m_A + m_B)^{1/2}} \frac{R_p}{\lambda}\right]$

TABLE 7.1: Diffusiophoretic Force Equations

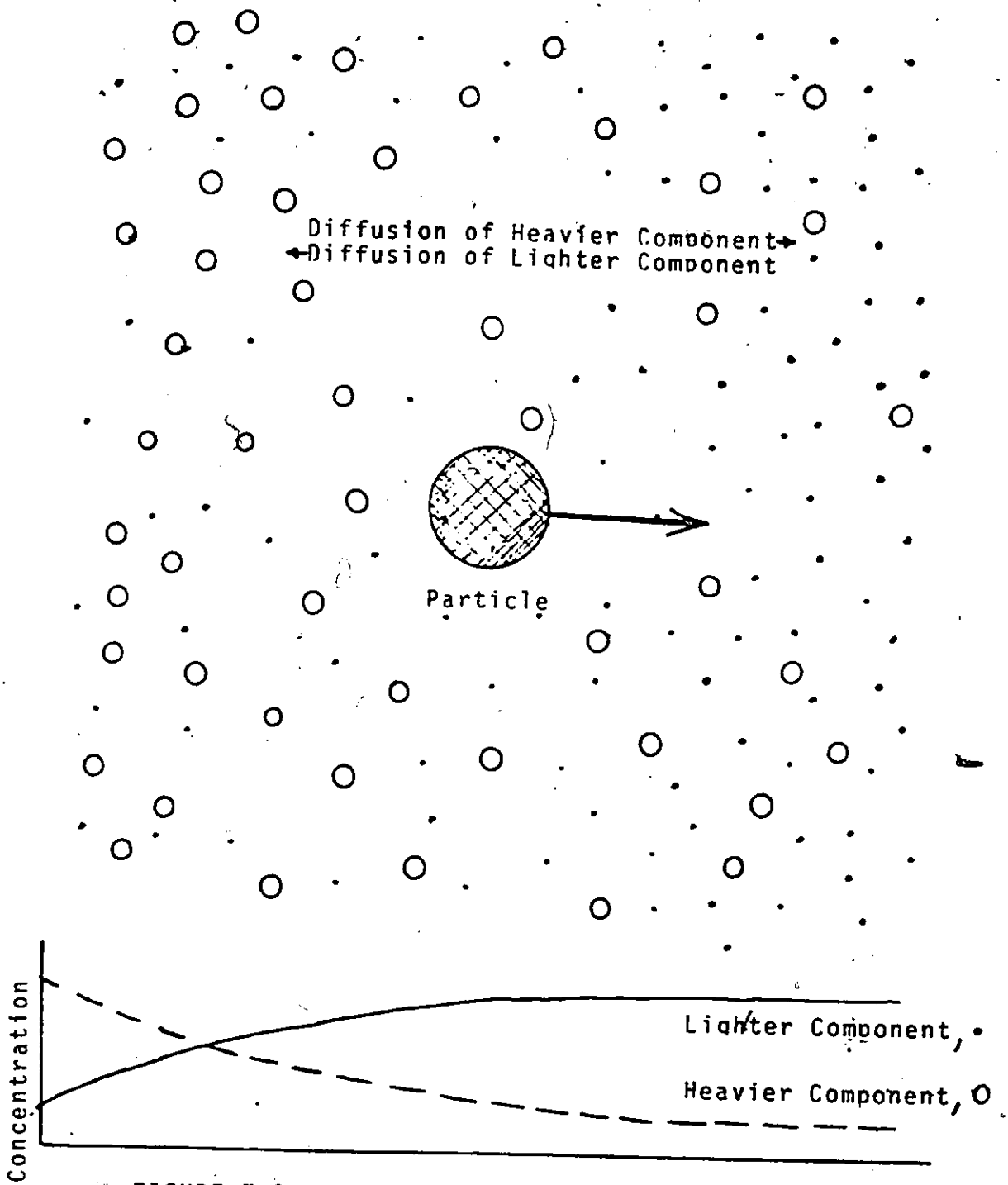

FIGURE 7.1: Spherical Particle in an Isothermal Binary Gas Mixture

the Knudsen number

$$N_{Kn_{R_p}} = \frac{\lambda}{R_p}$$

can be obtained.

As with the case of thermal force, three arbitrary classifications are used to facilitate analysis of the diffusiophoretic force: [20]

i. the slip-flow regime $0 < N_{Kn_{R_p}} < .25$

ii. the free-molecular regime, $10 < N_{Kn_{R_p}} < \infty$

iii. the transition regime $.25 < N_{Kn_{R_p}} < 10$

In the slip-flow regime, the mean free path of the gas, λ, is small compared to the size of the aerosol particle [$\lambda << R_p$ and $N_{Kn_{R_p}} \to 0$]. An acceptable theory for this set of conditions was developed by Schmitt and Waldmann [11].

In the free molecular regime, the mean free path of the gas, λ, is much greater than the size of the aerosol particle [$\lambda >> R_p$ and $N_{Kn_{R_p}} \to \infty$]. In this limiting case, the gas molecule velocity distribution function is not affected by the presence of the particle. Waldmann's [10] theory is valid for the free-molecular regime.

For the transition regime, where the mean free path of the gas, λ, is of the same order of magnitude as the size of the

particle, no reasonably acceptable theory has yet been developed.

No quantitative analysis has been reported in the literature for the diffusiophoretic force over the entire range of $0 < N_{Kn_{R_p}} < \infty$.

1. Slip-Flow Regime

Schmitt and Waldmann [11] developed a theory for the diffusiophoretic force in the slip-flow regime. A continuum mechanics approach was used to obtain expressions for both the diffusiophoretic force and velocity.

In their development, Schmitt and Waldmann specified the following boundary conditions:

i. Stefan flow (i.e. mass average velocity) prevailed far away from the particle

ii. the tangential velocity at the particle surface was assumed to be Kramers and Kistemaker's slip velocity [16].

Kramers and Kistemaker [16] had shown that the fluid velocity parallel to a solid surface does not vanish at the boundary when diffusion occurs parallel to the surface. In other words, a slippage of the gas occurs at the boundary. The velocity at the boundary was called 'diffusion-creep' analogously to 'thermal-creep'.

The Navier-Stokes equations for creeping flow around spheres were solved, subject to the assumptions previously made,

to obtain the diffusiophoretic force, F_d for two cases.

The diffusiophoretic force exerted on a particle at rest by an isothermal binary gas mixture, for which the average molecular velocity was taken to be zero, was given by [11]:

$$F_d = -6\pi\mu R_p \left(\frac{M_A - M_B}{\gamma_A M_A + \gamma_B M_B + \sqrt{M_A M_B}} \right) D_{AB} \nabla \gamma_A \qquad (7\text{-}5)$$

where

F_d = diffusiophoretic force, dynes

μ = viscosity of the mixture, gm/(cm sec)

R_p = radius of the particle, cm

M_A = molecular weight of component A, gm/gm-mole

M_B = molecular weight of component B, gm/gm-mole

γ_A = mole fraction of component A

γ_B = mole fraction of component B

D_{AB} = binary diffusivity of component A through B, cm^2/sec

∇ = differential operator, cm^{-1}

For a particle suspended in a stationary carrier gas (species B) through which a vapour (species A) is diffusing, the diffusiophoretic force, F_d, exerted on the particle by an isothermal binary gas mixture, for which an average molecular velocity exists, is given by [11]:

$$F_d = -6\pi\mu R_p \left[1 + \left(\frac{M_A - M_B}{\gamma_A M_A + \gamma_B M_B + \sqrt{M_A M_B}}\right)\gamma_B\right]\frac{D_{AB}}{\gamma_B}\nabla\gamma_A \qquad (7\text{-}6)$$

where

μ = viscosity of the mixture, gm/(cm sec)

R_p = radius of particle, cm

M_A = molecular weight of component A, gm/(gm-mole)

M_B = molecular weight of component B, gm/(gm-mole)

γ_A = mole fraction of component A

γ_B = mole fraction of component B

D_{AB} = binary diffusivity of component A through B, cm^2/sec

∇ = differential operator, cm^{-1}

In order to establish the validity of the diffusiophoretic force equation (7-5), Waldmann and Schmitt [17] performed experiments in a modified Millikan oil drop apparatus [18]. Experimental results did not agree with the values predicted by equation (7-5). After studying various gases, the authors suggested the following empirical relationship for the diffusiophoretic force in the slip-flow regime.

$$F_d = -6\pi\mu R_p \left[1 + \left(A_w \frac{M_A - M_B}{M_A + M_B} + B_w \frac{d_A - d_B}{d_A + d_B}\right)\gamma_B\right]\frac{D_{AB}}{\gamma_B}\nabla\gamma_A \qquad (7\text{-}7)$$

where

A_w and B_w = two empirical constants whose value depend on the gas mixture, dimensionless

d_A = diameter of molecule A, cm

d_B = diameter of molecule B, cm

2. Free-Molecular Regime

In the free-molecular regime, where the mean free path of the gas, λ, is much larger than the size of the aerosol particle [$\lambda >> R_p$ and $N_{Kn_{R_p}} \to \infty$], the heavier molecules striking the particle will have a greater momentum than the lighter molecules. Consequently a net momentum is imparted to the particle in the direction in which the heavier molecules are diffusing. That is, relative to a reference frame in which the diffusion fluxes are equal, the resulting velocity of the particle will be in the same direction as the heavier molecules are diffusing.

Waldmann [10] developed a diffusiophoretic force equation for the free-molecular regime by calculating the net momentum imparted to the particles on colliding with the gas molecules. In order to evaluate the net momentum imparted to the particles, a knowledge of the velocity distribution function of the approaching molecules and the law of reflection of the gas molecules by the particles was necessary.

Waldmann [10] assumed that the velocity distribution function of the gas molecules was not affected by the presence of the particle. The Chapman and Cowling approach [19] was used to express the velocity distribution function in terms of Sonine polynomials. The first term of this sum is the Maxwellian distribution and subsequent terms denote the deviation from Maxwellian behavior. Waldmann [10] neglected all terms after the second because considering further terms would have resulted in extremely complicated expressions.

In order to find the velocity distribution of molecules leaving the surface, Waldmann assumed that a fraction, equal to the "coefficient of diffuse reflection", a, undergoes diffuse reflection and the remaining fraction (1 - a) is specularly reflected.

The Waldmann [10] treatment considered a spherical particle suspended in an isothermal multi-gas mixture whose components "i" have different mass velocities, v_i. The approach yielded the force exerted by the gas on such a particle as a result of net momentum transferred to the particle in the form

$$F_g = - \frac{32}{3 \bar{v}_i} R_p^2 \Sigma \left\{ \left(1 + \frac{\pi}{8} a_i\right) p_i \left(v_p - v_i\right) \right\} \qquad (7\text{-}8)$$

Substituting the following relations:

$$\bar{v}_i = \sqrt{\frac{8\ kT}{\pi\ m_i}} \tag{4-49}$$

$$p_i = c_i kT \tag{7-9}$$

$$\gamma_i = \frac{c_i}{c} \tag{7-10}$$

into equation (7-8) gives

$$F_g = -\frac{2}{3} D_p^2 \sqrt{2\pi\ kT}\ \ c\ \Sigma\left\{\left(1 + \frac{\pi}{8} a_i\right) \gamma_i \sqrt{m_i}\ (v_p - v_i)\right\} \tag{7-11}$$

where

$\bar{v}_i$ = mean molecular velocity of component i, cm/sec

p_i = partial pressures of component i, dynes/cm^2

a_i = coefficient of diffuse reflection

R_p = radius of particle, cm

v_p = velocity of particle, cm/sec

v_i = mass velocity of component i, cm/sec

m_i = molecular mass of component i, gm

k = Boltzmann's constant, dyne cm/°K

T = absolute temperature of gas mixture, °K

γ_i = mole fraction of component i

c = molar density of gas mixture, gm-moles/cm^3

c_i = molar density of component i, gm-moles/cm^3

REFERENCES

1. Waldmann, L., and Schmitt, K. H., Thermophoresis and Diffusiophoresis of Aerosols, Aerosol Science, Edited by Davies, C. N., Academic Press, New York, p. 137 (1966).

2. Aitken, J., On the Formation of Small Clear Spaces in Dusty Air, Trans. Roy. Soc., Edinb., 32, 239 (1884).

3. *Deryaguin, B. V., and Dukhin, S. S., Diffusional Forces of Aerosol Particles, Doklady Akad. Nauk SSSR, 106, 851 (1956).

4. Deryaguin, B. V., and Dukhin, S. S., The Precipitation of Aerosol Particles at Interfaces Dust-Collection by a Diffusion Method. Importance to Medicine, Doklady Akad. Nauk SSSR, 111, 613 (1956).

5. Deryaguin, B. V., and Dukhin, S. S., The Theory of Force Interface of Resting Droplets at Any Distance at Phychometric Temperature, Doklady Akad. Nauk SSSR, 112, 445 (1957).

6. Facy, M. L., Sur un Mechanisme de Capture des Particules d' Aerosols par me une Gouttelette en Voie de Condensation-Evaporation, Compt. Rendus, 246, 3161 (1958).

7. Facy, M. L., Sur le Deplacement des Particules d'Aerosols au Cours des Processus de Diffusion Moleculaire, Compt. Rendus, 246, 102 (1958).

8. Freise, V., Mise En Evidence Du Courant De Convection Provoque Par la Diffusion, J. Chimie Physique, 54, 879 (1957).

9. Deryaguin, B. V., and Bakanov, S. P., The Theory of the Motion of Small Aerosol Particles in a Diffusion Field, Soviet Physics Doklady, 2, 563 (1957).

10. Waldmann, L., Wher die Kraft Eines Inhomogenen Gases auf Kleine Suspendierte Kugeln, Zeits. fur Naturf. 14a, 589 (1959).

11. Schmitt, K. H., Untersuchungen an Schwebstoffleilchen in Diffundierenden Gasen, Zeits. fur Naturf. 15a, 843 (1960).

12. Schmitt, K. H., Untersuchungen an Schwebstoffteilchen in Diffundierenden Wasserdamf, Zeits. fur Naturf. 16a, 144 (1961).

13. Mason, E. A, and Chapman, S., Motion of Small Suspended Particles in Nonuniform Gases, J. Chem. Phys. 36, 627 (1962).

*denotes incomplete holdings at time of writing

14. Brock, J. R., Forces on Aerosols in Gas Mixtures, J. Colloid Sci., 18, 489 (1963).

15. Brock, J. R., The Diffusion Force in the Transition Region of Knudsen Number, J. Colloid and Interface Sci., 27, 95 (1968).

16. Kramers, H. A., and Kistemaker, J., On the Slip of a Diffusing Gas Mixture Along a Wall, Physica, 10, 699 (1943).

17. Waldmann, L., and Schmitt, K. H., Thermophoresis and Diffusiophoresis of Aerosols, Aerosol Science, Edited by Davies, C. N., Academic Press, New York, p. 137 (1966).

18. Millikan, R. A., The Isolation of an Ion, A Precision Measurement of its Charge and The Correction of Stokes Law, Phy. Rev. 32, 382 (1911).

19. Chapman, S., and Cowling, T. G., The Mathematical Theory of Gases, Cambridge University Press, Cambridge (1964).

20. Hidy, G. M., Theory of Diffusive and Impactive Scavenging, p. 355, Proceedings of Precipitation Scavenging 1970 Symposium, Richland, Washington, June 1970, NTIS No. Conf. 700601.

VIII. DIFFUSIOPHORETIC VELOCITY

Aerosol particles suspended in a non-uniform but isothermal gas mixture move due to existing concentration gradients. In the steady state, under the influence of a concentration gradient in the gas mixture and friction, aerosol particles move with a constant velocity, v_d called the 'diffusiophoretic velocity'.

The force exerted by the gas on such particle is given by

$$F_g = F_d - F_D \tag{8-1}$$

where

F_g = force exerted by the gas on a moving particle, dynes

F_D = drag force, dynes

F_d = diffusiophoretic force, dynes

For the steady state case, the force F_g must vanish and the diffusiophoretic force, F_d, must be equal to the drag force, F_D.

In order to obtain the diffusiophoretic velocity, it is necessary to know either the force exerted by the gas, F_g, on the particle or the drag force, F_D.

A. Slip-Flow Regime

In the slip-flow regime, where the mean free path of the gas, λ, is small compared to the size of the aerosol particle [$\lambda << R_p$ and $N_{Kn_{R_p}} \rightarrow 0$], the drag force, F_D is given by Stokes law equation (5-2).

$$F_D = 6 \pi \mu R_p v_d \tag{5-2}$$

The diffusiophoretic force, F_d, exerted on the particle at rest by an isothermal binary gas mixture for which the average molecular velocity is taken to be zero, is given by Schmitt and Waldmann [1] as:

$$F_d = - 6 \pi \mu R_p \left(\frac{M_A - M_B}{\gamma_A M_A + \gamma_B M_B + \sqrt{M_A M_B}}\right) D_{AB} \nabla \gamma_A \tag{7-5}$$

Since the drag force, F_D must be equal to the diffusiophoretic force, F_d at steady-state, an otherwise free particle suspended in an isothermal binary gas mixture moves with the velocity [2]:

$$v_d = - \left(\frac{M_A - M_B}{\gamma_A M_A + \gamma_B M_B + \sqrt{M_A M_B}}\right) D_{AB} \nabla \gamma_A \tag{8-2}$$

where

v_d = diffusiophoretic velocity, cm/sec.

M_A = molecular weight of component A, gm/gm-mole

M_B = molecular weight of component B, gm/gm-mole

γ_A = mole fraction of component A

γ_B = mole fraction of component B

D_{AB} = binary diffusivity of component A through B, $cm^2/sec.$

The diffusiophoretic force, F_d, acting on a particle suspended in a stationary carrier gas (species B) through which a vapor (species A) is diffusing at a rate defined by an average molecular velocity is given by Schmitt and Waldmann [1] as

$$F_d = - 6\pi \mu R_p \left[1 + \left(\frac{M_A - M_B}{\gamma_A M_A + \gamma_B M_B + \sqrt{M_A M_B}}\right)\gamma_B\right] \frac{D_{AB}}{\gamma_B} \nabla \gamma_A \qquad (7\text{-}6)$$

Employing equation (7-6) and equation (5-2), the particle velocity [2] in the vapor diffusion field becomes

$$v_d = - \left[1 + \left(\frac{M_A - M_B}{\gamma_A M_A + \gamma_B M_B + \sqrt{M_A M_B}}\right)\gamma_B\right] \frac{D_{AB}}{\gamma_B} \nabla \gamma_A \qquad (8\text{-}3)$$

where

v_d = diffusiophoretic velocity, cm/sec

M_A = molecular weight of component A, gm/gm-mole

M_B = molecular weight of component B, gm/gm-mole

γ_A = mole fraction of component A

γ_B = mole fraction of component B

D_{AB} = binary diffusivity of component A through B, $cm^2/sec.$

B. Free-Molecular Regime

In the free-molecular regime, where the mean free path of the gas is larger than the size of the particle [$\lambda >> R_p$ and $N_{Kn_{R_p}} \to \infty$], the particle is considered to be a large molecule. In this case, the force exerted by the gas on a particle suspended in an isothermal multi-gas mixture is given by Waldmann [3] as:

$$F_g = -\frac{2}{3} D_p^2 \sqrt{2\pi kT}\, c \sum_i \left\{\left(1 + \frac{\pi}{8} a_i\right) \gamma_i \sqrt{m_i}\, (v_p - v_i)\right\} \qquad (7\text{-}11)$$

In the steady-state, the force F_g must vanish. Thus, under the influence of the diffusiophoretic force and drag the otherwise free particle moves with the velocity

$$v_p = \frac{\left(1 + \frac{\pi}{8} a_1\right)\sqrt{m_1}\, \gamma_1 v_1 + \left(1 + \frac{\pi}{8} a_2\right) \sqrt{m_2}\, \gamma_2 v_2 + \ldots}{\left\{\sum_i \left(1 + \frac{\pi}{8} a_i\right) \sqrt{m_i}\, \gamma_i\right\}} \qquad (8\text{-}4)$$

By introducing

$$\sigma_i = \frac{\left(1 + \frac{\pi}{8} a_i\right) \gamma_i \sqrt{m_i}}{\sum_k \left\{\left(1 + \frac{\pi}{8} a_k\right) \gamma_k \sqrt{m_k}\right\}}; \quad \text{where } \Sigma \sigma_i = 1 \qquad (8\text{-}5)$$

and

$$v_p = \Sigma \sigma_i v_i \tag{8-6}$$

where

v_p = diffusiophoretic velocity, cm/sec

a_i = thermal reflection coefficient of component i

γ_i = mole fraction of component i

m_i = molecular mass of component i, gm

v_i = molecular velocity of component i, cm/sec.

Equation (8-4) can be rewritten by introducing diffusion velocities either in the local reference system moving with mass average velocity, u, or the local particle reference system moving with average molecular velocity, w.

If the mass diffusion velocity, V_i and the particle diffusion velocity, W_i, are defined [4]:

$$v_i - u = V_i \tag{8-7}$$

$$v_i - w = W_i \tag{8-8}$$

it follows that

$$v_i = u + V_i = w + W_i \tag{8-9}$$

where by definition [2]

$$u = \frac{\sum_i \rho_i v_i}{\sum \rho_i} = \sum \tau_i v_i \qquad (8\text{-}10)$$

and

$$w = \frac{\sum m_i v_i}{\sum m_i} = \sum \gamma_i v_i \qquad (8\text{-}11)$$

The quantities $\tau_i = \frac{\rho_i}{\rho} = \frac{m_i}{m} \gamma_i$

where $(\rho_i = m_i c_i,\ \rho = \sum \rho_i = mc)$ (8-12)

are the mass fractions of the mixture. Since $\sum \sigma_i = 1$, equation (8-6) transforms to

$$v_p = u + \sum \sigma_i V_i = w + \sum \sigma_i W_i \qquad (8\text{-}13)$$

Fick's diffusion law is introduced to discuss special cases. For simplicity, a binary mixture is considered. Fick's law expressed in terms of molecular diffusion velocities and mole fractions, is then

$$\gamma_1 W_1 = -\gamma_2 W_2 = -D_{12} \nabla \gamma_1 \qquad (8\text{-}14)$$

where

D_{12} = binary diffusivity of component 1 through 2, cm^2/sec.

Two specific cases [2] will be considered in some detail. For the first case, in which the average molecular

velocity of the mixture is taken to be zero, it can be shown that for a multi-gas mixture diffusing the relationship

$$v_p = \sum_i \sigma_i W_i \tag{8-15}$$

is obtained from equation (8-13). By expanding equation (8-15) for a binary mixture, the diffusiophoretic velocity is obtained as

$$v_p = - \frac{(1 + \frac{\pi}{8} a_1) \sqrt{m_1} - (1 + \frac{\pi}{8} a_2) \sqrt{m_2}}{(1 + \frac{\pi}{8} a_1) \gamma_1 \sqrt{m_1} + (1 + \frac{\pi}{8} a_2) \gamma_2 \sqrt{m_2}} D_{12} \nabla \gamma_1 \tag{8-16}$$

When $a_1 = a_2$, equation (8-16) reduces to

$$v_p = - \frac{\sqrt{m_1} - \sqrt{m_2}}{\gamma_1 \sqrt{m_1} + \gamma_2 \sqrt{m_2}} D_{12} \nabla \gamma_1 \tag{8-17}$$

This implies that aerosol particles move in the direction of the diffusion flux, $\gamma_1 W_1$ of the heavier component. When $m_1 = m_2$ (i.e. equal molecular masses), a small suspended particle will not move.

In order to compare the diffusiophoretic velocity with the average mass velocity, u, of the diffusing gas, the average mass velocity can be written from equations (8-10), (8-11) and (8-12) in the form:

$$u = w + \sum_i \tau_i W_i$$

$$= w + \sum_i \frac{m_i}{m} \gamma_i W_i \tag{8-18}$$

For a binary mixture with w = 0

$$u = \left(\frac{m_1 - m_2}{m}\right) \gamma_1 W_1 \tag{8-19}$$

from equation (8-18)

Substituting $\gamma_1 W_1$ from equation (8-14) into equation (8-19) yields

$$u = -\left(\frac{m_1 - m_2}{m}\right) D_{12} \nabla \gamma_1 \tag{8-20}$$

With $m = m_1 \gamma_1 + m_2 \gamma_2$, equation (8-17) becomes

$$v_p = -\left(\frac{m_1 - m_2}{m_1 + \sqrt{m_1 m_2}}\right) D_{12} \nabla \gamma_1 \tag{8-21}$$

If $m_1 \approx m_2$

$$v_p \approx -\frac{1}{2}\left(\frac{m_1 - m_2}{m}\right) D_{12} \nabla \gamma_1$$

$$\approx \frac{1}{2} u \tag{8-22}$$

and the particle moves with half of the average mass velocity of the gas. But if $m_1 >> m_2$ and $\gamma_1 \approx \gamma_2$, the particle moves at a rate equivalent to the average mass velocity of the gas.

The other case concerns vapour molecules (species 1) diffusing through an inert stationary gas (species 2, $v_2 = 0$). For this system the average mass and average molecular velocities are not zero. When $v_2 = 0$, equation (8-9) reduces to

$$w = -W_2 \tag{8-23}$$

Substituting equation (8-14) into equation (8-23) yields

$$w = -W_2 = -\frac{1}{\gamma_2} D_{12} \nabla \gamma_1 \tag{8-24}$$

Similarly,

$$v_1 = w + W_1 = -W_2 + W_1$$

$$= -\frac{1}{\gamma_2} D_{12} \nabla \gamma_1 - \frac{1}{\gamma_1} D_{12} \nabla \gamma_1$$

$$= \frac{-1}{\gamma_1 \gamma_2} D_{12} \nabla \gamma_1 \tag{8-25}$$

From equations (8-24) and (8-25)

$$v_1 = \frac{1}{\gamma_1} w \tag{8-26}$$

With v_1 from equations (8-25) and (8-26), the steady state velocity of a small suspended particle can be obtained from equation (8-6) in the form:

$$v_p = -\frac{\sigma_1}{\gamma_1}\frac{1}{\gamma_2}D_{12}\nabla\gamma_1 = \frac{\sigma_1}{\gamma_1}w \qquad (8\text{-}27)$$

where

$$\sigma_1 = \frac{(1+\frac{\pi}{8}a_1)\gamma_1\sqrt{m_1}}{(1+\frac{\pi}{8}a_1)\gamma_1\sqrt{m_1}+(1+\frac{\pi}{8}a_2)\gamma_2\sqrt{m_2}} \qquad (8\text{-}28)$$

If $m_1 = m_2$ (i.e. equal molecular masses) and $a_1 = a_2$

$$\text{then } \frac{\sigma_1}{\gamma_1} = 1 \qquad (8\text{-}29)$$

and

$$v_p = -\frac{1}{\gamma_2}D_{12}\nabla\gamma_1 = w \qquad (8\text{-}30)$$

In order to compare the diffusiophoretic velocity, v_p, with the mass average velocity, u, of the diffusing gas, the mass average velocity can be written from equations (8-10), (8-11), and (8-26) as:

$$u = \tau_1 v_1 = \frac{\tau_1}{\gamma_1}w = \frac{m_1}{m}w \qquad (8\text{-}31)$$

Substituting for w from equation (8-31) into equation (8-27) yields

$$v_p = \frac{\sigma_1 m}{\gamma_1 m_1}u \qquad (8\text{-}32)$$

where

v_p = diffusiophoretic velocity, cm/sec

m = molecular mass of mixture, gm

m_1 = molecular mass of component 1, gm

u = average mass velocity, cm/sec

This means that the particles do not move with the average mass velocity. Now, the particle velocity is dependent upon the composition and the molecular mass ratio of the gas. Nevertheless the particle velocity is always in the same direction as the average mass velocity, u, or average molecular velocity, w.

REFERENCES

1. Schmitt, K. H., and Waldmann, L., Untersuchungen an Schwebstoffteilchen in Diffundierendun Gasen, Zeits. fur Naturf. 15a, 843 (1960).

2. Waldmann, L., and Schmitt, K. H., Thermophoresis and Diffusiophoresis of Aerosols, Edited by Davies, C. N., Academic Press, New York p. 13 (1966).

3. Waldmann, L., Wher die Kraft Eines Inhomogenen Gases auf Kleine Suspendierte Kugeln, Zeits. fur Naturf. 14a, 589 (1959).

4. Bird, R. B., Steward, W. E., and Lightfoot, E. N., Transport Phenomena, John Wiley and Sons, Inc. New York, p. 497 (1966)

IX. EXPERIMENTAL INVESTIGATIONS

Diffusiophoresis is a phenomenon involving aerosol particles that move as a result of concentration gradients established in a non-uniform, but isothermal gas mixture. Quantitative investigations on diffusiophoresis are reviewed briefly to establish

i. the validity of theoretical analyses, and

ii. the quantitative inconsistencies that have been reported.

A. Schmitt and Waldmann

The experimental investigations by Schmitt and Waldmann [1, 2] were specifically oriented towards the validation of their theoretical analyses [3, 4].

1. Equipment

Figure 9.1 shows schematically the arrangement of apparatus for measurements in a diffusion field. The two gases, which mix by diffusion, were initially in the large equal volume vessels, V_1 and V_2. A Millikan condensor, consisting of two circular screens N_1 and N_2 was placed in the middle of a small vertical tube connecting the two vessels. The aerosol particles,

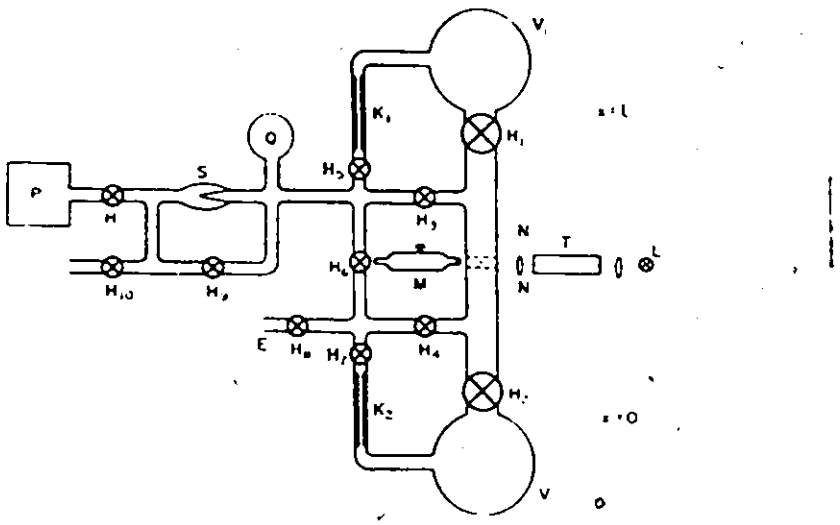

FIGURE 9.1: Apparatus for Diffusiophoresis Measurements [2]

situated between the screens, were illuminated by the lamp L through the trough T. These particles were observed through the microscope M. The pressure which could be lowered by means of a pump P, was monitored by a mercury pressure gauge Q.

2. Experimental Method

The upper vessel, V_1, was filled with the lighter gas component while the lower vessel, V_2, contained the heavier gas. Schmitt and Waldmann used mixtures of N_2 with H_2, C_2H_2, C_2H_4 (isobar), C_2H_6, O_2, Ar, CO_2, C_3H_8 and CO_2 with C_3H_8 (isobar). The experimental temperature was always about 20°C.

The aerosol was brought between the screens N_1 and N_2 through the inlet E. The particle diameter could be determined by observing the speed of free fall of that aerosol particle through the microscope M.

In order to measure diffusion at atmospheric pressure, the taps H_1 and H_2 to the vessels containing the two gas components were opened. After a linear concentration gradient was attained in the connecting tube, times of free fall and rise of an aerosol particle were measured. The taps H_1 and H_2 were then closed. The gas in the connecting tube now had the same composition as during the time of diffusion. Once again, times of free fall and rise of an aerosol particle in the homogeneous gas mixture were measured and the corresponding speeds were calculated.

The difference in the speeds with and without diffusion yielded the diffusiophoretic speed of the particle.

3. Results

Figure 9.2 shows, in terms of a dimensionless scale, the diffusiophoretic velocity of silicone oil drops in the diffusion field of N_2 with C_2H_2, C_2H_4 (isobar), C_2H_6, O_2, Ar, C_3H_8 (isobar) and CO_2 with C_3H_8 (isobar). The diffusion coefficients for the reduction of the velocities are given on the right side. The experimental curves are dashed for small $\frac{R_p}{\lambda}$ ratios, since

the measurements are difficult to make because of rapid diffusion. Theoretical values, given by the Waldmann equation (8-17) for the free-molecular regime, are indicated by the horizontal lines on the left side. A reasonably good agreement with equation (8-17) for $\frac{R_p}{\lambda} << 1$ is indicated by Figure 9.2.

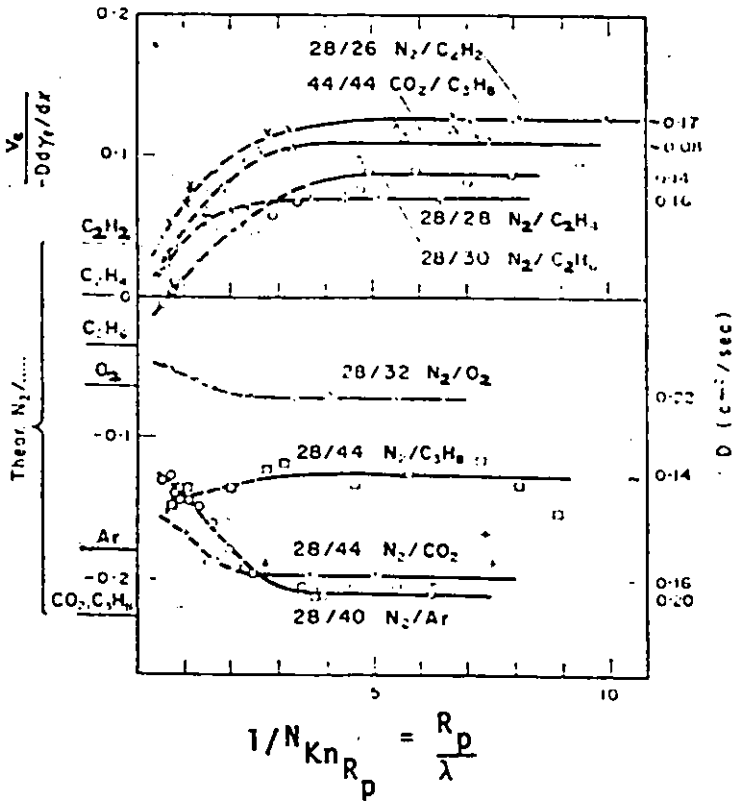

FIGURE 9.2: Reduced Diffusiophoretic Velocity of Silicone Oil Drops in Mixtures of N_2 with Different Gases and CO_2 with C_3H_8. D refers to 1 atmosphere 293°K; the Numbers on the Curves Denote Molecular Weights [2]

For the slip-flow regime, the measured values of the factor

$$\epsilon = A_w\left(\frac{M_A - M_B}{M_A + M_B}\right) + B_w\left(\frac{d_A - d_B}{d_A + d_B}\right) \qquad (9\text{-}1)$$

in the diffusiophoretic force equation (7-7) are in excellent agreement with the calculated values as shown in Table 9-1.

B. Goldsmith et. al

Goldsmith, Delafied, Cox and May [5, 6] showed that diffusiophoresis could be employed to separate submicron particles continuously from a gas stream.

1. Equipment

Figure 9-3 shows a schematic representation of the experimental arrangement. Nichrome aerosols were generated by passing dry filtered air over an electrically heated nichrome wire. The particles were made radioactive by adsorbing thorium on them. A Pollak counter [7] was used to detect the radioactive particles. The vapour pressure gradient box was prepared by placing two lining papers, saturated in sulphuric acid and water respectively, on each plate of the box as shown in Figure 9.3.

2. Experimental Method

The marked nichrome aerosol was passed between two parallel plates with spacing ranging from 2 to 6 mm. Across the

Gas	N_2	H_2	C_2H_2	C_2H_4	C_2H_6	D_2	A_r	CO_2	C_3H_8	CO_2/C_3H_8
Molecular Weight, M	28	2	26	28	30	32	40	44	44	--
Diameter, d(Å)	3.68	2.97	4.22	4.23	4.42	3.43	3.42	4.00	5.06	--
μ(Poise) 20°C	175	88	102	101	92	203	222	147	80	--
D (cm^2/sec) 20°C, 760 Torr	--	0.76	0.17	0.16	0.14	0.22	0.20	0.16	0.14	0.18
ε (measured)		0.9	0.13	0.073	0.085	-0.10	-0.22	-0.20	-0.13	0.11
ε (calculated)		0.65	0.11	0.073	0.063	-0.10	-0.21	-0.17	-0.04	0.12
% Relative Error		-38.0	-18.0	0	-35.0	0	5.0	18	225	8.0

TABLE 9-1: Comparison of Measured Values of ε with the Calculated Values According to Equation (8-3) with A_W = 0.95 and B_W = -1.05 [2]

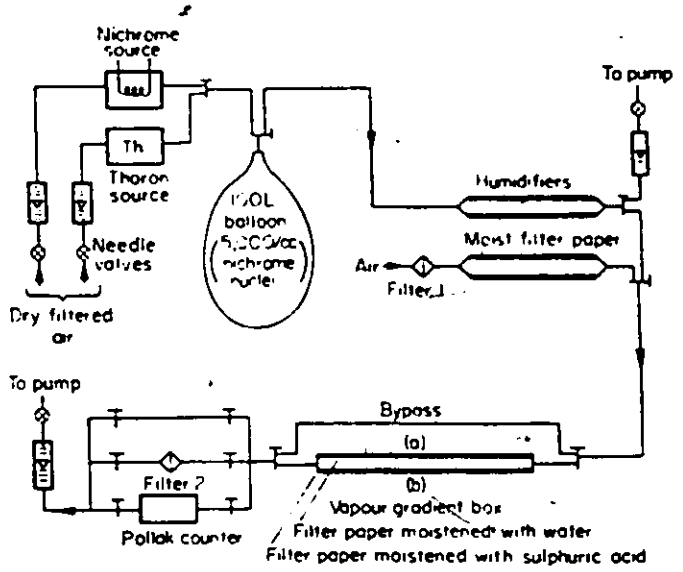

FIGURE 9-3: The Experimental Arrangement Used in the Measurement of Velocities Imposed on Particles by Diffusing Water Vapor in Air [6]

spacing controlled water-vapor pressure gradients were achieved by the strength of sulphuric acid. Both millipore filter and Pollak counter measurements of the aerosol were taken for each vapor pressure gradient.

3. Experimental Results

In all measurements, the filter paper saturated with sulphuric acid was found to be radioactive. This indicated that the particles were deposited on the surface towards which the vapor diffused.

The velocity of the submicron particles was a linear function of the vapour pressure gradient as shown in Figure 9.4. The magnitude of the diffusiophoretic velocity was given by

$$v_d = \left(1.9 \times 10^{-4}\right) \frac{dp_1}{dx} \qquad \text{where} \qquad (9.2)$$

$\frac{dp_1}{dx}$ = water vapour pressure gradient in x-direction, mb/cm

v_d = diffusiophoretic velocity, cm/sec

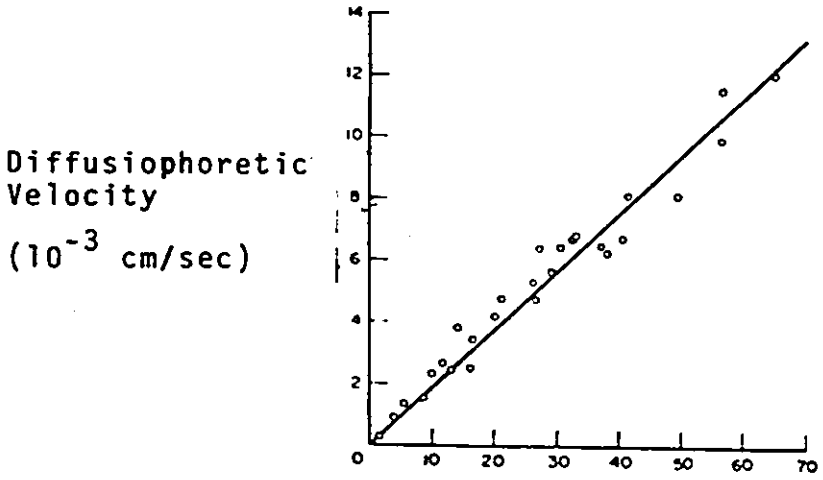

FIGURE 9.4: The Diffusiophoretic Velocity in Air as a Function of Water-Vapour Pressure Gradient [6]

For the case where $\gamma_1 << \gamma_2$ (i.e. the water vapor pressure small compared to the total pressure), Waldmann's diffusiophoretic equation (8.17) reduces to

$$v_d = - \frac{\sqrt{m_1}}{\gamma_1 \sqrt{m_1} + \gamma_2 \sqrt{m_2}} \frac{D_{12}}{p_2} \frac{dp_1}{dx} \qquad (9.3)$$

where

$\frac{dp_1}{dx}$ = partial pressure gradient of vapour in x-direction, mb/cm

m_1 = molecular mass of vapor, gm

m_2 = molecular mass of gas, gm

γ_1 = mole fraction of vapor

γ_2 = mole fraction of gas

D_{12} = binary diffusivity of component 1 through, 2, cm^2/sec

Substituting in equation (9.2) for water vapor diffusing in air at standard temperature and pressure yields the equation

$$v_d = -\left(1.89 \times 10^{-4}\right) \frac{dp_1}{dx} \qquad \text{where} \qquad (9.4)$$

$\frac{dp_1}{dx}$ = partial pressure gradient of vapour in x-direction, mb/cm

v_d = diffusiophoretic velocity, cm/sec

Equation (9.4) is in excellent agreement with the experimental result given by equation (9.2).

REFERENCES

1. Schmitt, K. H., Untersuchungen an Schwebstoffteilchen in Diffundierenden Wasserdamf Zeits. fur Naturf. 16a, 144 (1961).

2. Schmitt, K. H., and Waldmann, L., Thermophoresis and Diffusiophoresis of Aerosols, Aerosol Science, Edited by Davies, C. N., Academic Press, New York (1966).

3. Waldmann, L., Wher die Kraft Eines Inhomogenen Gases auf Kleine Suspendierte Kugeln, Zeits. fur Naturf. 14a, 589 (1959).

4. Schmitt, K. H., and Waldmann, L., Untersuchungen an Schwebsto ffteilchen in Diffundierenden Gasen, Zeits. fur Naturf. 15a, 843 (1960).

5. Goldsmith, P., Delafied, H. J., and Cox, L. C., The Role of Diffusiophoresis in the Seavenging of Radioactive Particles From the Atmosphere, Quarterly J. Roy. Met. Soc., 89, 43 (1963).

6. Goldsmith, P., and May, F. G., Diffusiophoresis and Thermophoresis in Water Vapour Systems, Aerosol Science, Edited by Davies, C. N., Academic Press, p. 163 (1966).

7. *Metnieks, A. L., and Pollak, L. W., Geophy. Bull., Dublin 16 (1959).

*denotes incomplete holdings at time of writing

X. ANALYSIS OF FINE PARTICULATE COLLECTION MECHANISMS FOR COUNTER-CURRENT FLOW IN A SPRAY SCRUBBER

In the absence of reliable experimental performance evaluations gas cleaning devices have been rated solely on the basis of theoretical analyses. Traditionally, Ministry of the Environment personnel have essentially used the design criteria of Calvert [1], which account for particle collection by inertial impaction only. As might be expected such evaluations invariably fall short of manufacturer's claims. One possible solution to this dilemma would involve rigorous field testing of each piece of control equipment to obtain grade efficiency curves relating particulate collection efficiency to particle size. In principle such curves can be developed for any gas cleaning device because reliable grain loading and particle sizing techniques are available; however, the costs become prohibitive when several alternate control units are considered for any specific source. As a result, the ability to model each type of collector in terms of fundamental collection mechanisms is still of paramount importance.

In view of the increasing emphasis on the collection of fine particulate matter (loosely defined as solid or liquid airborne aerosols less than 3-5 microns) which

cannot be removed economically by inertial impaction, pollution control equipment manufacturers are striving to utilize collection mechanisms which were previously neglected. Fine particle removal is considered in terms of flux forces resulting from temperature, concentration and electrical gradients, and from the flux of matter or energy as well as magnetic fields.

This critical review of theoretical and experimental studies on thermophoresis (temperature gradient phenomenon) and diffusiophoresis (concentration gradient phenomenon) provides design and approvals engineers with a comprehensive background on these two potentially promising techniques for fine particulate removal. Consistent with the aims of the overall research program, emphasis is focussed on demonstrating the application of diffusiophoresis and thermophoresis to the modelling of wet scrubbers.

A counterflow spray tower has been chosen initially for detailed analysis to demonstrate the derivation of design curves for collection by:

i. inertial impaction
ii. interception
iii. Brownian diffusion
iv. thermophoresis, and
v. diffusiophoresis

Single Drop Collection Efficiency for Flux Force Mechanism

A single drop collection efficiency is normally defined as the fraction of particles within the limiting stream lines approaching the single drop collector which are deposited on the collecting drop. The rate at which particles approach the spherical droplet collector is given by:

$$\underbrace{\left[\begin{array}{l}\text{projected area}\\ \text{of spherical}\\ \text{collector}\end{array}\right]}_{\pi R_c^2} \underbrace{\left[\begin{array}{l}\text{relative}\\ \text{gas}\\ \text{velocity of}\\ \text{approach to}\\ \text{collector}\end{array}\right]}_{v_{rel}} \underbrace{\left[\begin{array}{l}\text{number of}\\ \text{solid parti-}\\ \text{cles per}\\ \text{unit volume}\\ \text{of gas}\end{array}\right]}_{n_p} = \pi R_c^2 \, v_{rel} \, n_p$$

where

R_c = radius of collecting drop, cm

v_{rel} = free stream gas velocity relative to sphere, cm/sec

n_p = number of solid particles per unit volume, particles/cm^3

The deposition rate on a single drop by any flux mechanism can be expressed as:

$$\underbrace{\left[\begin{array}{l}\text{surface area}\\ \text{per drop}\end{array}\right]}_{4\pi R_c^2} \cdot \underbrace{\left[\begin{array}{l}\text{particle flux}\\ \text{due to flux}\\ \text{force}\end{array}\right]}_{N_F = u_F n_p} = 4\pi R_c^2 \, u_F \, n_p$$

where

u_F = particle velocity due to flux force, cm/sec

N_F = solid particle flux due to flux force, particles/$(cm^2 sec)$

The efficiency of particle collection due to a flux mechanism thus becomes

$$\eta_F = \frac{(4\pi R_c^2) u_F \; n_p}{(\pi R_c^2) \; v_{rel} \; n_p} = \left(\frac{4u_F}{v_{rel}}\right) \qquad (10\text{-}1)$$

where

η_F = single drop collection efficiency due to any flux force

The ratio, u_F/v_{rel}, is defined as the flux deposition number [2]:

$$N_{FD} = \frac{u_F}{v_{rel}} = \frac{\text{particle transport by flux forces}}{\text{particle transport by fluid flow}} \qquad (10\text{-}2)$$

so that

$$\eta_F = 4N_{FD} \qquad (10\text{-}3)$$

Calvert et al [2] have shown that the flux deposition number can be related to a modified form of the Peclet number,

N_{Pe}, and that comparable mathematical models exist for deposition by diffusion and flux forces.

B. Overall Collection Efficiency Expressions for Counter-Current Flow in a Spray Scrubber

Expressions for overall collection efficiencies due to inertial impaction, interception, Brownian diffusion and flux forces are derived in order to assess the relative importance of each mechanism.

1. Inertial Impaction

In this derivation of the overall collection efficiency due to inertial impaction, it is assumed that:

i. liquid distribution is uniform

ii. particulate and collector drop sizes are uniform

iii. flow rates of liquid and gas are uniform

iv. distribution of particulates in any horizontal plane is uniform

v. liquid drop hold-up is constant throughout the scrubber

vi. no wall losses for particulate and liquid occur

vii. no condensation or evaporation occur

An elemental volume of cross-sectional area A_1 and height, dz, in a counter-current spray scrubber is shown in Figure 10-1. For the element, input - output = 0 since there is neither accumulation nor generation of particulates in the system. A mass balance on the particulates can be expressed as:

$$\left\{\begin{array}{l}\text{rate at}\\ \text{which part-}\\ \text{iculates are}\\ \text{entering the}\\ \text{scrubber with}\\ \text{the gas}\\ \text{stream}\end{array}\right\} - \left\{\begin{array}{l}\text{rate at}\\ \text{which part-}\\ \text{iculates are}\\ \text{leaving the}\\ \text{scrubber in}\\ \text{the gas}\\ \text{stream}\end{array}\right\} - \left\{\begin{array}{l}\text{rate of}\\ \text{particulate}\\ \text{removal by}\\ \text{liquid}\\ \text{droplets}\end{array}\right\} = 0$$

to yield

$$v_g A_1 C_1 - v_g A_1 \left(C_1 + \frac{dC_1}{dz} dz\right) - \left\{\begin{array}{l}\text{particulate}\\ \text{removal rate}\\ \text{by liquid}\\ \text{droplets}\end{array}\right\} = 0 \qquad (10\text{-}4)$$

where

v_g = velocity of gas stream, cm/sec

A_1 = cross-sectional area of scrubber, cm^2

C_1 = concentration of particulate at position, z, in the scrubber, gm/cm^3

$\frac{dC_1}{dz}$ = concentration gradient, gm/cm^4

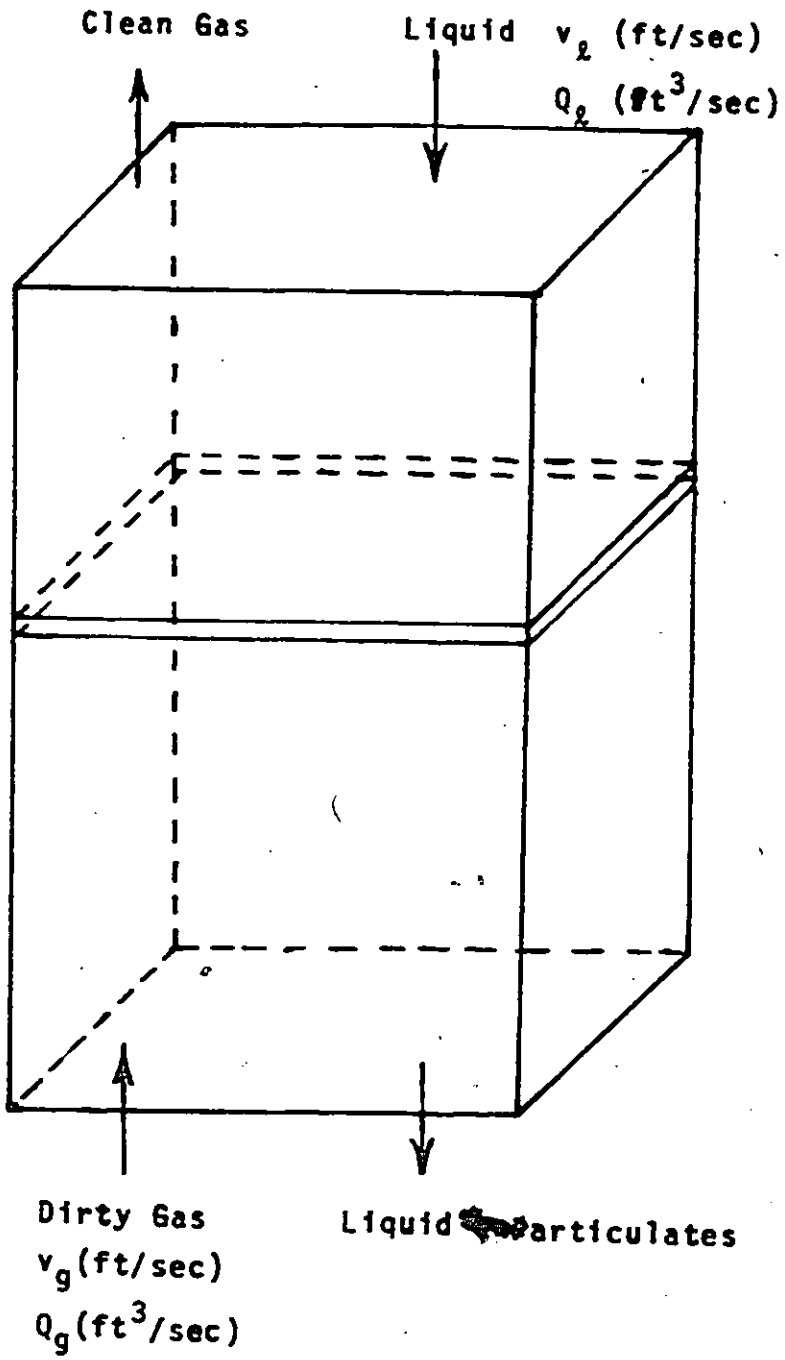

FIGURE 10.1: Counter-Current Spray Scrubber

If inertial impaction is considered to be the sole mechanism for solid particle removal, the collection rate can be expressed in terms of a single drop impaction collection efficiency, η_I, obtained from

$$\left\{\begin{array}{l}\text{number of}\\ \text{liquid}\\ \text{droplets}\\ \text{in the}\\ \text{control}\\ \text{volume}\end{array}\right\}\left\{\begin{array}{l}\text{projected}\\ \text{area of}\\ \text{drop}\end{array}\right\}\left\{\begin{array}{l}\text{relative}\\ \text{gas vel-}\\ \text{ocity of}\\ \text{approach}\end{array}\right\}\left\{\begin{array}{l}\text{concen-}\\ \text{tration}\\ \text{of part-}\\ \text{iculates}\\ \text{in the}\\ \text{element}\end{array}\right\}\left\{\begin{array}{l}\text{single}\\ \text{drop col-}\\ \text{lection}\\ \text{efficiency}\\ \text{by impaction}\end{array}\right\}$$

$$= N(\pi R_c^2)\, v_{te}\, C_1\, \eta_I \qquad (10\text{-}5)$$

where

N = number of liquid droplets in the element

R_c = radius of collecting drop, cm

v_{te} = terminal velocity of collecting drop, cm/sec

C_1 = concentration of solid particles at height z, in the scrubber, gm/cm^3

η_I = single drop collection efficiency due to impaction

Substituting equation (10-5) into equation (10-4) yields

$$v_g A_1 C_1 - v_g A_1 \left(C_1 + \frac{dC_1}{dz}\, dz\right) - N(\pi R_c^2)\, v_{te}\, C_1\, \eta_I = 0 \qquad (10\text{-}6)$$

which simplifies to

$$-v_g A_1 dC_1 = N\pi R_c^2 \, v_{te} \, C_1 \, \eta_I \qquad (10\text{-}7)$$

The drop hold-up, H_d, defined as the volume fraction of liquid in a differential volume is

$$H_d = \frac{Q_\ell}{v_\ell A_1} \qquad (10\text{-}8)$$

where

Q_ℓ = volumetric flow rate of liquid, cm^3/sec

v_ℓ = velocity of liquid drop, cm/sec

A_1 = cross-sectional area of scrubber, cm^2

H_d = drop hold-up, $\frac{cm^3 \text{ of liquid}}{cm^3 \text{ of total volume}}$

For uniform drop size and uniform liquid distribution, the total volume of the collecting drops in the control volume must equal the liquid hold-up in the control volume according to

$$N\left(\frac{4}{3}\pi R_c^3\right) = A_1 dz \, H_d \qquad (10\text{-}9)$$

Therefore

$$N = \frac{3}{4} \frac{A_1 \, dz \, H_d}{\pi \, R_c^3} \qquad (10\text{-}10)$$

Substituting for N from equation (10-10) into equation (10-7) and rearranging yields:

$$-\frac{dC_l}{C_l} = \frac{3}{4}\frac{A_l\ v_{te}\ H_d\ \eta_I\ dz}{v_g\ A_l\ R_c} \qquad (10\text{-}11)$$

The droplet hold up, H_d from equation (10-8) is then substituted into equation (10-11) to give:

$$-\frac{dC_l}{C_l} = \frac{3}{4}\frac{A_l\ v_{te}\ \eta_I\ dZ}{Q_g\ v_\ell\ R_c} \qquad (10\text{-}12)$$

Integrating equation (10-12) using the boundary conditions:

$z = 0$, $C_l = C_i$ and $z = Z$, $C_l = C_o$

gives

$$-\int_{C_i}^{C_o}\frac{dC_l}{C_l} = \int_0^Z \frac{3}{4}\frac{Q_\ell}{Q_g}\frac{v_{te}\ \eta_I\ dz}{v_\ell\ R_c} \qquad (10\text{-}13)$$

which becomes

$$\ln\frac{C_o}{C_i} = \frac{-3\ Q_\ell\ v_{te}\ \eta_I\ Z}{4\ Q_g\ v_\ell\ R_c} \qquad (10\text{-}14)$$

where

C_i = concentration of particulate matter in inlet gas stream, gm/cm^3

C_o = concentration of particulate matter in outlet gas stream, gm/cm^3

Z = height of scrubber, cm

By convention, the overall particulate collection efficiency of control equipment, E_o, is defined as:

$$E_o = \frac{C_i - C_o}{C_i} = 1 - \frac{C_o}{C_i} \qquad (10\text{-}15)$$

The overall particulate collection efficiency due to the sole mechanism of inertial impaction is obtained from equations (10-14) and (10-15) as:

$$E_I = 1 - \exp\left[\frac{-3Q_\ell \, v_{te} \, \eta_I \, Z}{4 \, Q_g \, v_\ell \, R_c}\right] \qquad (10\text{-}16)$$

The single drop collection efficiency due to impaction η_I, is given by Calvert et al [3] as

$$\eta_I = \left[\frac{N_I}{N_I + 0.35}\right]^2 \qquad (10\text{-}17)$$

where

N_I = inertial impaction parameter

Equation (10-17) may be written as:

$$\eta_I = \left[\frac{1}{1 + \frac{0.35}{N_I}}\right]^2 \qquad (10\text{-}18)$$

and the inertial impaction parameter, N_I, from equation (3-1) substituted into equation (10-18) to yield:

$$\eta_I = \left[\frac{1}{1 + \frac{0.35\ (18\mu\ D_c)}{C_1\ \rho_p\ D_p^2\ v_{rel}}} \right]^2 \qquad (10\text{-}19)$$

It is obvious from equation (10-19) that as the particle diameter, D_p, approaches zero, the single droplet collection efficiency due to impaction also approaches zero.

2. Interception

Treatment of particulate matter as point masses provides an incomplete measure of particle removal by a spherical obstruction in terms of the inertial impaction efficiency, η_I. When the finite size of real particles is considered, it becomes apparent that some particles, whose centres follow a fluid streamline around an obstruction, may still make contact with the collecting drop. Particle removal by interception will occur as long as the particle centre passes the collector at a distance less than $D_p/2$.

According to Ranz and Wong[4] the interception efficiency, η_{Int}, for spherical collectors is given by:

$$\eta_{Int} = (1 + N_R)^2 - \left(\frac{1}{1 + N_R}\right) \qquad (10\text{-}20)$$

when the inertial impaction parameter, N_I, approaches zero.

where

$N_R = D_p/D_c$, the interception parameter.

In a counter-flow spray scrubber, the liquid drops must be sufficiently large for their settling velocities to be greater than the gas velocity. Normal drop sizes in pre-formed counter-current sprays range from 200-600μ [3]. Thus for fine particles, the interception parameter, N_R, will seldom exceed 0.025. This means that the overall collection efficiency due to interception, E_{Int}, will be negligible since the value of N_R must exceed unity for the interception effect to be significant [5].

3. Brownian Diffusion

Fine particles can move across gas stream lines flowing past a spherical collector due to random bombardment by gas molecules. As a result some of the particles strike the spherical collector and are removed from the gas stream. In the derivation of an expression for overall collection efficiency by Brownian diffusion, all the assumptions made

in the case of inertial impaction are valid.

Again, an elemental volume of height, dz, is considered in a counter-current spray scrubber as shown in Figure 10-1. A particulate mass balance over this elemental volume gives:

$$v_g A_1 C_1 - v_g A_1 \left(C_1 + \frac{dC_1}{dz}\, dz\right) - \left\{\begin{array}{l}\text{particulate}\\ \text{removal rate}\\ \text{by liquid}\\ \text{drops}\end{array}\right\} = 0 \qquad (10\text{-}4)$$

Levich [5] has shown that the rate of deposition, R_B, on a spherical collector by Brownian diffusion for low Reynolds numbers ($N_{Re_c} < 3$) and high Schmidt number ($N_{Sc} \approx 10^6$) is given by:

$$R_B = 2\pi \mathcal{D}_p R_c C_1 N_{Re_c}^{1/3} N_{Sc}^{1/3} \qquad (10\text{-}21)$$

where

R_B = rate of deposition on a spherical collector by Brownian diffusion, gm/sec

$\mathcal{D}_p$ = particle diffusivity, cm^2/sec

R_c = radius of spherical collector, cm

C_1 = concentration of particulate in the scrubber, gm/cm^3

N_{Re_c} = $D_c v_{rel} \rho/\mu$, Reynolds number, dimensionless

N_{Sc} = $\mu/(\rho D_p)$ Schmidt number, dimensionless

v_{rel} = velocity of gas stream relative to spherical collector, cm/sec

ρ = gas density, gm/cm^3

D_c = diameter of spherical collector, cm

For uniform drop size and uniform liquid distribution, equation (10-9)

$$N(\tfrac{4}{3} \pi R_c^3) = A_1 \, dz \, H_d \qquad (10\text{-}9)$$

is valid. Substituting into equation (10-9) for drop hold-up, H_d, from equation (10-8) and rearranging yields

$$N = \frac{3}{4} \frac{Q_\ell \, dz}{v_\ell \pi R_c^3} \qquad (10\text{-}22)$$

The particulate removal rate by liquid drops in the element is:

$$\left\{\begin{matrix}\text{number of}\\ \text{drops in the}\\ \text{element}\end{matrix}\right\} \left\{\begin{matrix}\text{rate of}\\ \text{deposition}\\ \text{on a single}\\ \text{drop}\end{matrix}\right\} = NR_B \qquad (10\text{-}23)$$

Substitution of equations (10-21), (10-22) and (10-23) into equation (10-4) yields

$$-v_g A_1 dC_1 = \frac{3 Q_\ell \mathcal{D}_p N_{Re_c}^{1/3} N_{Sc}^{1/3} C_1 dz}{2 v_\ell R_c^2} \qquad (10\text{-}24)$$

Rearranging and integrating between the appropriate limits leads to

$$\ln \frac{C_i}{C_o} = - \frac{3 Q_\ell \mathcal{D}_p N_{Re_c}^{1/3} N_{Sc}^{1/3} Z}{2 Q_g v_\ell R_c^2} \qquad (10\text{-}25)$$

The overall particulate collection efficiency by the sole mechanism of Brownian diffusion becomes:

$$E_B = 1 - \exp \left[- \frac{3 Q_\ell \mathcal{D}_p N_{Re_c}^{1/3} N_{Sc}^{1/3} Z}{2 Q_g v_\ell R_c^2} \right] \qquad (10\text{-}26)$$

4. Flux Forces

a. Overall Collection Efficiency

In a spray scrubber flux forces generated by temperature and concentration gradients can improve fine particle collection efficiency. In the derivation of an expression for overall collection efficiency by flux forces, all the assumptions made in the case of inertial impaction are considered valid.

Again an elemental volume of height, dz, is considered for a counter-current spray scrubber as shown in Figure 10-1. In the particulate mass balance equation:

$$v_g A_1 C_1 - v_g A_1 [C_1 + (\frac{dC_1}{dz})\, dz] - \{\text{particulate removal rate by liquid drops}\} = 0 \quad (10\text{-}4)$$

a new expression is required for the particulate removal rate in terms of the flux forces exerted by the collecting drops.

An effective drop-particle interaction time can be approximated by

$$\tau = \frac{2R_c}{v_{te}} \quad (10\text{-}27)$$

which represents an average time for a particle to pass by a collecting drop. A particle under the influence of a flux force would be moved through a distance

$$S_1 = \tau u_F = \left(\frac{2R_c}{v_{te}}\right) u_F \qquad (10\text{-}28)$$

assuming a constant flux force velocity, u_F, over the time interval, τ

Particles will be removed from an effective volume, V_e, for each drop according to:

$$V_e = \frac{4\pi}{3} \left[\left(R_c + 2R_c \frac{u_F}{v_{te}}\right)^3 - R_c^3\right] \qquad (10\text{-}29)$$

which simplifies to:

$$V_e = \frac{4}{3} \pi \left(6 \frac{u_F}{v_{te}}\right) R_c^3 \qquad (10\text{-}30)$$

neglecting second and higher order terms in u_F/v_{te}. The total volume in which flux forces are operative will be determined by the number of drops in the control volume, $A_1\, dz$, according to

$$N\ V_e = \left[\frac{3}{4}\frac{Q_\ell}{v_\ell}\ \frac{dz}{\pi R_c^3}\right]\left[\frac{4}{3}\pi\ \left(6\frac{u_F}{v_{te}}\right) R_c^3\right] \qquad (10\text{-}31)$$

as given by equations (10-22) and (10-30). Simplifying equation (10-31) and multiplying by C_1, the average particulate concentration in the control volume, gives the total particulate removed in the control volume by all the drops as

$$C_1\ N\ V_e = C_1\ \left(6\frac{u_F}{v_{te}}\right)\frac{Q_\ell}{v_\ell}\ dz \qquad (10\text{-}32)$$

Since this removal is achieved in the time, τ, the particulate removal rate by all the drops is given by:

$$\frac{C_1\ N\ V_e}{\tau} = 3\ C_1\ \frac{u_F}{v_\ell}\ \frac{Q_\ell}{R_c}\ dz \qquad (10\text{-}33)$$

Substituting equation (10-33) into equation (10-4) and simplifying leads to

$$\frac{dC_1}{C_1} = -\ 3\ \frac{u_F}{v_\ell}\ \frac{Q_\ell}{Q_g}\ \frac{dz}{R_c} \qquad (10\text{-}34)$$

Integration between the appropriate limits provides

$$\ln\ \frac{C_o}{C_i} = -\ 3\ \frac{u_F}{v_\ell}\ \frac{Q_\ell}{Q_g}\ \frac{Z}{R_c} \qquad (10\text{-}35)$$

The overall particulate collection efficiency by flux forces

$$E_F = 1 - \exp\{-3 \frac{u_F}{v_\ell} \frac{Q_\ell}{Q_g} \frac{Z}{R_c}\} \qquad (10\text{-}36)$$

is obtained by substituting for $\frac{C_o}{C_i}$ in equation (10-15).

b. Thermophoresis

In order to estimate the overall thermophoretic collection efficiency, E_T, thermophoretic velocities, v_t, at different temperature gradients as well as the total collecting surface area in the spray scrubber, A_c, are required.

i. Thermophoretic Velocity

Epstein's thermophoretic velocity equation for the slip flow regime

$$v_t = -\frac{3}{2}\left[\frac{k_g}{2k_g + k_p}\right]\frac{\mu}{\rho T}\left(\frac{dT}{dX}\right) \qquad (5\text{-}4)$$

$$(10\text{-}37)$$

can be used to estimate the thermal flux force velocity for $N_{Kn_{R_p}} = \lambda/R_p \to 0$. Calvert et.al. [3] employed a modified form of Epstein's equation, which included the Cunningham correction factor, C_1, to calculate the thermophoretic velocity as a function of temperature gradient in the form

$$v_t = -\frac{3}{2}\left[\frac{k_g}{2k_g + k_p}\right]\frac{C_1\ \mu}{\rho T}\left(\frac{dT}{dx}\right) \qquad (10\text{-}38)$$

Figure 10-2 illustrates the effect of operating temperature and pressure on thermophoretic velocities in air for 1 and 0.1μ diameter particles, when the ratio of k_p/k_g equals 10.

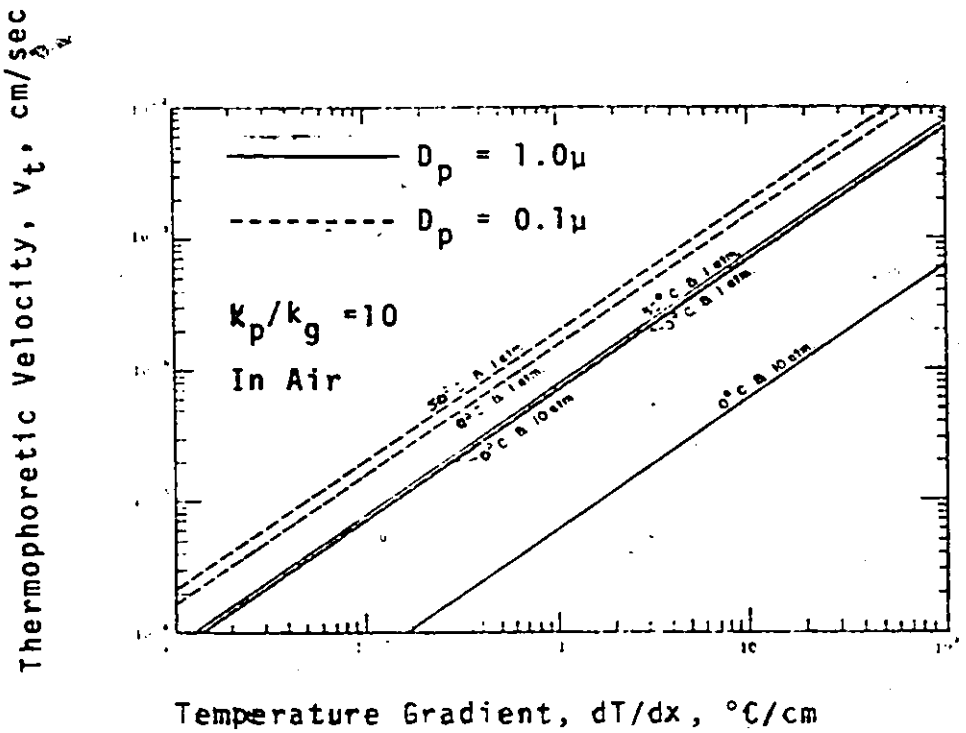

FIGURE 10.2: Thermophoretic Velocity as a Function of Temperature Gradient for Different Operating Conditions [3]

ii. Overall Collection Efficiency

The total collecting surface area from all drops in the scrubber is given by:

$$A_c = \left(\frac{3}{4}\frac{Q_\ell}{v_\ell}\frac{Z}{\pi R_c^3}\right)(4\pi R_c^2) = \frac{3\,Q_\ell\,Z}{v_\ell\,R_c} \qquad (10\text{-}39)$$

As a result the overall thermophoretic flux force collection efficiency equation (10-36) can be simplified to

$$E_T = 1 - \exp\left\{\frac{-A_c v_t}{Q_g}\right\} \qquad (10\text{-}40)$$

Figures 10-3 and 10-4 give the collection efficiency curves for a spray tower at various A_c/Q_g ratios, resulting from thermophoresis acting alone on 0.1 and 1 micron particles respectively at a temperature of 0°C and absolute pressure of 1 atm. Thermophoretic velocities used in deriving these design efficiency curves were obtained from equation (10-38).

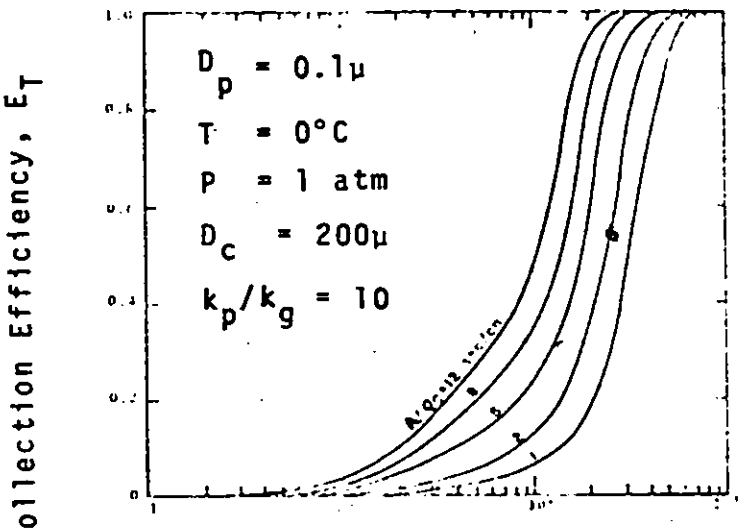

FIGURE 10-3: Collection Efficiency of Aerosol Particles by Spheres Due to Thermophoresis at Different A_c/Q_g Ratios [3]

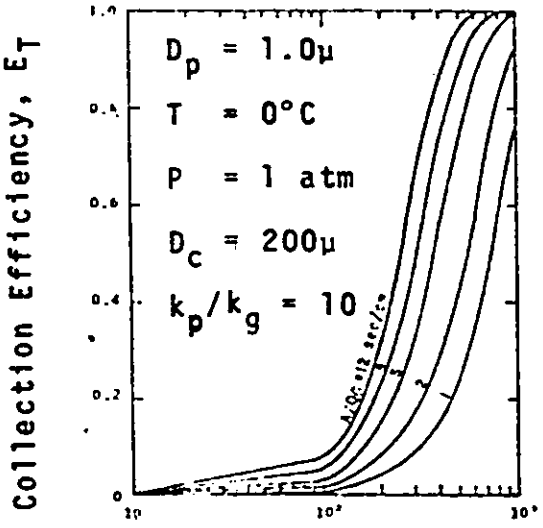

FIGURE 10-4: Collection Efficiency of Aerosol Particles by Spheres Due to Thermophoresis at Various A_c/Q_g Ratios [3]

c. Diffusiophoresis

In order to estimate the overall diffusiophoretic collection efficiency, E_d, diffusiophoretic velocities, v_d, at different vapor pressure gradients as well as the total collecting surface area in the spray scrubber, A_c, are required.

i. Diffusiophoretic Velocity

Waldman's expression for predicting the diffusiophoretic particle velocity in the free-molecular regime [$\lambda > R_p$]

$$V_d = \sigma_1 V_1 + \sigma_2 V_2 \qquad (10\text{-}41)$$

where

σ_1, σ_2 = definition according to equation (8-5)

V_1, V_2 = molecular velocities of components 1 and 2, cm/sec

has been found to apply with only 10% error even when $R_p/\lambda = 1$ [3]. For the case in which vapor molecules (species 1) diffuse radially towards a collecting drop through air (species 2), stationary,with respect to the drop in the radial direction, v_2 equals zero and equation (10-41) simplifies to

$$v_d = \sigma_1 v_1 \qquad (10\text{-}42)$$

By assuming that the thermal reflection coefficients, a_1 and a_2, are equal equation (8-5) reduces to

$$\sigma_1 = \frac{\gamma_1 \sqrt{m_1}}{\gamma_1 \sqrt{m_1} + \gamma_2 \sqrt{m_2}} \qquad (10\text{-}43)$$

or

$$\sigma_1 = \frac{\gamma_1 \sqrt{M_1}}{\gamma_1 \sqrt{M_1} + \gamma_2 \sqrt{M_2}} \qquad (10\text{-}44)$$

since (m_i) (Avogadro's Number) = M_i.

Substitution for σ_1 into equation (10-42) yields

$$v_d = \left[\frac{\gamma_1 \sqrt{M_1}}{\gamma_1 \sqrt{M_1} + \gamma_2 \sqrt{M_2}} \right] v_1 \qquad (10\text{-}45)$$

According to Equation(8-8) the molecular velocity of the diffusing vapor, v_1, equals the sum of the systems molar average velocity, w, and the vapor diffusion velocity, W_1, given by Fick's 1st law of diffusion as

$$W_1 = \frac{-D_{12}}{\gamma_1} \nabla \gamma_1 \qquad (10\text{-}46)$$

From

$$v_i = w + W_i \tag{8-8}$$

it follows that

$$v_1 = w - \frac{\mathcal{D}_{12}}{\gamma_1} \nabla \gamma_1 \tag{10-47}$$

and

$$w = v_2 - W_2 = - W_2 \tag{10-48}$$

since v_2 is equal to zero.

From equation (8-14)

$$- W_2 = \frac{-\mathcal{D}_{12} \nabla \gamma_1}{\gamma_2} \tag{10-49}$$

thus

$$w = \frac{-\mathcal{D}_{12} \nabla \gamma_1}{\gamma_2} \tag{10-50}$$

and from equation (10-47)

$$v_1 = -\frac{\vartheta_{12} \nabla \gamma_1}{\gamma_2} - \frac{\vartheta_{12} \nabla \gamma_1}{\gamma_1} \qquad (10\text{-}51)$$

which simplifies to

$$v_1 = \frac{-\vartheta_{12} \nabla \gamma_1}{\gamma_1 \gamma_2} \qquad (10\text{-}52)$$

Accordingly

$$v_d = \left[\frac{-\sqrt{M_1}}{\gamma_1 \sqrt{M_1} + \gamma_2 \sqrt{M_2}}\right] \frac{\vartheta_{12}}{\gamma_2} \nabla \gamma_1 \qquad (10\text{-}53)$$

Assuming ideal gas behavior

$$\gamma_1 = \frac{p_1}{p} \text{ and } \gamma_2 = \frac{p_2}{p}$$

For one-dimensional diffusion in the x-direction equation (10-53) can be written in the form

$$v_d = \left[\frac{-\sqrt{M_1}}{p_1 \sqrt{M_1} + p_2 \sqrt{M_2}}\right] p \frac{\vartheta_{12}}{p_2} \left(\frac{dp_1}{dx}\right) \qquad (10\text{-}54)$$

The magnitude of the diffusivity of water vapor in air is given by [6] as

$$\mathcal{D}_{12} = 0.22 \left(\frac{T}{273}\right)^{1.75} \left(\frac{1}{p^*}\right) \qquad (10\text{-}55)$$

where

$\mathcal{D}_{12}$ = diffusivity of water vapor in air, cm^2/sec

T = absolute temperature, °K

p^* = total pressure, atm

The general expression for the diffusiophoretic velocity of sub-micron particles in air saturated with water vapor becomes

$$v_d = \left[\frac{-(0.9334)}{4.2426\ p_1 + 5.3759\ p_2}\right]\left(\frac{T}{273}\right)^{1.75} \left(\frac{1}{p^*}\right)\frac{p}{p_2}\left(\frac{dp_1}{dx}\right) \qquad (10\text{-}56)$$

where

p_1 = vapor pressure of liquid water at temperature T and pressure p, millibar

p_2 = vapor pressure of air at temperature T and pressure p, millibar

p = total system pressure, millibar

v_d = diffusiophoretic velocity, cm/sec

$\frac{dp_1}{dx}$ = vapor pressure gradient, millibar/cm

Figure 10-5 illustrates the diffusiophoretic velocities of sub-micron particles in air saturated with water vapor at various operating conditions for a range of assumed vapor pressure gradients

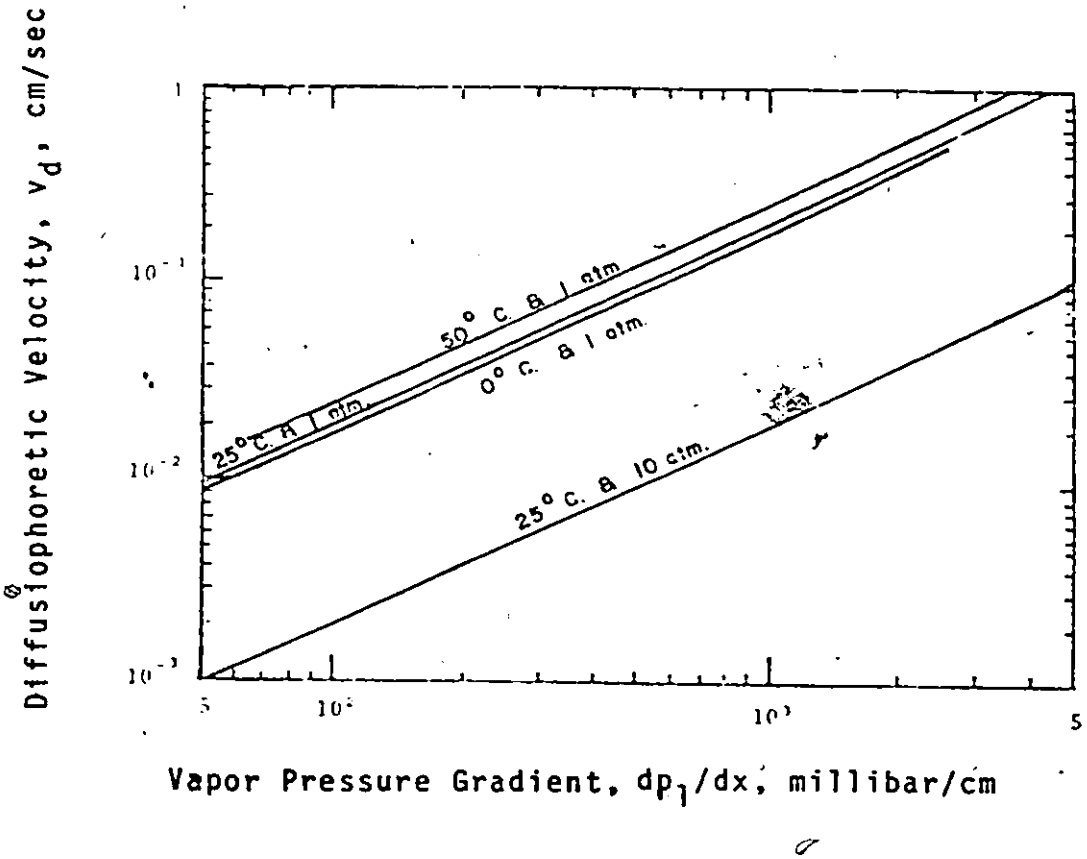

FIGURE 10-5: Diffusiophoretic Velocity of Sub-Micron Particles in Air Saturated with Water Vapor at Different Operating Conditions [3]

ii. Overall Collection Efficiency

For a total collecting surface area, A_c, given by equation (10-39), the overall diffusiophoretic flux force collection efficiency equation (10-36) for sub-micron particles becomes

$$E_d = 1 - \exp\left\{\frac{-A_c\, v_d}{Q_g}\right\} \qquad (10\text{-}57)$$

Figures (10-6) and (10-7) illustrate typical diffusiophoretic collection efficiencies in a spray scrubber operating with 200μ diameter collecting drops at atmospheric pressure and temperatures of 0°C and 25°C respectively.

5. Design Curves

The application of the combined particle collection mechanisms to any counter-flow spray scrubber requires stepwise integration of the rate equations for heat, mass, and momentum transport. In practice this is an iterative process requiring the development of a specific computer program. Preliminary attempts during this investigation form the basis for a new study that will provide practical design efficiency curves that can be used to evaluate commercial counter-current spray scrubbers. In addition the combined particle collection mechanisms will be extended to cocurrent wet collectors of the Venturi type.

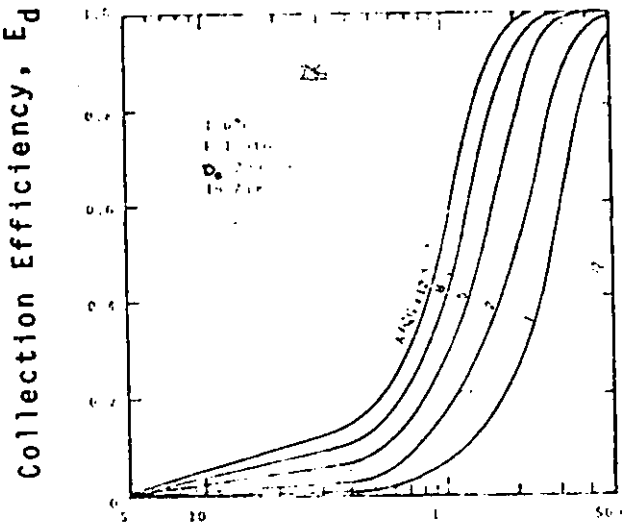

FIGURE 10-6: Collection Efficiency by Liquid Drops Due to Diffusiophoresis at Different A_c/Q_g Ratios [3]

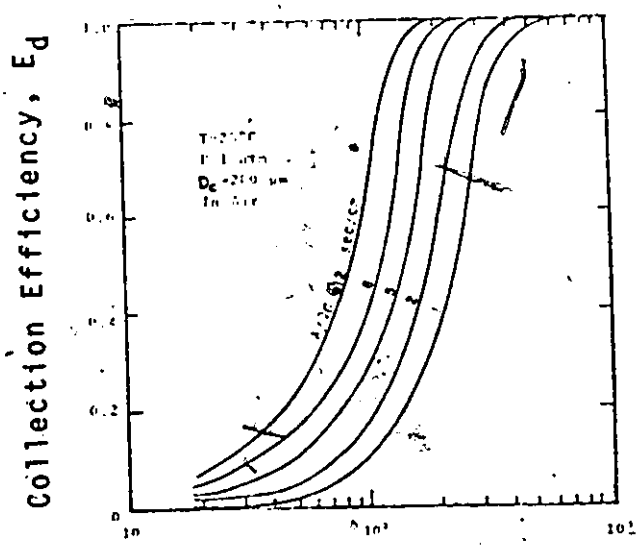

FIGURE 10-7: Collection Efficiency by Liquid Drops Due to Diffusiophoresis at Different A_c/Q_g Ratios [3]

REFERENCES

1. Calvert, S., Source Control By Liquid Scrubbing, Stern, A. C., Ed. Air Pollution, Academic Press, New York, 3, (1968).

2. Calvert, S., Goldshmid, J., Leith, D. and Jhaveri, N., Feasibility of Flux Force/Condensation Scrubbing for Fine Particle Collection, A.P.T. Inc. Prepared for U.S. Environmental Protection Agency, EPA Report - 650/2-73-036 (1973).

3. Calvert, S., Goldshmid, J., Leith, D., and Mehta, D., Scrubber Handbook, A.P.T., Inc., Distributed by NTIS, U.S. Department of Commerce, 5285 Port Royal Road, Springfield, Va 22151, 1, (1972).

4. Gnyp, A. W., Price, S. J. W., St. Pierre, C. C., Mozzon, D., and Smith, D., An Evaluation of Wet Collector Performance for Particulate Removal, Part I: Fundamentals, The Industrial Research Institute of the University of Windsor, p. 40 (1973).

5. *Levich, J., Physico-Chem. Hydrodyn. Acad. Sci., U.S.S.R., Moscow (1952).

6. Washburn, E. W., West, C. J., Dorsey, E. N., Bichowsky, F. R., Ring, M. D., Interdiffusion of Gases and Vapors, International Critical Tables, McGraw-Hill Book Company, Inc., New York, 5, 62 (1929).

*denotes incomplete holdings at the time of publication.

NOMENCLATURE

a_i	Coefficient of diffuse reflection of component i
a_m	Momentum accommodation coefficient of particle
a_t	Thermal accommodation coefficient of particle
A	Empirical constant appearing in the slip correction equation (5-9) Constant in the velocity distribution equation (4-13)
A_l	Cross-sectional area of scrubber, cm^2
A_c	Total surface area from all drops in the scrubber, cm^2
A_p	Projected area of an aerosol particle, cm^2
A_n	Constant in the temperature distribution equation (I-23)
A_w	Empirical constant in the diffusiophoretic equation (7-7)
B	Empirical constant appearing in the slip correction equation (5-9) Constant in the velocity distribution equation (4-13)
B_n	Constant in the temperature distribution equation (I-23)
B_w	Empirical constant in the diffusiophoretic equation (7-7)
c	Molar density of gas mixture, gm-moles/cm^3
c_m	Semi-empirical constant associated with velocity slip
c_n	Constant in the temperature distribution equation (I-28)
c_p	Specific heat of gas at constant pressure, Btu/(lb°F), cal/(gm °K)

C_v	Specific heat of gas at constant volume, Btu/(lb°F)
c_t	Semi-empirical constant associated with temperature jump
C	Empirical constant appearing in the slip correction equation (5-9)
C_l	Concentration of particulate at position, z, in the scrubber, gm/cm^3
	Cunningham correction factor, dimensionless
C_i	Concentration of particulate matter in inlet gas stream, gm/cm^3
C_o	Concentration of particulate matter in outlet gas stream, gm/cm^3
$\frac{dC_l}{dz}$	Concentration gradient, gm/cm^4
d_A	Diameter of molecule A, cm
d_B	Diameter of molecule B, cm
D_{AB}	Binary diffusivity of component A through B, cm^2/sec
D_c	Diameter of collecting element, cm
D_n	Constant in the temperature distribution equation (I-28)
D_p	Diameter of spherical particle, cm
$\mathcal{D}_p$	Diffusivity of particle, cm^2/sec
D_o	Diffusivity at 1 atmosphere pressure and 293°K, cm^2/sec
$\mathcal{D}_{12}$	Diffusivity of water vapor in air, cm^2/sec
D_{12}	Binary diffusivity of component 1 through 2, cm^2/sec
E	Electrical field intensity, practical volts/cm

E_B	Overall particulate collection efficiency due to Brownian diffusion
E_d	Overall particulate collection efficiency due to diffusiophoresis
E_F	Overall particulate collection efficiency due to a flux force
Σ_i	Average energy flux for incoming molecules at a point on the wall or particle surface, $cal/(cm^2 hr)$
E_I	Overall particulate collection efficiency due to inertial impaction
E_{Int}	Overall particulate collection efficiency due to interception
E_r	Average energy flux for departing molecules at a point on the wall or particle surface, $cal/(cm^2\ hr)$
E_T	Overall particulate collection efficiency due to thermophoresis
E_w	Energy flux which would prevail if the molecules leaving were in equilibrium with the wall or particle surface at the point, $cal/(cm^2 hr)$
E_o	Overall particulate collection efficiency of control equipment
f+	Velocity distribution function of leaving molecules
f-	Velocity distribution function of approaching molecules striking the surface assuming absence of the particle
f'	Velocity distribution function resulting from specular reflection on the surface element of the distribution function, f-
$F^{(+)}$	Maxwellian distribution arising from completely diffuse reflection
f_o^-	Velocity distribution function of approaching molecules striking the surface obtained by solution of the BGK model

F_d	Diffusiophoretic force, dynes
F_D	Drag force, dynes
F_E	Electrical force, dynes
F_g	Force exerted by the gas on the particle, dynes
F_{gr}	Gravitational force, dynes
F_t	Thermal force, dynes
F_t^*	Thermal force as given by equation (4-51), dynes
F_t^{**}	Thermal force as given by equation (5-11), dynes
g	Temperature jump distance, cm Gravitational acceleration, 980.6 cm/sec^2
G	Uniform gas temperature gradient away from the particle, °K/cm
G_i	Average tangential components of the momentum of molecules striking the wall or particle surface, gm cm/sec
G_r	Average tangential components of the momentum of molecules leaving the wall or particle surface, gm cm/sec
H_d	Drop hold-up, cm^3 liquid/cm^3 total volume
k	Boltzmann constant, dyne cm/°K
k_g	Thermal conductivity of gas, cal/(sec cm°K)
$(k_g)_{tr}$	Translational component of the thermal conductivity of gas, cal/(sec cm°K)
k_p	Thermal conductivity of particle, cal/(sec cm°K)
K_F	Constant in the diffusiophoretic force equation (7-1), dynes/cm
K_F'	Constant in the diffusiophoretic velocity equation (7-2)
K_F^*	Constant in the diffusiophoretic force equation (7-3), dynes

K_F^{**}	Constant in the diffusiophoretic velocity equation (7-4)
L	Plate spacing, cm
m	Molecular mass of gas, gm
M_A	Molecular weight of gas component A, gm/gm-mole
M_B	Molecular weight of gas component B, gm/gm-mole
M_1	Molecular weight of water vapor, gm/gm-mole
M_2	Molecular weight of air, gm/gm-mole
n	Positive integer
n_p	Number of solid particles per unit volume, particles/cm^3
N	Number of liquid drops in an element
N_F	Solid particle flux due to flux force, particles/(cm^2sec)
N_{FD}	Flux deposition number, u_F/v_{rel}
N_I	Inertial impaction parameter, $\frac{C_1 v_p \rho_p D_p^2}{18\mu D_c}$, dimensionless
$N_{Kn_{R_p}}$	Knudsen number, $\frac{\lambda}{R_p}$, dimensionless
N_{Kn_L}	Knudsen number, $\frac{\lambda}{L}$, dimensionless
N_{Pe}	Peclet number, $\frac{D_c v_{rel}}{C_p \mu \rho_p}$, dimensionless
N_{Pr}	Prandtl number, $\frac{C_p \mu}{k_g}$, dimensionless
N_R	Interception parameter, $\frac{D_p}{D_c}$, dimensionless

N_{Re_c}	Reynolds number based on collector, $\frac{D_c v_{rel} \rho}{\mu}$, dimensionless
N_{Sc}	Schmidt number, $\mu/(\rho \mathcal{D}_p)$, dimensionless
p	Absolute gas pressure, dyne/cm^2 Total system pressure, millibar
p_o	Static fluid pressure outside the boundary layer, dyne/cm^2
p_i	Partial pressure of component i, dynes/cm^2
p_n	Constant in the temperature distribution equation (I-28)
p*	Total pressure, atm
$p_{r,z}$	Total fluid stress acting on the surface in the z-direction, dynes/cm^2
p_1	Vapor pressure of liquid water at temperature T and pressure p, millibar
p_2	Vapor pressure of air at temperature T and pressure p, millibar
$\frac{dp_i}{dx}$	Partial pressure gradient of vapour in x-direction dynes/cm^3
$\frac{dp_1}{dx}$	Vapor pressure gradient, millibar/cm
$P_n(\cos\theta)$	n'th Legendre polynominal in cosθ
q	Charge on a particle, statcoulombs
Q_g	Volumetric flow rate of gas, cm^3/sec, ft^3/sec
Q_ℓ	Volumetric flow rate of liquid, cm^3/sec, ft^3/sec
$Q_n(\cos\theta)$	Reciprocal of the (n+1)'th Legendre polynominal in cosθ
r	Spherical co-ordinate variable
R	Gas constant, $\frac{cm^3\ atm}{gm\text{-}mole\ °K}$

R_B	Rate of deposition on a spherical collector by Brownian diffusion, gm/sec
R_c	Radius of spherical collector, cm
R_p	Radius of particle, cm
S_1	Distance that a particle moves under the influence of a flux force, cm
S	Length of periphery, cm
$\vec{ds}$	Unit normal of a surface element
T	Absolute gas temperature, °K
T_1	Absolute temperature of upper plate, °K
T_2	Absolute temperature of lower plate, °K
T_i	Temperature distribution inside aerosol particle, °K
T_o	Temperature distribution outside aerosol particle, °K
T_K	Gas temperature at wall or particle surface obtained by extrapolating uniform gas temperature profile back to wall or particle surface, °K
T_W	Wall or particle surface temperature, °K
∇T	Gas temperature gradient, °K/cm
$\frac{\partial T}{\partial n}$	Uniform gas temperature gradient away from wall or particle surface normal to the wall or particle surface, °K/cm
$\frac{\partial T}{\partial X}$	Gas temperature gradient in x-direction, °K/cm
$\frac{\partial T}{\partial S}$	Gas temperature gradient along surface in S-direction °K/cm
u	Mass average velocity, cm/sec

u_F	Particle velocity due to flux force, cm/sec
$\vec{v}$	Molecular velocity of gas, cm/sec
$\bar{v}$	Mean molecular velocity of gas, cm/sec
$\bar{v}_i$	Mean molecular velocity of component i, cm/sec
v_d	Diffusiophoretic velocity, cm/sec
V_e	Effective volume per drop from which particles will be removed by a flux force, cm^3/drop
v_f	Velocity of fall of particle, cm/sec
v_1	Molecular velocity of water vapor molecules, cm/sec
v_2	Molecular velocity of air molecules, cm/sec
v_g	Velocity of gas stream, cm/sec
v_K	Gas velocity at wall or particle surface relative to the wall or particle surface obtained by extrapolating uniform gas velocity profile back to wall or particle surface, cm/sec
v_ℓ	Velocity of liquid drop, cm/sec
v_p	Particle velocity, cm/sec
v_r	Velocity component of gas in r-direction, cm/sec Velocity rise of particle, cm/sec
v_{rel}	Free stream gas velocity relative to sphere, cm/sec
v_θ	Velocity component of gas in θ-direction, cm/sec
v_ϕ	Velocity component of gas in ϕ-direction, cm/sec
v_t	Thermophoretic velocity of particle, cm/sec

v_{tc}	Thermal creep velocity, cm/sec
v_{te}	Terminal velocity of collecting drop, cm/sec
v_x	Velocity component of gas in the x-direction, cm/sec
v_y	Velocity component of gas in the y-direction, cm/sec
v_z	Velocity component of gas in the z-direction
V_i	Mass diffusion velocity, cm/sec
$\frac{dv}{dz}$	Gas velocity gradient, taken positive in the direction away from the wall or particle surface, sec^{-1}
w	Average molecular velocity of system, cm/sec
W_i	Particle diffusion velocity, cm/sec Water vapor diffusion velocity, cm/sec
x	Rectangular co-ordinate variable
y	Rectangular co-ordinate variable
dz	Height of elemental scrubber volume, cm
z	Rectangular co-ordinate variable
Z	Height of scrubber, cm
z_∞	Distance from wall or particle surface beyond which gas temperature gradient is uniform, cm

Greek Symbols

α	Accommodation coefficient of particle
γ	Mole fraction, dimensionless
γ_i	Mole fraction of component i, dimensionless
γ_A	Mole fraction of component A, dimensionless
γ_B	Mole fraction of component B, dimensionless
γ_1	Mole fraction of water vapor, dimensionless
γ_2	Mole fraction of air, dimensionless
∇	Differential operator, cm^{-1}
ϵ	Defined by equation (9-1) as $\epsilon = A_w \left(\frac{M_A - M_B}{M_A + M_B}\right) + B_w \left(\frac{d_A - d_B}{d_A + d_B}\right)$
ζ	Coefficient of slip, cm
η_D	Single drop collection efficiency due to Brownian diffusion, dimensionless
η_F	Single drop collection efficiency due to any flux mechanism, dimensionless
η_I	Single drop collection efficiency due to inertial impaction, dimensionless
η_{Int}	Single drop collection efficiency due to interception, dimensionless
θ	Spherical co-ordinate variable
λ	Mean free path of gas, cm
μ	Gas viscosity, gm/(cmsec)

π 3.1416

ρ Gas density, gm/cm^3

ρ_p Particle density, gm/cm^3

σ_i Defined by equation (8-5) as

$$\sigma_i = \frac{(1 + \frac{\pi}{8} a_i) \quad \gamma_i \quad \sqrt{m_i}}{\sum_k \{(1 + \frac{\pi}{8} a_k) \gamma_k \quad \sqrt{m_k}\}}$$

σ_1 σ_i for water vapor diffusion

σ_2 σ_i for air diffusion

τ Effective drop-particle interaction time, $2R_c/v_{tc}$, sec

τ_i Mass fraction of component i, dimensionless

ϕ Spherical co-ordinate variable

APPENDIX I

Derivation of Epstein's Equation for the Thermal Force

APPENDIX I

Derivation of Epstein's Equation for the Thermal Force

For the case of a sphere, Epstein assumed that:

i. the mean free path of the gas was small relative to the radius of the aerosol particle

ii. a uniform temperature gradient existed in the gas at a great distance from the aerosol, and

iii. Fourier's heat conduction equation without convective terms could be used even though such a state would not exist because of thermal creep.

For steady state heat conduction through both the aerosol particle and surrounding gas, Laplace's equation

$$\nabla^2 T = 0 \qquad \text{(I-1)}$$

is valid.

For the spherical co-ordinates (r, θ, ϕ) shown in Figure A-1, Laplace's equation may be written

$$\frac{\partial}{\partial r}\left(r^2 \frac{\partial T}{\partial r}\right) + \frac{1}{\sin\theta} \frac{\partial}{\partial \theta}\left(\sin\theta \frac{\partial T}{\partial \theta}\right) + \frac{1}{\sin^2\theta} \frac{\partial T^2}{\partial \phi^2} = 0 \qquad \text{(I-2)}$$

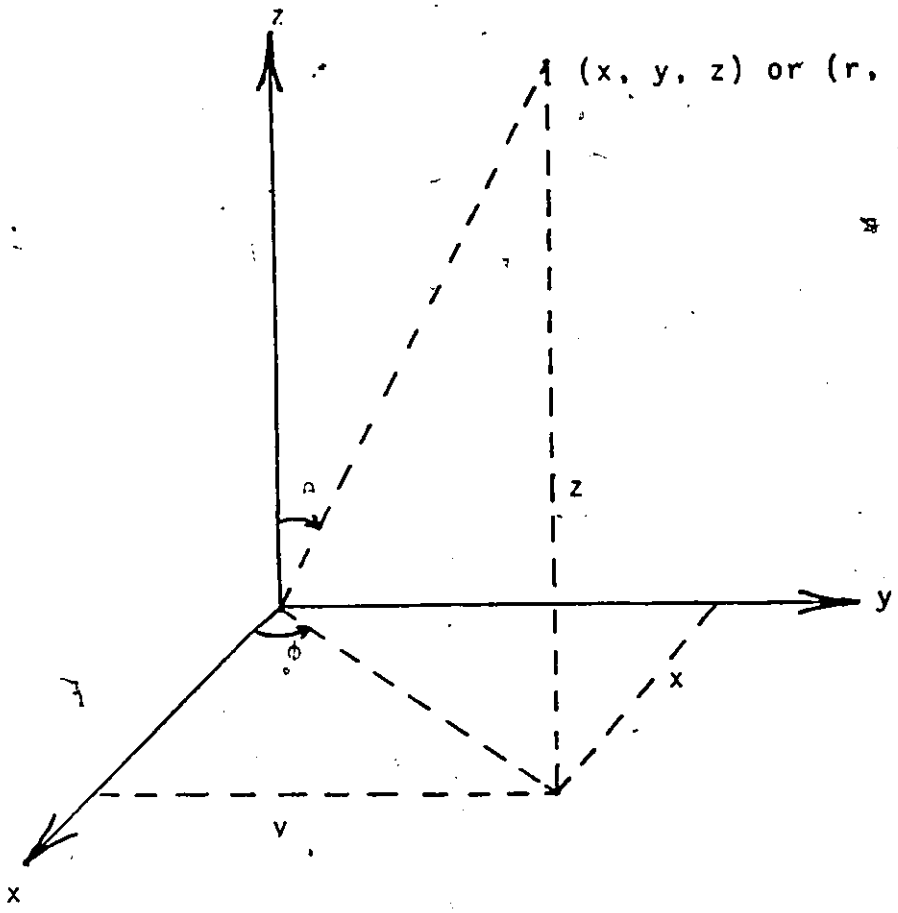

FIGURE A-1: Spherical Co-ordinates. The ranges of variables are $0 \leq r \leq \infty$, $0 \leq \theta \leq \pi$, and $0 \leq \phi \leq 2\pi$

When axial symmetry exists, T is independent of ϕ so that

$$\frac{\partial}{\partial r}\left(r^2 \frac{\partial T}{\partial r}\right) + \frac{1}{\sin\theta} \frac{\partial}{\partial \theta}\left(\sin\theta \frac{\partial T}{\partial \theta}\right) = 0 \qquad \text{(I-3)}$$

Substitute $T = R(r)\,\Theta(\theta)$ into the equation (I-3) and separate the variables to obtain:

$$\frac{1}{R}\frac{d}{dr}\left(r^2\frac{dR}{dr}\right) = -\frac{1}{\Theta}\frac{1}{\sin\theta}\frac{d}{d\theta}\left(\sin\theta\,\frac{d\Theta}{d\theta}\right) = \text{constant } k \qquad \text{(I-4)}$$

The choice of $n(n+1)$, where n is a positive integer, for the constant k results in the equations

$$r^2\frac{d^2R}{dr^2} + 2r\frac{dR}{dr} - n(n+1)R = 0 \qquad \text{(I-5)}$$

$$\frac{1}{\sin\theta}\frac{d}{d\theta}\left(\sin\theta\,\frac{d\Theta}{d\theta}\right) + n(n+1)\Theta = 0 \qquad \text{(I-6)}$$

In order to solve Euler's equation (I-5), the independent variable "r" is expressed in terms of "s" as $r = e^s$. This means

$$\frac{dr}{ds} = e^s \qquad \text{(I-7)}$$

or

$$\frac{ds}{dr} = e^{-s} = \frac{1}{r} \qquad \text{(I-8)}$$

From

$$\frac{dR}{dr} = \frac{dR}{ds}\frac{ds}{dr} = \frac{1}{r}\frac{dR}{ds} \qquad \text{(I-9)}$$

$$\frac{d^2R}{dr^2} = \frac{d}{dr}\left(\frac{1}{r}\frac{dR}{ds}\right) = \frac{1}{r^2}\frac{d^2R}{ds^2} - \frac{1}{r^2}\frac{dR}{ds} \qquad \text{(I-10)}$$

Substituting equations (I-9) and (I-10) into (I-5), we get

$$\frac{d^2R}{ds^2} + \frac{dR}{ds} - n(n+1)R = 0 \qquad \text{(I-11)}$$

Substituting $R = e^{ms}$ into the equation (I-11), we get

$$m^2 + m - n(n+1) = 0 \qquad \text{(I-12)}$$

$$m = \frac{-1 \pm \sqrt{1 + 4n(n+1)}}{2}$$

$$= \frac{-1 \pm (1 + 2n)}{2}$$

$$= n \text{ or } -(1+n) \qquad \text{(I-13)}$$

Hence the solution of equation (I-11) is

$$R = \begin{cases} e^{ns} \\ e^{-(n+1)s} \end{cases}, \text{ or} \qquad \text{(I-14)}$$

$$R = \begin{cases} r^n \\ r^{-(n+1)} \end{cases} \qquad \text{(I-15)}$$

Equation (I-6) is solved by first changing the independent variable from θ to η by means of the substitution $\eta = \cos\theta$. Equation (I-6) can be written as

$$\frac{d^2\Theta}{d\theta^2} + \cot\theta \frac{d\Theta}{d\theta} + n(n+1)\Theta = 0 \qquad \text{(I-16)}$$

The change of dependent variable gives

$$\frac{d\theta}{d\theta} = \frac{d\theta}{d\eta}\frac{d\eta}{d\theta} \quad \text{but} \quad \frac{d\eta}{d\theta} = -\sin\theta \tag{I-17}$$

and

$$\frac{d\theta}{d\theta} = -(\sin\theta)\frac{d\theta}{d\eta}, \text{ or } \frac{d}{d\theta} = -(\sin\theta)\frac{d}{d\eta} \tag{I-18}$$

$$\frac{d^2\theta}{d\theta^2} = \sin^2\theta \cdot \frac{d^2\theta}{d\theta^2} - \cos\theta \frac{d\theta}{d\eta} \tag{I-19}$$

Thus equation (I-16) can be simplified to:

$$\frac{d}{d\eta}\left[(1-\eta^2)\frac{d\theta}{d\eta}\right] + n(n+1)\,\theta = 0 \tag{I-20}$$

This is Legendre's equation. Since we require solutions which are finite over the closed interval $0 \leq \theta \leq \pi$ and since the only possible solutions are the Legendre's polynomials $P_n(\cos\theta)$, it is clear that n must be an integer and

$$\theta = \begin{cases} P_n(\eta) = P_\eta(\cos\theta) \\ Q_n(\eta) = Q_\eta(\cos\theta) \end{cases} \tag{I-21}$$

Thus equation (I-3) has solutions of the form

$$T = \begin{cases} r^n & P_n(\cos\theta) \\ r^{-(n+1)} & Q_n(\cos\theta) \end{cases} \tag{I-22}$$

which are valid inside the solid surface and for the surrounding gas. Subject to the assumptions previously made, since $Q_n(\cos\theta)$ is infinite for $\cos\theta = \pm 1$, the solution must not contain $Q_n(\cos\theta)$ because the temperature must be finite everywhere.

The most general form of the temperature distribution becomes:

$$T = \sum_{n=0}^{\infty} \left(A_n r^n + \frac{B_n}{r^{(n+1)}}\right) P_n(\cos\theta) \qquad \text{(I-23)}$$

a. Temperature Distribution Inside of the Aerosol Particle, T_i

Inside the spherical particle, the temperature distribution is

$$T_i = \sum_{n=0}^{\infty} \left(A_n r^n + \frac{B_n}{r^{n+1}}\right) P_n(\cos\theta) \qquad \text{(I-24)}$$

where A_n and B_n are constants to be determined from the proper boundary conditions

For $r \to 0$, $T_i \to \infty$, and since all solutions must be finite, including $r = 0$, then B_n must equal zero. This gives

$$T_i = \sum_{n=0}^{\infty} (A_n r^n) P_n(\cos\theta) \qquad \text{(I-25)}$$

b. Temperature Distribution Outside the Aerosol Particle, T_o

Equation (I-23) is written as:

$$T_o = \sum_{n=0}^{\infty} \left(C_n r^n + \frac{D_n}{r^{n+1}}\right) P_n(\cos\theta) \qquad \text{(I-26)}$$

for the temperature distribution in the surrounding gas, where C_n and D_n are constants to be evaluated employing the proper boundary conditions.

Since the temperature gradient was assumed to be constant away from the sphere (at $r \to \infty$), then

$$\left(\frac{\partial T_o}{\partial r}\right)_{r \to \infty} = G \cos\theta \quad \text{where} \qquad \text{(I-27)}$$

G is the magnitude of the temperature gradient. Thus for $r \to \infty$, equation (I-26) simplifies to

$$T_o = \sum_{n=0}^{\infty} \left(C_n r^n\right) P_n(\cos\theta) \qquad \text{(I-28)}$$

and

$$\left(\frac{\partial T_o}{\partial r}\right)_{r\to\infty} = \sum_{n=0}^{\infty} C_n (n\, r^{n-1}) P_n(\cos\theta) \qquad \text{(I-29)}$$

This gives $C_1 = G$ and $C_n = 0$ for $n \geq 2$. Also C_o has no physical meaning and is set equal to zero. Now since

$$P_1(\cos\theta) = \cos\theta \qquad \text{(I-30)}$$

it follows that

$$T_o = G r \cos\theta + \sum_{n=0} \frac{D_n}{r^{n+1}} P_n(\cos\theta) \qquad \text{(I-31)}$$

On the particle surface, where $r = R_p$, it follows that

$$T_i = T_o \tag{I-32}$$

Therefore

$$\sum_{n=0}^{\infty}\left(A_n R_p^n\right) P_n(\cos\theta) = G R_p \cos\theta + \sum_{n=0}^{\infty} \frac{D_n}{R_p^{n+1}} P_n(\cos\theta) \tag{I-33}$$

i.e.

$$A_0(1)(1) + A_1 R_p \cos\theta + A_2 R_p^2 \left(\tfrac{1}{2}\right)(3\cos^2\theta - 1) + \cdots\cdots$$

$$= G R_p \cos\theta + \frac{D_0(1)}{R_p} + \frac{D_1}{R_p^2}(\cos\theta) + \frac{D_2}{R_p^3}\left(\tfrac{1}{2}\right)(3\cos^2\theta - 1) + \cdots \tag{I-34}$$

Also at $r = R_p$,

$$-k_p\left(\frac{\partial T_i}{\partial r}\right) = -k_g\left(\frac{\partial T_o}{\partial r}\right) \tag{I-35}$$

where

k_p = thermal conductivity of the solid particle

k_g = thermal conductivity of the gas.

Therefore

$$k_p\left[\sum_{n=0}^{\infty} A_n n R_p^{n-1} P_n(\cos\theta)\right] = k_g\left[G\cos\theta + \sum_{n=0}^{\infty} \frac{D_n}{R_p^{n+2}} (-1)(n+1) P_n(\cos\theta)\right] \tag{I-36}$$

or

$$k_p \left[A_o(0)R_p^{-1}(1) + A_1(1)(\cos\theta) + A_2(2)R_p\left(\tfrac{1}{2}\right)(3\cos\theta^2 - 1) + \quad\right]$$

$$= k_g G(\cos\theta) + k_g \left[\frac{D_o(-1)(1)(1)}{R_p^2} + \frac{D_1(-1)2(\cos\theta)}{R_p^3} + \cdots\right] \quad \text{(I-37)}$$

Equating like terms in Equation (I-34) gives:

$A_o = D_o/R_p$, but $D_o = o$ by inspection of Equation (I-37)

$$A_1 R_p \cos\theta = GR_p (\cos\theta) + \frac{D_1}{R_p^2} (\cos\theta)$$

$$k_p A_1 (\cos\theta) = G k_g (\cos\theta) - \frac{D_o k_g}{R_p^2} - 2\frac{D_1 k_g (\cos\theta)}{R_p^3} \quad \text{(I-38)}$$

and

$$A_1 = G + \frac{D_1}{R_p^3} \quad \text{(I-39)}$$

Multiplying equation (I-38) by R_p yields

$$R_p k_p A_1 (\cos\theta) = R_p k_g G(\cos\theta) - \frac{k_g D_o R_p}{R_p^2} - \frac{R_p k_g D_1 2(\cos\theta)}{R_p^3} \quad \text{(I-40)}$$

From equations (I-39) and (I-40),

$$\frac{D_1 (\cos\theta)}{R_p^3} [k_p + 2 k_g] = k_g G(\cos\theta) - k_p G(\cos\theta) \quad \text{(I-41)}$$

and

$$D_1 = \frac{GR_p^3 (k_g - k_p)}{(k_p + 2 k_g)} \quad \text{(I-42)}$$

From equations (I-39) and (I-42)

$$A_1 = G \left[1 + \frac{k_g - k_p}{k_p + 2k_g}\right] \qquad \text{(I-43)}$$

Therefore

$$A_1 = G \left[\frac{3\, k_g}{k_p + 2\, k_g}\right] \qquad \text{(I-44)}$$

On substituting the above value of A_1 into equation (I-25) the final form of the temperature distribution inside the sphere is found to be:

$$T_i = G \left[\frac{3\, k_g}{k_p + 2\, k_g}\right] r(\cos\theta) \qquad \text{(I-45)}$$

Substituting the value of D_1 in equation (I-31) yields

$$T_o = G\, r(\cos\theta) + \frac{G\, R_p^3}{r^2} \left[\frac{k_g - k_p}{k_p + 2\, k_g}\right] (\cos\theta) \qquad \text{(I-46)}$$

The temperature distribution in the surrounding gas is then

$$T_o = G \left[r + \frac{(k_g - k_p)}{(k_p + 2\, k_g)} \frac{R_p^3}{r^2}\right] (\cos\theta) \qquad \text{(I-47)}$$

Now the temperature gradient over the surface can be found. On the surface, the temperature varies only in the θ-direction. From

$$\left(\frac{\partial T}{\partial S}\right) = \left(\frac{1}{r} \frac{\partial T}{\partial \theta}\right)_{r = R_p} \qquad \text{(I-48)}$$

where

S = distance along the surface in the direction of increasing temperature

$$\frac{\partial T}{\partial S} = \frac{1}{R_p}\left(\frac{\partial T_o}{\partial \theta}\right)_{r = R_p} = \frac{1}{R_p}\left(\frac{\partial T_i}{\partial \theta}\right)_{r = R_p} \qquad \text{(I-49)}$$

which reduces to

$$\frac{\partial T}{\partial S} = -\left[\frac{3\,k_g}{2\,k_g + k_p}\right] \quad G(\sin\theta) \qquad \text{(I-50)}$$

c. Velocity Distribution

The velocity components in rectangular co-ordinates for steady state flow of a constant density gas past a fixed spherical particle using the boundary conditions

i. $v_x = 0,\ v_y = 0,\ v_z = 0$, for $r = R_p$ and

ii. $v_x = 0,\ v_y = 0,\ v_z = v$ for $r = \infty$

are given by Lamb [1] as

$$v_x = \left(B - \frac{Ar^2}{6\mu}\right)\frac{\partial}{\partial x}\left(\frac{z}{r^3}\right) \qquad \text{(I-51)}$$

$$v_y = \left(B - \frac{Ar^2}{6\mu}\right)\frac{\partial}{\partial y}\left(\frac{z}{r^3}\right) \qquad \text{(I-52)}$$

$$v_z = v + \left(B - \frac{Ar^2}{6\mu}\right)\frac{\partial}{\partial z}\left(\frac{z}{r^3}\right) + \frac{2A}{3\mu\, r} \qquad \text{(I-53)}$$

where

μ is gas viscosity

A and B are constants to be evaluated, flow is parallel to the z-axis, and the origin is at the centre of the spherical particle. For spherical co-ordinates the variables are related to x, y, z as:

$$x = r \sin\theta \cos\phi \tag{I-54}$$

$$y = r \sin\theta \sin\phi \tag{I-55}$$

$$z = r \cos\theta \tag{I-56}$$

Also

$$r = \sqrt{x^2 + y^2 + z^2} \tag{I-57}$$

$$\theta = \arctan\left(\frac{\sqrt{x^2 + y^2}}{z}\right) \tag{I-58}$$

$$\phi = \arctan\frac{y}{x} \tag{I-59}$$

In terms of spherical co-ordinates, it follows that

$$\frac{\partial}{\partial x}\left(\frac{z}{r^3}\right) = \frac{r^3 \frac{\partial z}{\partial x} - z \frac{\partial}{\partial x}(r^3)}{r^6}$$

$$= -\frac{r\cos\theta}{r^6} \frac{3}{2}(x^2 + y^2 + z^2)^{1/2} 2x$$

$$= -\frac{3}{r^3} \cos\theta \sin\theta \cos\phi \tag{I-60}$$

Substituting the value of $\frac{\partial}{\partial x}\left(\frac{z}{r^3}\right)$ from equation (I-60) into equation (I-51) yields

$$v_x = \left(B - \frac{Ar^2}{6\mu}\right)\left(\frac{-3}{r^3}\cos\theta \sin\theta \cos\phi\right)$$

$$= -\frac{3B}{r^3}\sin\theta \cos\theta \cos\phi + \frac{A}{2\mu r}\sin\theta \cos\theta \cos\phi \qquad \text{(I-61)}$$

In terms of spherical co-ordinates, it follows that

$$\frac{\partial}{\partial y}\left(\frac{z}{r^3}\right) = \frac{r^3 \frac{\partial z}{\partial y} - z \frac{\partial}{\partial y}(r^3)}{r^6}$$

$$= -\frac{r\cos\theta}{r^6}\frac{3}{2}(x^2 + y^2 + z^2)^{1/2}\, 2y$$

$$= -\frac{3}{r^3}\cos\theta \sin\theta \sin\phi \qquad \text{(I-62)}$$

Substituting the value of $\frac{\partial}{\partial y}\left(\frac{z}{r^3}\right)$ from equation (I-62) in equation (I-52) yields

$$v_y = \left(B - \frac{Ar^2}{6\mu}\right)\left(-\frac{3\cos\theta \sin\theta \sin\phi}{r^3}\right)$$

$$= -\frac{3B}{r^3}\cos\theta \sin\theta \sin\phi + \frac{A}{2\mu r}\sin\theta \cos\theta \sin\phi \qquad \text{(I-63)}$$

In terms of spherical co-ordinates, it follows that

$$\frac{\partial}{\partial z}\left(\frac{z}{r^3}\right) = \frac{r^3 \frac{\partial z}{\partial z} - z \frac{\partial}{\partial z}(r^3)}{r^6}$$

$$= \frac{1}{r^3} - \frac{r\cos\theta}{r^6} \frac{3}{2}(x^2 + y^2 + z^2)^{1/2} 2z$$

$$= \frac{1 - 3\cos^2\theta}{r^3} \qquad \text{(I-64)}$$

Substituting the value of $\frac{\partial}{\partial z}\left(\frac{z}{r^3}\right)$ from equations (I-64) into equation (I-53) gives

$$v_z = v + \left(B - \frac{Ar^2}{6\mu}\right)\left[\frac{1 - 3\cos^2\theta}{r^3}\right] + \frac{2A}{3\mu r}$$

$$= v - \frac{B}{r^3}(2 - 3\sin^2\theta) + \frac{A}{2\mu r}(1 + \cos^2\theta) \qquad \text{(I-65)}$$

For spherical co-ordinates, the variables are related to v_x, v_y and v_z as:

$$v_r = (\sin\theta\ \cos\phi)\, v_x + (\sin\theta\ \sin\phi)\, v_y + (\cos\theta)\, v_z \qquad \text{(I-66)}$$

$$v_\theta = (\cos\theta\ \cos\phi)\, v_x + (\cos\theta\ \sin\phi)\, v_y + (-\sin\theta)\, v_z \qquad \text{(I-67)}$$

$$v_\phi = (-\sin\phi)\, v_x + (\cos\phi)\, v_y + (0)\, v_z \qquad \text{(I-68)}$$

Substituting for v_x, v_y and v_z from equations (I-61), (I-63) and (I-65) respectively into equation (I-66) yields

$$v_r = (\sin\theta\cos\phi)\left[-\frac{3B}{r^3}\sin\theta\cos\theta\cos\phi + \frac{A}{2\mu r}\sin\theta\cos\theta\cos\phi\right]$$

$$+ \sin\theta\sin\phi\left[-\frac{3B}{r^3}\sin\theta\cos\theta\sin\phi + \frac{A}{2\mu r}\sin\theta\cos\theta\sin\phi\right]$$

$$+ \cos\theta\left[v - \frac{B}{r^3}(2 - 3\sin^2\theta) + \frac{A}{2\mu r}(1 + \cos^2\theta)\right]$$

$$= -\frac{3B}{r^3}\sin^2\theta\cos\theta\left[\cos^2\phi + \sin^2\phi\right]$$

$$+ \frac{A}{2\mu r}\sin^2\theta\cos\theta\left[\cos^2\phi + \sin^2\phi\right]$$

$$+ v\cos\theta - \frac{2B}{r^3}\cos\theta + \frac{3B}{r^3}\sin^2\theta\cos\theta + \frac{A}{2\mu r}\cos\theta + \frac{A}{2\mu r}\cos^3\theta$$

$$= v\cos\theta - \frac{2B}{r^3}\cos\theta + \frac{A}{2\mu r}\sin^2\theta\cos\theta + \frac{A}{2\mu r}\cos\theta\left[1 + \cos^2\theta\right]$$

$$= v\cos\theta - \frac{2B\cos\theta}{r^3} + \frac{A}{2\mu r}\sin^2\theta\cos\theta + \frac{A}{2\mu r}\cos\theta(2 - \sin^2\theta)$$

$$= v\cos\theta - \frac{2B}{r^3}\cos\theta + \frac{2A}{2\mu r}\cos\theta$$

$$\text{i.e.} \quad v_r = \left(v - \frac{2B}{r^3} + \frac{A}{\mu r}\right)\cos\theta \qquad \text{(I-69)}$$

Substituting for v_x, v_y, and v_z from equations (I-61), (I-63), and (I-65) respectively into equation (I-67) gives

$$v_\theta = (\cos\theta\cos\phi)\left[\frac{-3B}{r^3}\sin\theta\cos\theta\cos\phi + \frac{A}{2\mu r}\sin\theta\cos\theta\cos\phi\right]$$

$$+ \cos\theta\sin\phi\left[\frac{-3B}{r^3}\sin\theta\cos\theta\sin\phi + \frac{A}{2\mu r}\sin\theta\cos\theta\sin\phi\right]$$

$$+ (-\sin\theta)\left[v - \frac{B}{r^3}(2 - 3\sin^2\theta) + \frac{A}{2\mu r}(1 + \cos^2\theta)\right.$$

$$= \frac{-3B}{r^3}\sin\theta\cos^2\theta\cos^2\phi - \frac{3B}{r^3}\sin\theta\cos^2\theta\sin^2\phi$$

$$-\frac{3B}{r^3}\sin^2\theta\sin\theta + \frac{2B}{r^3}\sin\theta - v\sin\theta + \frac{A}{2\mu r}\sin\theta\cos^2\theta\cos^2\phi$$

$$+ \frac{A}{2\mu r}\sin\theta\cos^2\theta\sin^2\phi - \frac{A}{2\mu r}\sin\theta - \frac{A}{2\mu r}\sin\theta\cos^2\theta$$

$$= -\frac{3B}{r^3}\sin\theta\cos^2\theta[\cos^2\theta + \sin^2\theta] - \frac{3B}{r^3}\sin^2\theta\sin\theta$$

$$+ \frac{2B}{r^3}\sin\theta - \frac{A}{2\mu r}\sin\theta - v\sin\theta\ , \text{ or}$$

$$v_\theta = -\left(v + \frac{B}{r^3} + \frac{A}{2\mu r}\right)\sin\theta \qquad \text{(I-70)}$$

Substituting for v_x, v_y and v_z from equations (I-61), (I-63) and (I-65) respectively into equation (I-68) yields

$$v_\phi = (-\sin\phi)\left[\frac{-3B}{r^3}\sin\theta\cos\theta\cos\phi + \frac{A}{2\mu r}\sin\theta\cos\theta\cos\phi\right]$$

$$+ \cos\phi\left[\frac{-3B}{r^3}\cos\theta\sin\theta\sin\phi + \frac{A}{2\mu r}\sin\theta\cos\theta\sin\phi\right]$$

$$+ (0)\left[v + \frac{B}{r^3}(2 - 3\sin^2\theta + \frac{A}{2\mu r}(1 + \cos^2\theta)\right], \text{ or}$$

$$v_\phi = 0 \qquad \text{(I-71)}$$

For the resulting expressions

$$v_r = \left(v - \frac{2B}{r^3} + \frac{A}{\mu r}\right)\cos\theta \qquad \text{(I-69)}$$

$$v_\theta = -\left(v + \frac{B}{r^3} + \frac{A}{2\mu r}\right)\sin\theta \qquad \text{(I-70)}$$

$$v_\phi = 0 \qquad \text{(I-71)}$$

The following boundary conditions are applicable:

i. there is no flow except near the surface of the sphere. Hence, $v = 0$

ii. the normal velocity, v_r, must be zero at the surface of the particle where $r = R_p$

iii. the tangential velocity, v_θ, at the surface of the particle where $r = R_p$, is assumed to be Maxwell's slip velocity given by equation (4-1) in section (IV-A) with these boundary conditions

$$v_r = \left(\frac{-2B}{R_p^3} + \frac{A}{\mu R_p}\right) \cos\theta = 0 \qquad \text{(I-72)}$$

$$v_\theta = -\left[\frac{B}{R_p^3} + \frac{A}{2\mu R_p}\right] \sin\theta = \frac{3}{4}\frac{\mu}{\rho T}\frac{\partial T}{\partial s} \qquad \text{(I-73)}$$

$$v_\phi = 0 \qquad \text{(I-74)}$$

In terms of equation (I-50), equation (I-73) can be written as

$$-\left[\frac{B}{R_p^3} + \frac{A}{2\mu R_p}\right] \sin\theta = -\frac{3}{4}\frac{\mu}{\rho T}\left[\frac{3\,k_g}{2k_g + k_p}\right] G \sin\theta \qquad \text{(I-75)}$$

By setting

$$K = \frac{3\,k_g}{2\,k_g + k_p}, \qquad \text{(I-76)}$$

equation (I-75) reduces to

$$8\mu\rho T B + 4\rho T R_p^2 A - 6\mu^2 R_p^3 K G = 0 \qquad \text{(I-77)}$$

Equation (I-72) can be written as:

$$A R_p^2 \cos\theta - 2\mu B \cos\theta = 0 \qquad \text{(I-78)}$$

By solving equations (I-77) and (I-78), it follows that

$$A = \frac{9 R_p}{4}\left(\frac{\mu^2}{\rho T}\right)\left(\frac{k_g}{2 k_g + k_p}\right) G \qquad \text{(I-79)}$$

$$B = \frac{A R_p^2}{2\mu} \qquad \text{(I-80)}$$

Finally, we obtain for the velocity over the surface of the sphere by substituting for A and B into equation (I-73)

$$v_\theta = -\frac{9}{4}\left(\frac{\mu}{\rho T}\right)\left(\frac{k_g}{2k_g + k_p}\right) G \sin\theta \qquad \text{(I-81)}$$

d. The Thermal Force

The force acting on the sphere in the direction of flow as shown in Figure A-2 is given by the integral over the surface in the z-direction.

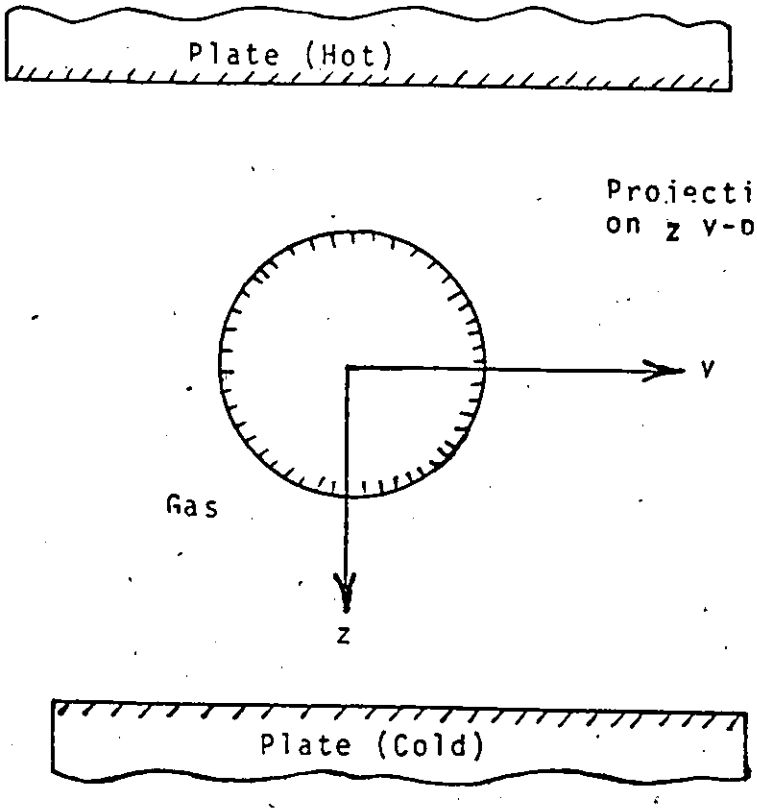

FIGURE A-2: Flow of a Spherical Particle in a Gas Under a Temperature Gradient

At each point on the particle surface, there is a fluid stress acting perpendicularly to the surface. The surface area, on which the fluid stress acts, is $R^2 \sin\theta \, d\theta \, d\phi$ [2]. Therefore

$$F_t = \int_0^{2\pi} \int_0^{\pi} p_{r,z=R_p}(r,\theta) \, R^2 \sin\theta \, d\theta \, d\phi \qquad \text{(I-82)}$$

and

$$F_t = 2\pi R_p^2 \int_0^{\pi} p_{r,\, z=R_p}(r,\theta) \sin\theta \, d\theta \qquad \text{(I-83)}$$

The total fluid stress acting on the surface of the sphere in the z-direction is given by Lamb [1] as

$$p_{r,z} = \frac{-x}{r} p_o + \left(Ar - \frac{6\mu B}{r}\right) \frac{\partial}{\partial z}\left(\frac{z}{r^3}\right) - \frac{A}{r^2} \qquad \text{(I-84)}$$

By substituting the value of x and $\frac{\partial}{\partial z}\left(\frac{z}{r^3}\right)$ from equations (I-56) and (I-64) into the equation (I-84) it is possible to write

$$p_{r,\, z = R_p} = - p_o \cos\theta + \left(AR_p - \frac{6\mu B}{R_p}\right) \frac{1}{R_p^3} (1 - 3\cos^2\theta) - \frac{A}{R_p^2}$$

$$= - p_o \cos\theta - \frac{6\mu B}{R_p^4} - 3\left(\frac{A}{R_p^2} - \frac{6\mu B}{R_p^4}\right) \cos^2\theta \qquad \text{(I-85)}$$

Substituting equation (I-85) into equation (I-83) yields

$$F_t = 2\pi R_p^2 \left[-p_o \int_0^{\pi} \cos\theta \sin\theta \, d\theta - \frac{6\mu B}{R_p^4} \int_0^{\pi} \sin\theta \, d\theta \right.$$

$$\left. - 3 \left(\frac{A}{R_p^2} - \frac{6\mu B}{R_p^4}\right) \int_0^{\pi} \cos^2\theta \sin\theta \, d\theta\right]$$

$$= 2\pi R_p^2 \left[0 - \frac{12\mu B}{R_p^4} - 2 \left(\frac{A}{R_p^2} - \frac{6\mu B}{R_p^4}\right)\right]$$

$$= - 4\pi A \qquad \text{(I-86)}$$

Substituting for A from equation (I-79) into equation (I-86) leads to

$$F_t = -9\pi R_p \left(\frac{k_g}{2\,kg + kp}\right)\left(\frac{\mu^2}{\rho T}\right) G \qquad \text{(I-87)}$$

This is Epstein's equation for the thermal force in the slip-flow regime.

REFERENCES

1. Lamb, H., Hydrodynamics, p. 597, Sixth Edition, Cambridge University Press, New York (1957).

2. Bird, R. B., Steward, W. E., and Lightfoot, E. N., Transport Phenomena, p. 58, John Wiley and Sons, Inc., New York (1966).

VITA AUCTORIS

1950 Born in Muvattupuzha, Kerala, India

1965 Received the Secondary School Leaving Certificate from the Higher Secondary School Board of Kerala, India

1967 Received the Pre-Degree Certificate from the University of Kerala, India

1973 Received the Degree of Bachelor of Technology in Chemical Plant Engineering from the Regional Engineering College, Warangal, (affiliated to the Osmania University, Hyderabad), Andhra Pradesh, India

1975 Received the Degree of Master of Applied Science in Chemical Engineering at the University of Windsor, Windsor, Ontario, Canada